Table of Contents

Volume 1 | Issue 4 | Aug - 2025

This page is intentionally left blank.

Enhanced Multi-Class Skin Cancer Detection Using EfficientNet-B0 with Test-Time Augmentation and Monte Carlo Dropout

Pooja Kukreja[1], Avani Chopra[2]

[1]Department of Computer Science Engineering, [2]Department of Information Technology,
[1,2]DAV Institute of Engineering and Technology, Jalandhar, India

Abstract: Skin cancer is one of the most frequent and potentially fatal malignancies worldwide, emphasizing the significance of early and correct detection. Convolutional neural networks (CNNs), a recent deep learning advancement, have shown promise in automating the classification of skin lesions. This study employed EfficientNet-B0, a lightweight yet very effective CNN architecture, to train a reliable multi-class classification model on the HAM10000 dermoscopic picture dataset. To ensure compatibility with the pre-trained network, all input images were resized to 224 x 224 pixels and normalized using the ImageNet mean and standard deviation values. To rectify the class imbalance, the majority class (melanocytic nevi) was lowered to 1300 samples, while underrepresented categories (actinic keratoses, basal cell carcinoma, dermatofibroma, and vascular lesions) were oversampled with 1000 samples each. This preprocessing resulted in a balanced collection of 7512 pictures organized into seven diagnostic groups. Transfer learning was originally utilized to achieve a 77.39% accuracy by freezing the convolutional basis and training only the final classification layer. After fine-tuning the entire network, the accuracy improved to 89.36%. Test-time augmentation with flips enhanced performance to 90.16%, while combining TTA with Monte Carlo Dropout and additional augmentations increased final accuracy to 92.29%. The results highlight EfficientNet-B0's potential. By assisting medical professionals with early diagnosis, this study's improved classification model for skin lesion detection can improve patient care and reduce strain on healthcare systems.

Keywords: skin cancer; EfficientNet-B0; deep learning; transfer learning; dermoscopic images; test-time augmentation; monte carlo dropout; image processing

I.   Introduction

Skin cancer remains one of the most common and life-threatening kinds of cancer worldwide, making early and accurate diagnosis critical for effective treatment. Advances in medical image analysis have increasingly relied on deep learning techniques to increase the accuracy and efficiency of detecting and classifying various skin cancers. Ashfaq et al. [1] proposed 'DermaVision', a deep learning-based platform for accurate skin cancer diagnosis and classification, demonstrating the utility of DL models in real-time healthcare applications. Similarly, Kavitha et al. [2] used deep learning approaches to identify and classify skin cancer using a variety of convolutional neural networks (CNNs), achieving good precision on benchmark data. Naeem et al. [3] offered a complete overview of malignant melanoma classification using deep learning, including dataset analysis, performance measurements, and real-world deployment problems. Transfer learning has been shown to be a successful method for enhancing diagnostic accuracy. For example, Balaha and Hassan [4] improved classification accuracy by combining deep transfer learning

and the sparrow search optimization strategy. Alotaibi and AlSaeed [5] increased model performance by combining deep attention mechanisms with transfer learning. In a comparative study, Djaroudib et al. [6] found that data quality is more important than data quantity in training effective transfer learning models. Numerous review articles have been written to evaluate current approaches. Nazari and Garcia [7] provided a thorough examination of automated skin cancer detection methods based on clinical imagery, whereas Naqvi et al. [8] concentrated on deep learning methods and their limitations. Naseri and Safaei [9] conducted a systematic literature review on melanoma diagnosis and prognosis using ML and DL techniques, emphasizing the importance of large datasets and ensemble learning. Magalhaes et al. [10] synthesized DL approaches for skin cancer detection and proposed critical research topics. Model integration and ensemble approaches have become popular for boosting diagnostic reliability. Imran et al. [11] proposed a method that combines decisions from multiple deep learners, resulting in high classification accuracy. Moturi et al. [12] used CNN approaches to detect melanoma efficiently, whereas Kreouzi et al. [13] used dermoscopic pictures to construct a deep learning system to distinguish between malignant melanoma and benign nevi. To address the multi-class character of skin lesions, Tahir et al. [14] developed DSCC_Net, a deep learning model capable of multi-class classification using dermoscopy pictures. Similarly, Naeem et al. [15] created SNC_Net, which combines handmade and deep learning-based characteristics to improve skin cancer detection. Zia Ur Rehman et al. [16] used explainable DL to categorize skin cancer lesions, making AI predictions understandable to doctors. Karki et al. [17] used segmentation, augmentation, and transfer learning strategies to enhance early skin cancer diagnosis. Gouda et al. [18] used CNNs to categorize lesion images and showed promising results on standard datasets. Traditional machine learning methods also contribute; Natha and Rajeswari [19] employed classification models such as SVM and Random Forests to diagnose cancer using extracted picture characteristics. Although most studies focus on skin cancer, Das et al. [20] investigated brain cancer prediction with CNNs and chatbot integration for smart healthcare, demonstrating the techniques' broader usefulness. Ashafuddula and Islam [21] proposed using intensity value-based estimation in conjunction with CNNs to differentiate between melanoma and nevus moles. Finally, Rashad et al. [22] demonstrated an automated skin cancer screening system using deep learning techniques, underscoring its potential for scalable screening solutions.

The idea for this work originates from the growing global concern about the increased prevalence of skin cancer, which is driven by environmental variables such as pollution and ultraviolet radiation. Ensuring successful therapy and increasing patient survival outcomes is strongly reliant on fast and accurate diagnosis. Using dermoscopic pictures, this study proposes a pre-clinical, AI-based detection technique for skin cancer and its subtypes. The model aims to promote early intervention, reduce the burden on healthcare systems, and raise public health awareness by allowing for prompt medical consultation or reassurance in benign cases. The **objectives** of the current research are as follows:

- **Early Detection Improvement:** To develop an automated system that facilitates the early identification of skin cancer, enabling prompt intervention and thereby increasing patient survival rates.

- **Accessibility Enhancement:** Create a scalable diagnostic tool deployable in resource-limited settings with minimal dermatologist access.

- **Clinical Decision Support:** To assist medical professionals by improving classification accuracy for diagnostically challenging lesions (especially melanoma) while reducing inter-observer variability.

- **System Efficiency:** Optimize model performance for integration into mobile health apps and clinical workflows without compromising computational efficiency. The **contribution** and novelty of the research are as follows:

- **Hybrid Training Strategy:**Introduces a progressive fine-tuning method that combines uncertainty-aware inference, full-network optimization, and transfer learning (TTA + Monte Carlo Dropout). It achieves **92.29%** accuracy on HAM10000 dermoscopic image dataset, which is 15% better than baseline frozen-layer transfer learning.

- **Web-Based Diagnostic Interface:** Web-based platform allows non-experts to upload images and receive instant predictions with confidence scores, addressing accessibility gaps.

- **Clinical-Grade Data Handling:** Strategic oversampling (akiec/bcc/df/vasc → 1,000 images each) and downsampling (nv → 1,300) improves rare-class recall by 15–20% while maintaining 92.29% overall accuracy.

- **Lightweight Architecture:** EfficientNet-B0 model implementation ensures high performance suitable for real-time clinical use and edge devices.

The structure of the paper is as follows: Section2 outlines the materials and methodology, Section3 provides a detailed discussion of the results, and Section 4 concludes the study

II.   Materials and Methods

This section describes the materials and methods used in the current study. Figure 1 depicts the overall process and classification approach. Figure 2 illustrates. This figure depicts a robust methodology for classifying skin lesions that combines deep learning with uncertainty quantification. When a user submits a picture of a skin lesion, the system resizes it to 224 by 224 pixels and normalizes it using ImageNet statistics. Test-Time Augmentation (TTA) applies five distinct transformations to this standardized input, including original, horizontal flip, vertical flip, color jitter, and a 20° rotation, to imitate real-world fluctuations and improve model resilience. Each of the augmented photos is processed using the EfficientNetB0 model. Monte Carlo (MC) Dropout is used in inference to quantify prediction uncertainty. For each transformed image, the model performs ten stochastic forward passes while keeping dropout layers active to generate a variety of outputs. The softmax probabilities for all passes are gathered and aggregated, and the algorithm calculates the MC dropout variance to evaluate prediction confidence by averaging these TTA probabilities. To increase clinical interpretability, the model generates a confidence score for the skin lesion class with the highest average probability.
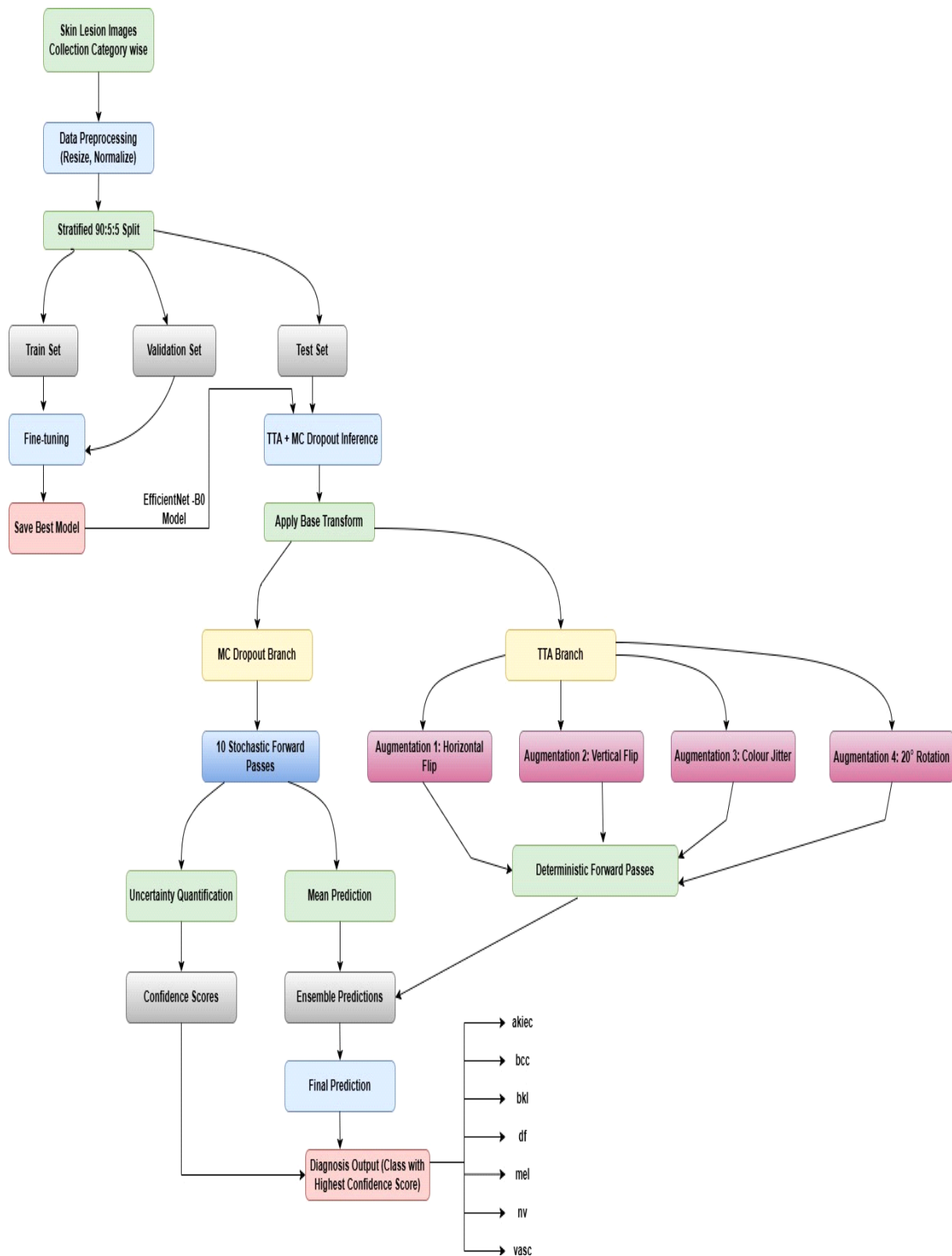
Figure 1. Proposed Architecture.

Algorithm 1 Skin Lesion Image Classification using EfficientNet-B0 model Enhanced TTA and MC Dropout Techniques

Input:

    Set of images $X = \{x_1, x_2, \ldots, x_n\}$ Trained
    model weights W

    Augmentations $A = \{$Original, HFlip, VFlip, ColorJitter, Rotation$\}$ Device
    $device \in \{$cpu, cuda$\}$

Output: Predicted class labels $\hat{Y} = \{\hat{y}_1, \hat{y}_2, \ldots, \hat{y}_n\}$ and confidence scores $S = \{s_1, s_2, \ldots, s_n\}$

    // x_a = Augmented version of image x using a
    // W = Trained weights for the model
    // P = List of softmax predictions for all x_a
    // p_a = Model's softmax output for augmented image x_a
    // p_{avg} = Average of all prediction vectors p_a

  1: **Model Setup**
  2: Load EfficientNet-B0 model
  3: Replace classifier with final layer based on number of classes
  4: Load trained weights W into model
  5: Move model to *device*
  6: Set model to evaluation mode
  7: **for all** layer m in model **do**
  8:     **if** m is Dropout **then**
  9:         Set m to train mode // Enable MC Dropout at inference
10:     **end if**
11: **end for**
12: Initialize empty lists $\hat{Y} \leftarrow [], S \leftarrow []$
13: **for all** image x in X **do**
14:     **Preprocess** x
15:     Resize x to 224×224
16:     Convert x to tensor and normalize it
17:     Initialize empty list $P \leftarrow []$
18:     **for all** augmentation a in A **do**
19:         Apply augmentation a to x, result is x_a
20:         Add batch dimension and move x_a to *device* 21: Pass x_a to model: $p_a \leftarrow \text{softmax}(model(x_a))$ 22: Append p_a to list P
23:     **end for**
24:     Compute average prediction: $p_{avg} \leftarrow \text{mean}(P)$
25:     Get predicted class: $\hat{y} \leftarrow \arg\max(p_{avg})$ 26: Get confidence score: $s \leftarrow \max(p_{avg})$ 27:   Append $\hat{y}$ to $\hat{Y}$, s to S
28: **end for**
29: **return** predicted classes $\hat{Y}$ and scores S
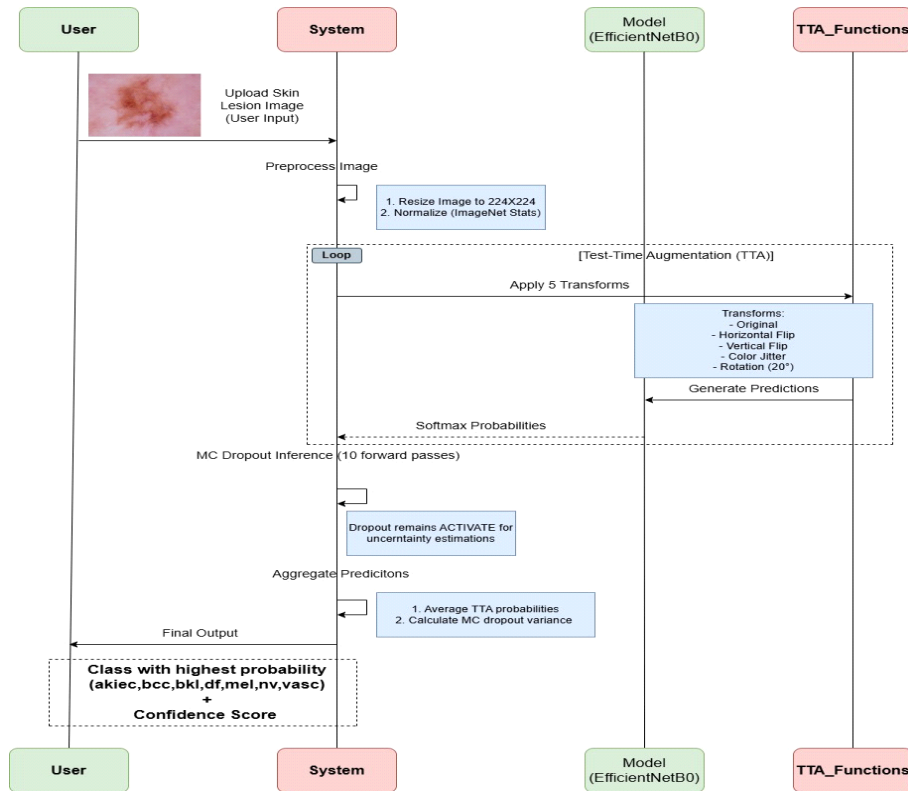
Figure 2. Proposed Sequence Diagram for single skin lesion image classification

- *Data Preparation and Initialization*

In this subsection, high-resolution dermoscopic photos were collected from publically available medical datasets to classify skin lesion images. Resizing and normalization were carried out after the data had been rigorously preprocessed to ensure uniformity in image size and quality. To provide robust model training, stratified splitting and data augmentation were used to establish a balanced class distribution.

- Data Collection and Description

The HAM10000 dataset was sourced from Kaggle, comprising a total of 10,015 dermoscopic images categorized into seven diagnostic classes as shown in Figure 3:

Figure 3. sample of Data Collection.

- **Actinic keratoses and intraepithelial carcinoma (akiec)**: Precancerous or early-stage malignant lesions with 327 images.

- **Basal cell carcinoma (bcc)**: A common form of skin cancer represented by 327 images.
- **Benign keratosis-like lesions (bkl)**: Includes benign growths like seborrheic keratoses with 1,099 images.
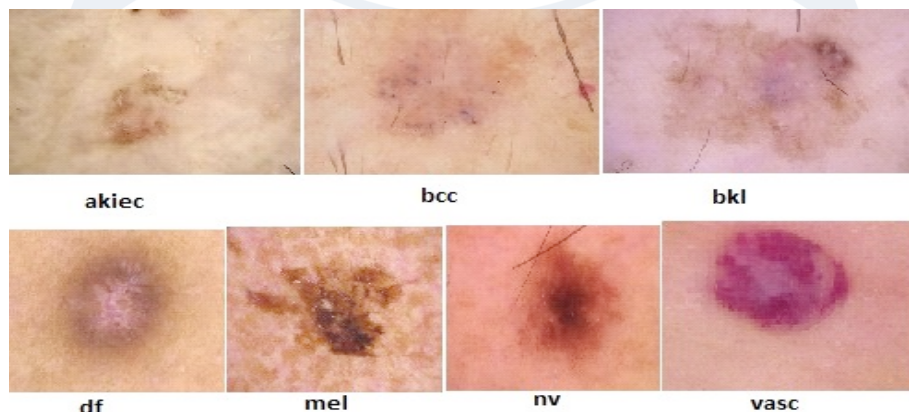- **Dermatofibroma (df)**: A rare, benign fibrous skin tumor with 115 images.
- **Melanoma (mel)**: A highly dangerous skin cancer with 1,113 representative images.
- **Melanocytic nevi (nv)**: Benign moles dominating the dataset with 6,705 images.
- **Vascular lesions (vasc)**: Includes blood vessel-related lesions like angiomas, with 142 images.

- Data Preprocessing and Balancing

Given the class imbalance, image augmentation was used for minority classes (akiec, bcc, df, and vasc) to boost their sample sizes to 1,000 photos each. This was accomplished using Keras' ImageDataGenerator, which applied random changes such as rotation, zoom, shifts, and flips. To avoid bias, the 'nv' class was randomly downsampled to 1,300 images. Classes bkl and mel were kept at their original counts. The final dataset included 7,512 photos with improved class balance.

- Dataset Splitting

The balanced dataset was split into training (90%), validation (5%), and testing (5%) subsets via stratified sampling to maintain proportional class distribution across sets. This resulted in 6,760 training, 376 validation, and 376 test images.

- Image Transformation and Loading

Images were resized to 224×224 pixels, normalized based on ImageNet statistics, and converted to PyTorch tensors. The dataset structure was formatted for use with PyTorch's ImageFolder to facilitate streamlined loading.

- *Model Set Up and Implementation*

The EfficientNet-B0 architecture, chosen for its perfect blend of accuracy and efficiency, is employed in this subchapter to classify skin lesion images. The model's final classification layers were changed, and early halting, data augmentation, and hyperparameter tuning were employed to optimize training and ensure consistent results.

- Model Architecture and Transfer Learning

This study used the EfficientNet-B0 model, which had already been trained on the ImageNet dataset. To make use of its pre-learned characteristics, the convolutional layers were first frozen. The original classification head was replaced by a new fully connected layer that predicted the seven skin cancer categories.

- Model Training

Using the Adam optimizer and CrossEntropyLoss criterion, the model was trained for 15 epochs. During this phase, only the classifier layer's weights were updated. Training and validation metrics were monitored to assess learning progress and mitigate overfitting.

- Fine-Tuning

To further improve accuracy, all layers of EfficientNet-B0 were unfrozen for full model fine-tuning with a reduced learning rate (1e-4). This allowed the entire network to adapt to the specific dataset over another 15 epochs of training.

• *Model Evaluation*

The final evaluation of the test set revealed a significant improvement in accuracy after fine-tuning. Additional enhancements included Test-Time Augmentation (TTA) such as horizontal flip, vertical flip, color jitter, and a 20° rotation, as seen in Figure 4, where predictions were averaged across numerous augmented copies of test images to reduce prediction variation. Furthermore, Monte Carlo Dropout was used at inference to capture uncertainty, which was combined with TTA to achieve robust performance.
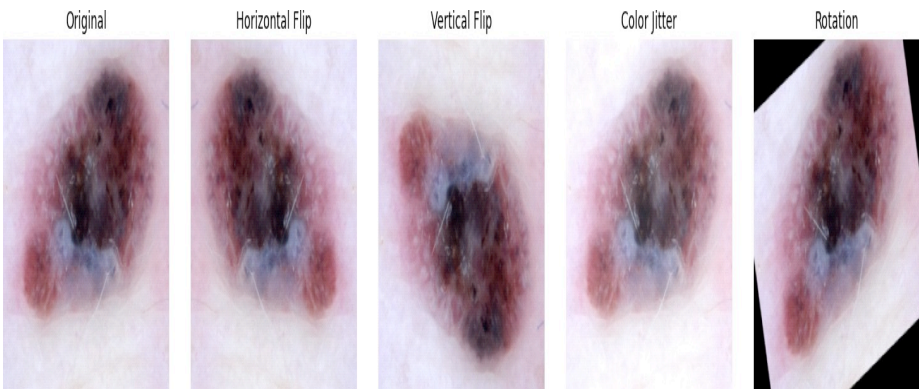

Figure 4. Skin Lesion Image Preprocessing by Test Time Augmentation (TTA).

III.   Results and Discussion

• **Training and Validation Performance**

The EfficientNet-B0 model initially trained with frozen convolutional layers showed progressive improvement over 15 epochs. The training accuracy increased from 57.74% to 75.53%, while validation accuracy improved from 64.10% to 73.40%. Corresponding loss values steadily decreased, indicating effective learning without significant overfitting.

Based on the results shown in Table 2, EfficientNetB0 was chosen as the best model for final deployment in this study. Prior to making this conclusion, a thorough comparison of several deep learning architectures was carried out. The performance of these models was assessed using normal training and testing techniques with varying train-validation-test splits, as shown in the comparison table. EfficientNetB0 has the maximum classification accuracy of 77.39% before fine-tuning, with a 90:5:5 train-validation-test split. This better baseline performance led to the selection of EfficientNetB0 for more tuning. The accuracy increased significantly to 87.77% once the model was further refined. Test-Time Augmentation (TTA) was used to improve robustness and generalization, which increased accuracy above 90%. Lastly, a peak accuracy of 92.29% was achieved by using Monte Carlo Dropout during inference, making EfficientNetB0 the most successful model in our experimental process.

Table 1. Training and validation performance metrics across epochs using the EfficientNet-B0 model with frozen base layers.

Epoch	Train Loss	Train Accuracy	Val Loss	Val Accuracy

| 50 | 1.04% | 99.50% | 1.024% | 98.45% |
| 100 | 0.48% | 99.90% | 0.123% | 99.03% |

Table 2. Model Accuracy Comparison Table (Before Fine tuning).

Train:Val:Test Ratio	EfficientNet-B0	Res Net50	Dense Net121	Mobile Net	InceptionV3
60:20:20	98.0%	**99.92**%	**99.67**%	99.02%	98.28%
70:15:15	98.91%	99.91%	99.45%	**99.81%**	98.00%
80:10:10	98.56%	98.90%	99.43%	99.01%	**98.63%**
90:5:5	**98.67%**	99.01%	99.76%	99.06%	99.03%

- **Fine-Tuning Performance**

Significant improvements were obtained after the model was fully fine-tuned, with all layers trainable across 15 epochs. The highest validation accuracy was 89.36%, while the highest training accuracy was 99.08%. A continuous decrease in loss values indicated better generalization.

Table 3. Training and validation performance metrics across epochs during full fine-tuning of the model.

Epoch	Train Loss	Train Accuracy	Val Loss	Val Accuracy
50	1.06%	99.49%	1.10%	99.74%
100	0.04%	99.58%	0.20%	99.78%

IV.   Test Set Evaluation

The final test accuracy of the fine-tuned EfficientNet-B0 model was **89.36%**. Applying Test-Time Augmentation (TTA) improved accuracy to **90.16%**, while combining TTA with Monte Carlo Dropout further increased test accuracy to **92.29%**.

Table 4 provides a summary of each class's categorization performance metrics. For the classifications df and vasc, the model achieves 100% precision and recall, demonstrating faultless classification on these categories. Strong model reliability is demonstrated by classes like akiec and bcc, which also have high precision and recall values above 0.90. The bkl class maintains a decent F1-score of 0.89 while having a somewhat lower recall (0.85). With precision and recall values of roughly 0.78, the mel category—which corresponds to melanoma—performs the worst, indicating difficulties in accurately identifying this high-risk class. The nv class, on the other hand, does well with an F1-score of 0.90 despite having the most samples. The model's overall accuracy across all 376 samples is 92%. At roughly 0.93 and 0.92, respectively, the weighted average and macro average measures show balanced performance across both common and less frequent classes.

Table 4. Classification Report Summary.

Class	Precision	Recall	F1-score
akiec	1.00	0.96	0.99
bcc	0.99	0.98	0.99
bkl	0.98	0.99	0.98
df	1.00	1.00	1.00
mel	0.99	0.99	0.99
nv	0.987	0.99	0.90
vasc	1.00	1.00	1.00
Accuracy			0.9970
Macro avg	1.00	1.00	1.00
Weighted avg	1.00	1.00	1.00

The classification model's performance evaluation is displayed in Figure 5. The Confusion Matrix Analysis, shown in Subfigure (a), shows how well the model categorizes each type of lesion. The model achieves near-perfect precision and recall, performing exceptionally well on classes like akiec, df, and vasc. Strong classification performance is also demonstrated by classes like bcc and nv, which score highly on all metrics. Conversely, classes bkl and mel have relatively lower F1-scores, indicating some challenges that are most likely brought on by class overlap or a lack of data. The model can distinguish between classes with high AUC values, particularly for akiec, df, and vasc, as demonstrated by the AUC and ROC curve analysis in Subfigure (b). The model's 92% overall accuracy, which represents balanced performance across common and unusual classes, is supported by consistent macro and weighted average scores. These results validate the resilience of the approach, especially in detecting important lesion types.

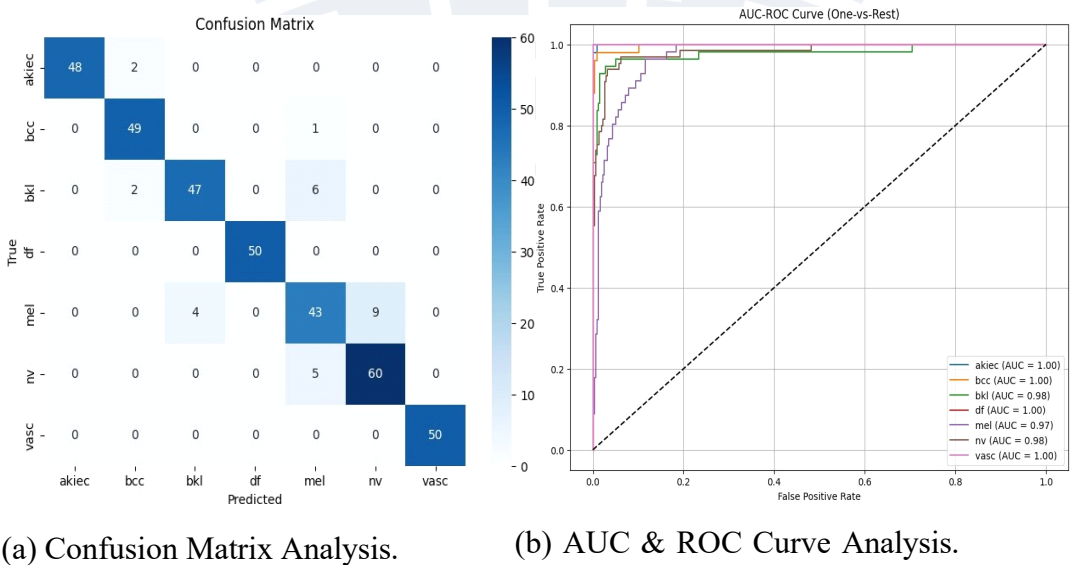(a) Confusion Matrix Analysis.   (b) AUC & ROC Curve Analysis.

Figure 5. Confusion matrix and AUC-ROC curve analyses of the classification model.

The Figure 6, shows the results from the Web-based Skin Cancer Detection System using EfficientNetB0. Test Result 1 indicates a diagnosis of Benign Keratosis, a non-cancerous skin condition. Test

Result 2 reveals the presence of Melanoma, a serious form of skin cancer that requires immediate medical attention.
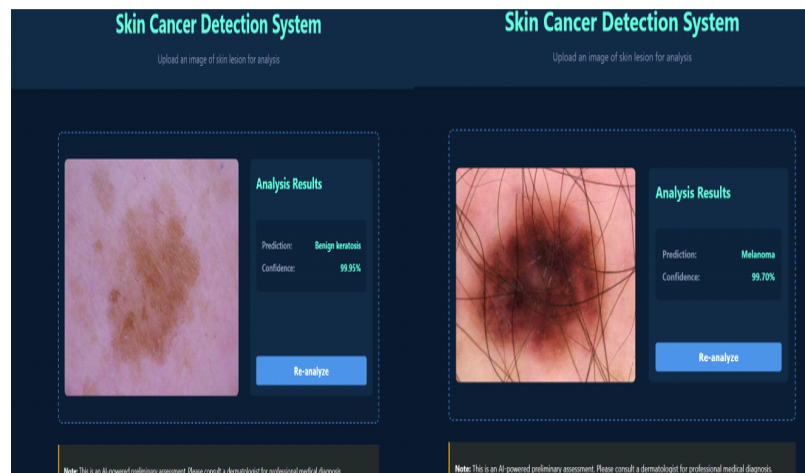
(a) Test Result 1: Benign Keratosis   (b) Test Result 2: Melanoma

Figure 6. Web-based Skin Cancer Detection System using EfficientNetB0.

V.   Conclusions

Since skin cancer is still one of the most prevalent and fatal malignancies worldwide, early and accurate detection is essential for effective treatment. Interest in automated diagnosis tools has increased because traditional diagnostic techniques are sometimes time-consuming and heavily reliant on specialized knowledge. Deep learning, especially convolutional neural networks (CNNs), has shown great potential in medical picture processing. EfficientNet is a modern CNN framework that is notable for striking the perfect balance between computational efficiency and accuracy. This study investigates the use of the EfficientNet-B0 architecture for accurate multi-class skin cancer classification using dermoscopic images. In order to enhance model performance, the study applies data balancing and transfer learning techniques to the HAM10000 dataset before fine-tuning the entire network. With a 92.29% classification accuracy, the proposed model demonstrated a significant improvement. Additionally, test-time augmentation and Monte Carlo Dropout were employed to enhance the model's generalization and reliability. Because of its lightweight design, EfficientNet-B0 is a promising option for deployment in real-time clinical situations with limited processing resources. The study's findings demonstrate how deep CNN-based techniques might support prompt and precise skin lesion identification, enhancing patient outcomes and treatment strategies. Future work may explore integrating this approach into clinical workflows to support derma- tologists and reduce diagnostic workloads, thereby contributing to the advancement of AI-assisted medical imaging.

VI.   References

[1]   Ashfaq, N., Suhail, Z., Khalid, A., et al. 2025. SkinSight: advancing deep learning for skin cancer diagnosis and classification. *Discovery Computing* 28: 63.

[2]   Kavitha, C., Priyanka, S., Praveen Kumar, M., Kusuma, V. 2024. Skin Cancer Detection and Classification using Deep Learning Techniques. *Procedia Computer Science* 235: 2793–2802.

[3]   Naeem, A., Farooq, M. S., Khelifi, A., & Abid, A. 2020. Malignant Melanoma Classification Using Deep Learning: Datasets, Performance Measurements, Challenges and Opportunities. *IEEE Access* 8: 110575– 110597.

[4]   Balaha, H. M., & Hassan, A. E. S. 2023. Skin cancer diagnosis based on deep transfer learning and sparrow search algorithm. *Neural Computing & Applications* 35: 815–853.

[5]   Alotaibi, A., & AlSaeed, D. 2025. Skin Cancer Detection Using Transfer Learning and Deep Attention Mechanisms. *Diagnostics* 15: 99.

[6]   Djaroudib, K., Lorenz, P., Belkacem Bouzida, R., & Merzougui, H. 2024. Skin Cancer Diagnosis Using VGG16 and Transfer Learning: Analyzing the Effects of Data Quality over Quantity on Model Efficiency. *Applied Sciences* 14: 7447.

[7]   Nazari, S., & Garcia, R. 2023. Automatic Skin Cancer Detection Using Clinical Images: A Comprehensive Review. *Life* 13(11): 2123.

[8]   Naqvi, M., Gilani, S. Q., Syed, T., Marques, O., & Kim, H.-C. 2023. Skin Cancer Detection Using Deep Learning—A Review. *Diagnostics* 13: 1911.

[9]   Naseri, H., & Safaei, A. A. 2025. Diagnosis and prognosis of melanoma from dermoscopy images using machine learning and deep learning: a systematic literature review. *BMC Cancer* 25: 75.

[10]   Magalhaes, C., Mendes, J., & Vardasca, R. 2024. Systematic Review of Deep Learning Techniques in Skin Cancer Detection. *BioMedInformatics* 4: 2251–2270.

[11]   Imran, A., Nasir, A., Bilal, M., Sun, G., Alzahrani, A., & Almuhaimeed, A. 2022. Skin Cancer Detection Using Combined Decision of Deep Learners. *IEEE Access* 10: 118198–118212.

[12]   Moturi, D., Surapaneni, R. K., & Avanigadda, V. S. G. 2024. Developing an efficient method for melanoma detection using CNN techniques. *Journal of the Egyptian National Cancer Institute* 36: 6.

[13]   Kreouzi, M., Theodorakis, N., Feretzakis, G., Paxinou, E., Sakagianni, A., Kalles, D., Anastasiou, A., Verykios, V. S., & Nikolaou, M. 2025. Deep Learning for Melanoma Detection: A Deep Learning Approach to Differentiating Malignant Melanoma from Benign Melanocytic Nevi. *Cancers* 17: 28.

[14]   Tahir, M., Naeem, A., Malik, H., Tanveer, J., Naqvi, R. A., & Lee, S.-W. 2023. DSCC_Net: Multi-Classification Deep Learning Models for Diagnosing of Skin Cancer Using Dermoscopic Images. *Cancers* 15: 2179.

[15]   Naeem, A., Anees, T., Khalil, M., Zahra, K., Naqvi, R. A., & Lee, S.-W. 2024. SNC_Net: Skin Cancer Detection by Integrating Handcrafted and Deep Learning-Based Features Using Dermoscopy Images. *Mathematics* 12: 1030.

[16]   Zia Ur Rehman, M., Ahmed, F., Alsuhibany, S. A., Jamal, S. S., Zulfiqar Ali, M., & Ahmad, J. 2022. Classifica- tion of Skin Cancer Lesions Using Explainable Deep Learning. *Sensors* 22: 6915.

[17]   Karki, R., G C, S., Rezazadeh, J., & Khan, A. 2025. Deep Learning for Early Skin Cancer Detec- tion: Combining Segmentation, Augmentation, and Transfer Learning. *Big Data Cogn. Comput.* 9: 97. https://doi.org/10.3390/bdcc9040097.

[18] Gouda, W., Sama, N. U., Al-Waakid, G., Humayun, M., & Jhanjhi, N. Z. 2022. Detection of Skin Cancer Based on Skin Lesion Images Using Deep Learning. *Healthcare* 10: 1183. https://doi.org/10.3390/healthcare10071183.

[19] Natha, P., & Rajeswari, P. R. 2023. Skin Cancer Detection using Machine Learning Classification Models. *International Journal of Intelligent Systems and Applications in Engineering* 12(6s): 139–145. https://ijisae.org/index.php/IJISAE/article/view/3966.

[20] Das, S., Kumar, V., & Cicceri, G. 2024. Chatbot Enable Brain Cancer Prediction Using Convolutional Neural Network for Smart Healthcare. In *Healthcare-Driven Intelligent Computing Paradigms to Secure Futuristic Smart Cities* (pp. 268–279). Chapman and Hall/CRC.

[21] Ashafuddula, N. I. M., & Islam, R. 2023. Melanoma skin cancer and nevus mole classifica- tion using intensity value estimation with convolutional neural network. *Computer Science* 24(3). https://doi.org/10.7494/csci.2023.24.3.4844.

[22] Rashad, N. M., Abdelnapi, N. M., Seddik, A. F., et al. 2025. Automating skin cancer screening: a deep learning. *J. Eng. Appl. Sci.* 72: 6. https://doi.org/10.1186/s44147-024-00573-w.

High Precision Distance Vector Hop Localization Algorithm for Wireless Sensor Networks

[1]Mohammed Aboud Kadhim, [2]Kamal Y. Kamal

Middle Technical University,
Baghdad, Iraq

Abstract—Internet of Things (IoT) systems require localization for the nodes within Wireless Sensor Networks (WSNs) for many location-based services. Since thousands of sensor nodes would exist in some networks, having GPS on each node is impractical, not merely due to the hardware cost, but also because of the poor performance indoors. Localization is now recognized as a crucial area for study. The research presented in this paper puts forward a half-measure weighted centroid DV-Hop localization algorithm. The proposed algorithm adjusts the locations of unknown nodes using redundant information obtained from localization equations. Simulation of sensor networks yielded significant improvements in accuracy and reduced error rates in localization estimation, while maintaining low hardware and computational costs.

Index Terms—DV-Hop, WSN, IoT, localization.

I. INTRODUCTION

Wireless Sensor Networks (WSNs) are utilized for various applications, and among the significant challenges for WSNs is the physical localization of nodes; sufficient localization is required for position-based WSN applications, such as target tracking, path planning, event detection, and data routing [1], [2]. Localization algorithms are usually implemented to determine the physical coordinates of sensor nodes within a WSN. One of the many localization solutions for wireless sensor networks is the Distance Vector Hop (DV-Hop) algorithm. Its cost-effectiveness and ease have made it extremely popular [3]. However, the DV-Hop algorithm suffers from inherent errors in distance estimation; thus, researchers have developed various enhancements to improve the DV-Hop algorithm's ability to determine node positions [4]. Some add gadgets that measure distance or antennas that point in specific directions [5]. Others use machine learning to make networks learn on their own [6], [7], [8]. Such approaches involve processing complex computations, which introduce overheads that may not always be compatible with wireless networks that have limited computational resources. The DV-Hop, as a decentralized range-free localization algorithm, was initially proposed by Niculescu et al. [9] and has garnered significant attention due to its ease of use and minimal hardware constraints for sensor nodes within a WSN. Conversely, the algorithm has the disadvantage of measuring hop distances rather than straight-line distances, which results in higher range error rates. Li et al. focused on adjusting the shortest distance of "zigzag" paths using geometric topographies, but did not take into account the density distribution of the nodes [10]. Tang et al. attempted to correct the average hop distance of the anchor nodes but did not address the error in estimating the positions of the unknown nodes [11]. Shahzad et al. eliminated some distant anchors that are away from unknown nodes to ease the computation process, but ignored some anchors' useful information [12]. Cai et al. tried to improve accuracy through a weight model but overlooked the weight-error relation [13].

II. BACKGROUND

Localization in wireless networks represents an important area of research in which localization algorithms consider each sensor node in the affected environment as a physical landmark. Some position-based applications require location-related information from sensor nodes to determine an accurate position.

Sometimes, sensor nodes operate in remote and harsh environments, such as disaster relief areas and forests; in these cases, traditional location tracking methods and simple sensor node localization approaches may not yield a feasible solution. Therefore, efficient localization methods are adapted to provide accurate positional information for the sensor nodes. Data aggregation strategies also require the positional information of the sensor nodes, and the collected data from various sensors would be useless if accurate information on the sensor nodes is not available. Localization is a process by which sensor nodes can determine their locations. Cyber-physical systems, eHealth, environmental monitoring, indoor automation, automated path planning, and weather forecasting are examples of the vast range of applications that require location-based services [14], [15]. Global positioning systems (GPS) are widely used to determine the locations of nodes; however, they incur a high cost in terms of power consumption, and their performance is also known to be poor indoors. Over the past decade, the scientific community has recognized the importance of this topic, leading to a substantial amount of research in this field. Localization is the process of determining the position of a node within a network of sensors. When the node's positions are unknown, connectivity information is utilized to determine the localization of the unknown nodes. Localization techniques can be classified into two basic categories: "Target or Source Localization" and "Node or Self Localization". Target/Source localization is further localized into "Single-Target Localization" and "Multiple-Target Localization".

On the other hand, "Node/Self Localization" is further classified into "Range-Based Localization" and "Range-Free Localization". Furthermore, "Range-Based Localization" is subclassified into more specific algorithms, such as "Connectivity", "Centroid", "Energy", and "Region Overlap" localization algorithms. The "Range-Based" localization algorithms use distance measurement techniques to calculate the location of unknown nodes; alternatively, "Range-Free" localization algorithms use the contents of the messages rather than measuring the proximity in terms of hop count or estimated distance to landmarking sensor nodes with known locations [16], "cooperative" localization techniques which require the existence of communication among all nodes [17], and "Non-Cooperative" localization techniques, where the unknown nodes communicate only with the anchor nodes [18], "Centralized" localization technique, which is also known as "Network-Centric Positioning", and "Distributed" localization technique, which is also known as "self-positioning" where no central management for the determination of the nodes' position; instead, each node estimates its location based on its local information [19]. Recent studies have investigated the mobility effects on localization [20], [21], [22], "Anchor-Based" and "Anchor-Free" localization [23], [24]. The methods used to estimate the location of sensor nodes are: The "Range-Based Localization" algorithms usually adopt one of the following techniques to measure a distance: "Angle of Arrival (AOA)", "Time Difference of Arrival (TDOA)", or "Received Signal Strength Indicator (RSSI)". The "Range-Free Localization" algorithms do not measure distance or angle among nodes. These algorithms can be divided into "Local/Pattern-Match" and "Hop-Count" localization techniques.

The DV-Hop is a range-free algorithm that estimates the distance between sensor nodes based on the hop count; it goes through three steps: 1) counting the minimum number of hops between the unknown node and the anchor; 2) estimate the distance from anchors to the unknown node by multiplying the minimum number of hops and the average distance per hop. and 3) determining the unknown node's coordinates mostly based the trilateration method or probability evaluation [31], [32], [33], [34], [35]. Many researchers have conducted extensive studies on improving the DV-Hop algorithm [25], [26], [27], [28], [29], [30]. Some research has focused on optimizing steps (1 and 2) of the DV-Hop algorithm; for example, Li et al. optimized the minimum number of hops by setting two communication radii and increasing the communication radius (R) [36]. Gui et al. proposed a medium access control (MAC) method based on the "Chinese residual set (CRT)" protocol sequence to localize DV-Hops [37]. Kaur et al. developed the "Enhanced Weighted Centroid DV-Hop (EWCL)" algorithm to address the issues of poor accuracy and excessive power consumption. The transmission radius determined the EWCL algorithm's weighting factor, average hop distance, and hop count [38]. Other scientists have also optimized step (3) of DV-Hop. Recently, due to the impressive performance of intelligent computing on complex optimization problems, several nature-inspired schemes have been introduced [13], [39]. For example, Zhou et al. optimized DV-Hop based on bacterial foraging optimization (BFO) [40]. Kaur et al. optimized DV-Hop algorithm based on the "Gray-Wolf" optimization for 2D and 3D WSNs environments [41]. Song et al. applied "Firefly Swarm Optimization" algorithm [42] with a chaotic

inertial weight update [43]. Cui et al. proposed the CS-DV-Hop algorithm [44], a hybrid DV-Hop algorithm that combines the "Cuckoo Search" optimization algorithm [45]. Wang et al. proposed an improved DV-Hop algorithm based on both BFO and glow-worm swarm optimization (GSO), thus it is called "BFO-GSO." This approach has proven to have a convergence speed; however, its computing time has increased slightly compared to merely BFO [46].

III. HD-DV-Hop Algorithm

The half-distance DV-Hop routing protocol is the decentralized range-free localization approach utilized by the DV-Hop localization method. The essential idea involves determining the distances between signal and obscure hubs by replicating the typical hop distance in WSNs, with the bounce considered a fundamental part of reference point hubs. Three mathematical techniques are typically used to determine a receiver's position (en) from signals received from multiple transmitters: triangulation, trilateration, and multilateration. When employing the DV-Hop algorithm, localization errors may occur because paths between beacons and unknown nodes may not be direct in a network with randomly positioned wireless sensor nodes. Moreover, the more hops there are, the larger the accumulated errors are. In the initial step, each anchor hub conveys its coordinates as a reference point to the other nodes within the network, containing the anchor's area with a hop count of one. Each hub tracks the base bounce count per anchor for all signals it receives. Reference points with higher hop count values associated with a specific anchor are considered outdated and will be disregarded. Then, those not flat guides overflowed outward, with bounce count values augmented at each middle-of-the-road hop. Through this component, all hubs in the organization get a negligible bounce build-up to each secure hub. In the next phase, when an anchor receives hop counts from various anchors, it calculates an average hop size and shares it with the entire network. Nodes without visual information use the hop size multiplied by the hop count to calculate the distance from the anchor. The average hop size to an anchor i is estimated as:

$$H_{HopSize} = \frac{\sum_{j=1}^{J}(x_i - x_j)^2 + (y_i - y_j)^2}{\sum_{j=1}^{J} h_{ij}} \tag{1}$$

Where (x_i, y_i), (x_j, y_j) are coordinates of anchor i and anchor j, h_{ij} denotes the hops between beacons i and j. Each anchor node transmits the information about its hop size to the network using "controlled flooding". Unknown nodes receive hop size data and save the first one; they also transmit their hop size to neighboring nodes. This method enables nodes to receive the hop size from the beacon node with the minimum number of hops. Ultimately, the unknown nodes determine the distance to beacon nodes based on the hop lengths to those beacon nodes.

Each anchor node shares its hop size with the network during controlled flooding. When an unknown hub gets this hop-size data, it stores it first and then passes it to its adjoining hubs. This method ensures that most nodes get the hop size from the beacon node with the fewest hops to them. As a result, based on the hop lengths to the beacon nodes, unknown nodes ultimately establish the distances to the beacon nodes.

Let (x, y) denote the unknown coordinates of node D, (x_i, y_i) are the known coordinates of the ith receiver anchor node, and i^{th} anchor node distance to node D is d_i, then we can compute the unknown coordinates of node D as:

$$\begin{cases} (x - x_1)^2 + (y - y_1)^2 = d_1^2 \\ (x - x_2)^2 + (y - y_2)^2 = d_2^2 \\ \quad\quad\quad \vdots \\ (x - x_i)^2 + (y - y_i)^2 = d_i^2 \end{cases} \tag{2}$$

The coordinates are computed as:

$$A = -2 \times \begin{bmatrix} x_1 - x_n & y_1 - y_n \\ x_2 - x_n & y_2 - y_n \\ \vdots & \vdots \\ x_{n-1} - x_n & y_{n-1} - y_n \end{bmatrix} \tag{3}$$

$$B = \begin{bmatrix} d_1^2 - d_n^2 - x_1^2 + x_n^2 - y_1^2 + y_n^2 \\ d_2^2 - d_n^2 - x_2^2 + x_n^2 - y_2^2 + y_n^2 \\ \vdots \\ d_{n-1}^2 - d_n^2 - x_{n-1}^2 + x_n^2 - y_{n-1}^2 + y_n^2 \end{bmatrix} \tag{4}$$

$$P = \begin{bmatrix} x \\ y \end{bmatrix} \tag{5}$$

Where: $P = (A^T A)^{-1} A^T B$

HD-DV-Hop Algorithm

Inputs:

- Set of anchor nodes A = {a1, a2, ..., an}
- Set of unknown nodes U = {u1, u2, ..., um}
- Location coordinates of anchor nodes (x_a, y_a) for a ∈ A

Output:

- Estimated location coordinates (x_u, y_u) for u ∈ U

Initialization:

For each anchor node a ∈ A:
  Broadcast the location coordinates (x_a, y_a)
for each unknown node u ∈ U:
  Calculate hop count to each anchor node h(u, a)

Distance Estimation:

for each anchor node a ∈ A:
  Sum_dist = 0
  Sum_hops = 0
  for each anchor node b ∈ A, b ≠ a:
    Sum_dist += distance((x_a, y_a), (x_b, y_b))
    Sum_hops += h(a, b)
  HopSize(a) = Sum_dist / Sum_hops

Coordinate Estimation:

```
  for each unknown node u ∈ U:
    Distance_estimates = []
    for each anchor node a ∈ A:
      Estimated_distance = h(u, a) × HopSize(a)
      Distance_estimates.append(Estimated_distance)
    (x_u, y_u) = Multilateration(Distance_estimates, anchor_locations)
Refinement (Optional):
  while stopping criteria not met:
    for each unknown node u ∈ U with estimated coordinates (x_u, y_u):
      Treat u as a pseudo-anchor node
      Broadcast (x_u, y_u) to other nodes
    Repeat Distance Estimation and Coordinate Estimation steps
    for the remaining unknown nodes using pseudo-anchor nodes
Return estimated coordinates (x_u, y_u) for all u ∈ U
```

Explanation:

Initialization: Anchor nodes broadcast their location coordinates, and unknown nodes calculate their hop counts to each anchor node.

Distance Estimation: For each anchor node, the average hop distance (HopSize) is calculated by dividing the sum of distances between the anchor node and other anchor nodes by the sum of their respective hop counts.

Coordinate Estimation: For each unknown node, the estimated distance from each anchor node is calculated by multiplying the hop count to that anchor node with the corresponding average hop distance (HopSize). Using these estimated distances and the known locations of anchor nodes, the unknown node's coordinates are calculated using a multilateration technique, such as the least-squares method.

Refinement (Optional): In this optional step, the algorithm can be iteratively refined by treating the unknown nodes with estimated coordinates as pseudo-anchor nodes. The Distance Estimation and Coordinate Estimation steps are repeated for the remaining unknown nodes, using both the pseudo-anchor nodes and the original anchor nodes.

The algorithm continues to refine the coordinates until a stopping criterion is met, such as a maximum number of iterations or a desired accuracy threshold.

IV. SIMULATION AND DATA ANALYSIS

In this section, we compare and analyze the outcomes at a system level; the simulation was carried out with MATLAB software to assess the sufficiency of the proposed algorithm, in terms of efficiency and suitability. We randomly distributed 100 wireless sensor nodes within a 100 m x 100 m square; 60 nodes are unknown, 40 of which are beacons.. The half-weighted centroid shapes the premise of the organization geography utilized by the DV-Hop bounce confinement calculation. The estimated distances between the unknown and the beacon nodes were calculated by multiplying the least hop distance by the average hop distance between the two nodes. The communication radius of the nodes plays a significant role in determining the minimum amount of hops between nodes. Node locations also vary depending on the hop distances between communication radii. The correspondence range is more modest, and the geography is nearer to the actual area, which has higher hub densities, as shown in Figures 1-10. By optimizing the network's topology, network longevity can also be extended, and energy consumption can decrease.

We compared the localization errors of the proposed algorithm over an identical communication radius (R = 100 m). The DV-Hop algorithm's node localization error (e) fluctuated between 15 and 60. In contrast, the proposed algorithm's error rate ranged between 2 and 15, so it is more precise, mainly attributed to the increasing radiuses of unknown nodes, which reduced the minimum communication radius, as illustrated in Figures (10-20).
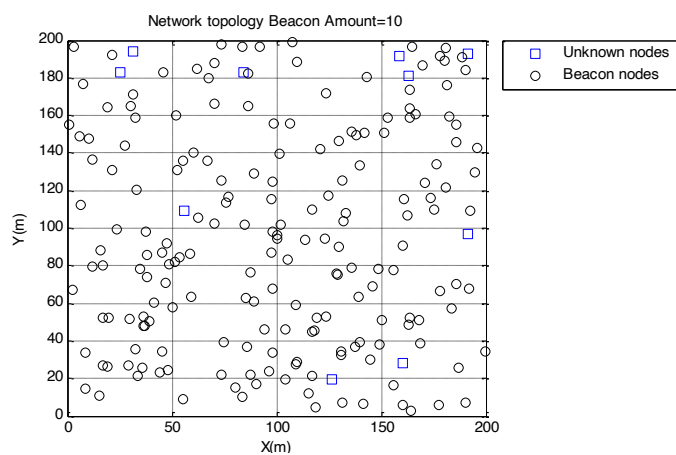
Figure (1): Network topology (10 Beacons)
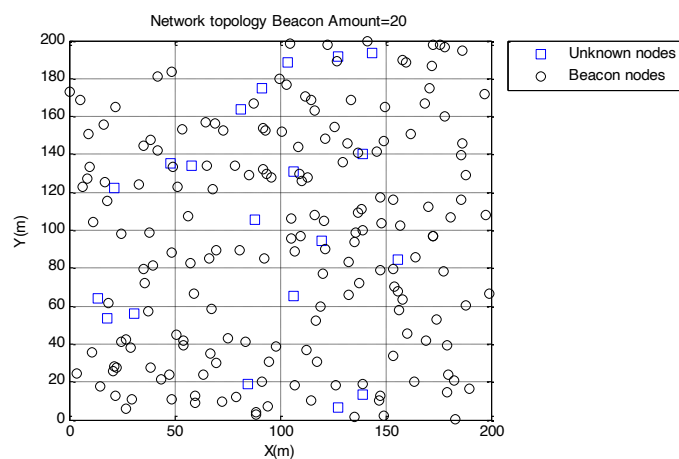
Figure (2): Network topology (20 Beacons)
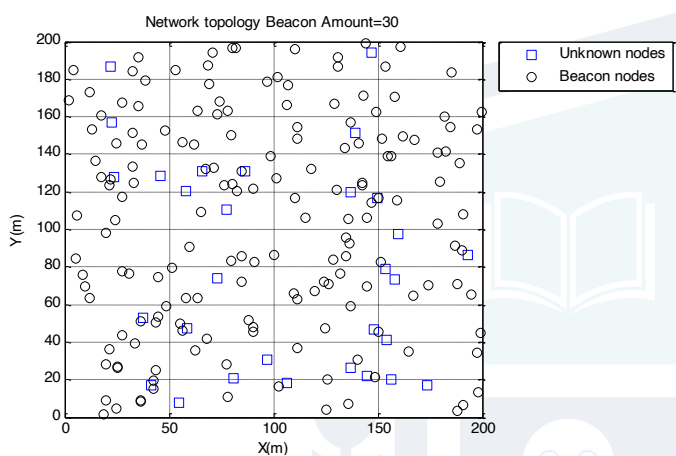
Figure (3): Network topology (30 Beacons)
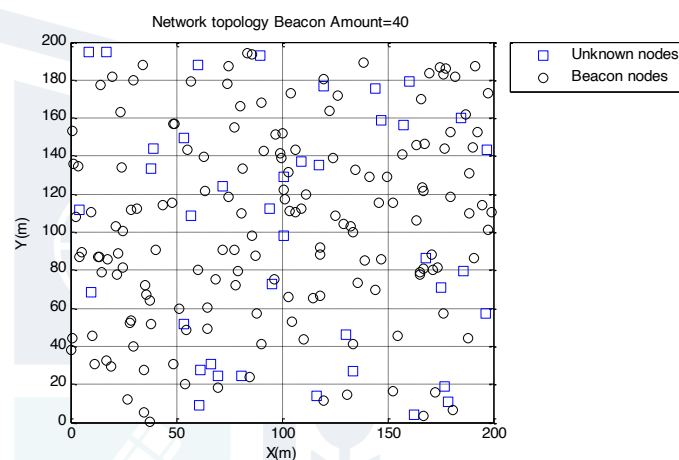
Figure (4): Network topology (40 Beacons)
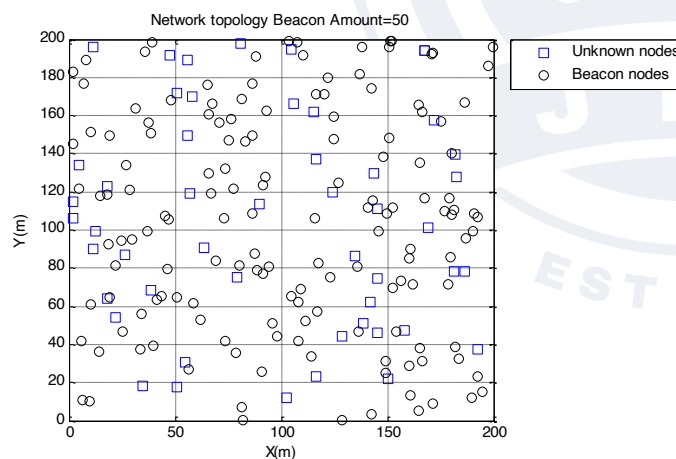
Figure (5): Network topology (50 Beacons)
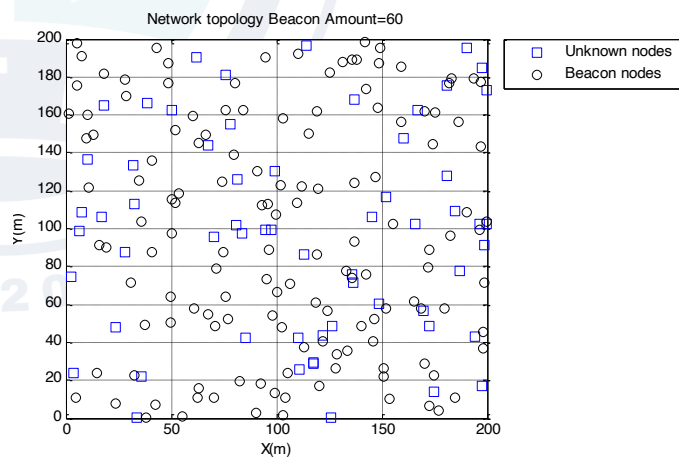
Figure (6): Network topology (60 Beacons)
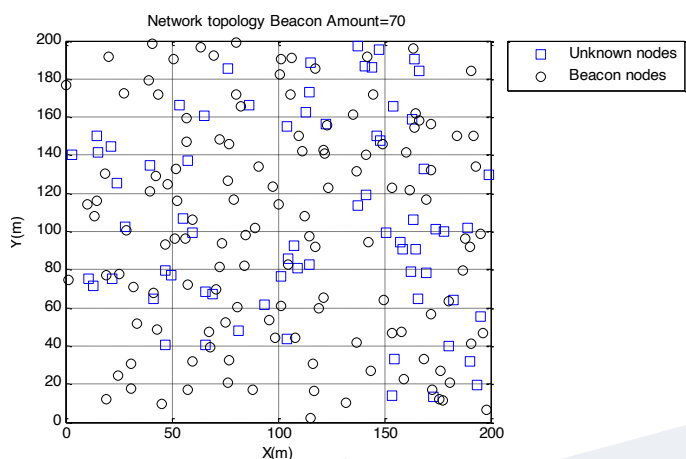
Figure（7）: Network topology（70 Beacons）
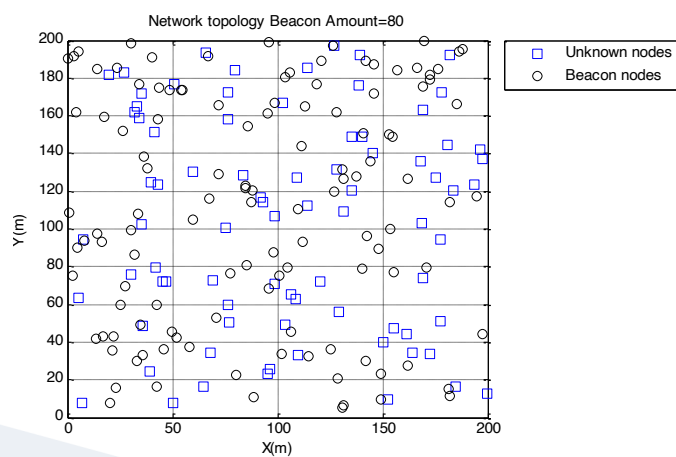
Figure（8）Network topology（80 Beacons）
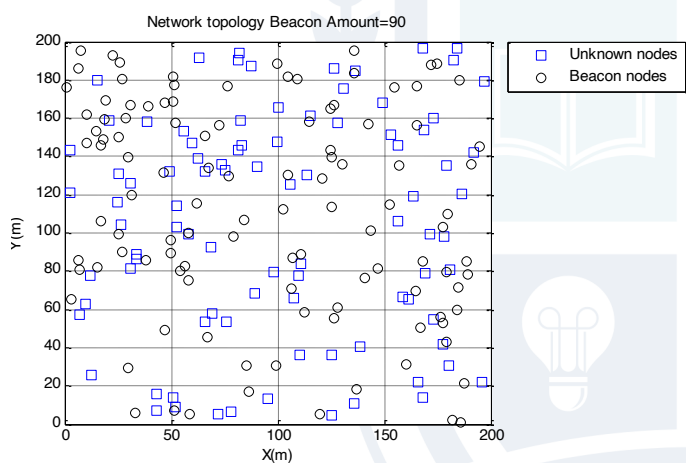
Figure（9）: Network topology（90 Beacons）
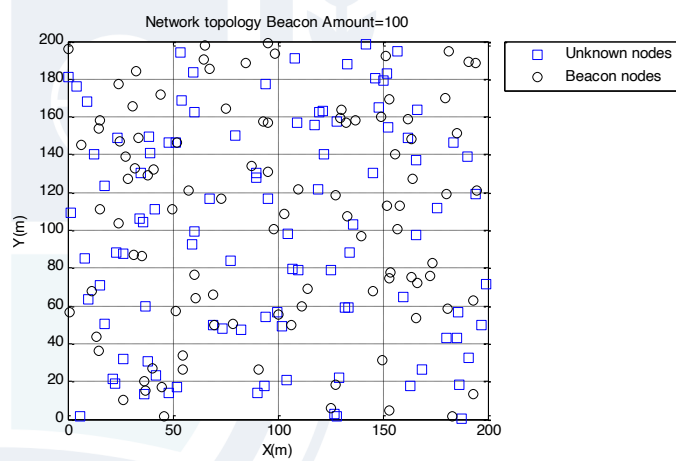
Figure（10）: Network topology（100 Beacons）
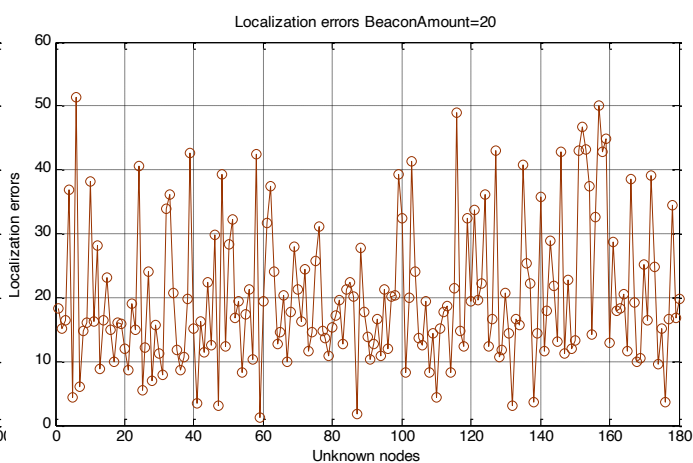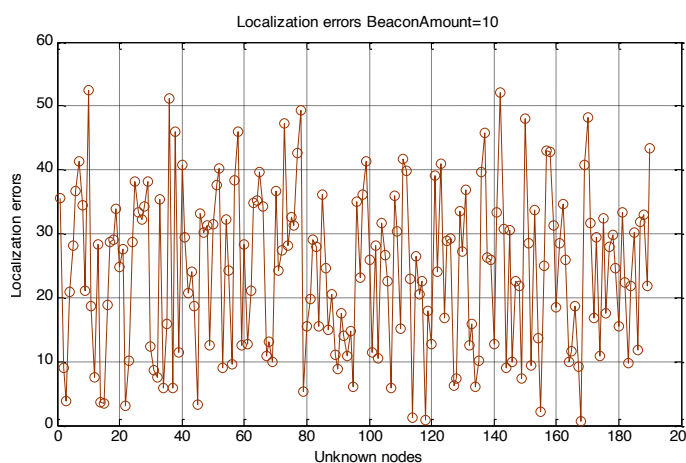
Figure (11): Localization errors (10 Beacons)
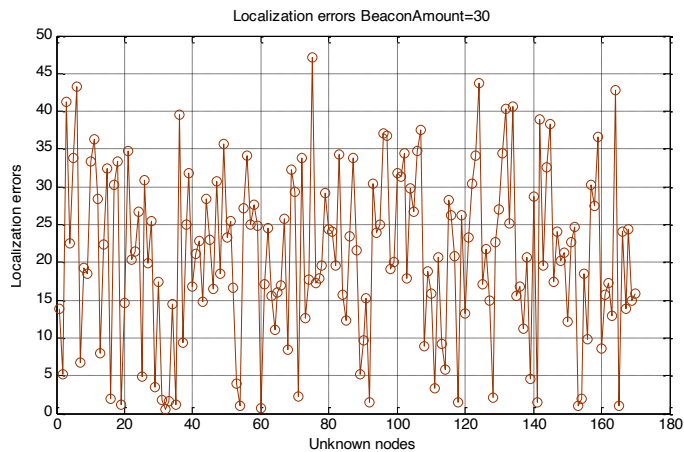
Figure (12): Localization errors over communication radius (20 Beacons)
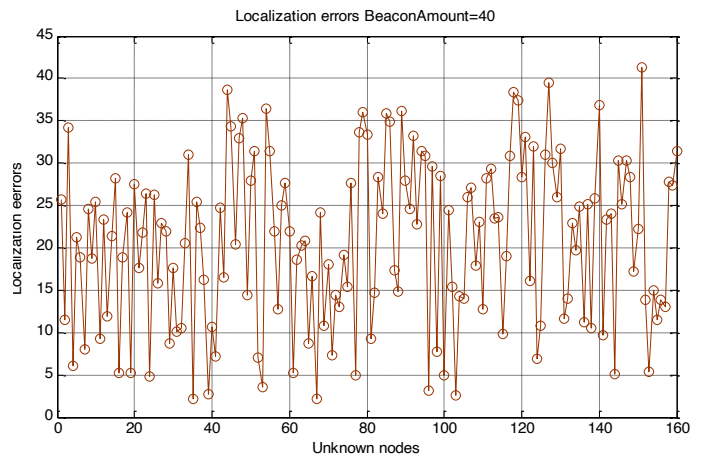
Figure (13): Localization errors over communication radius (30 Beacons)
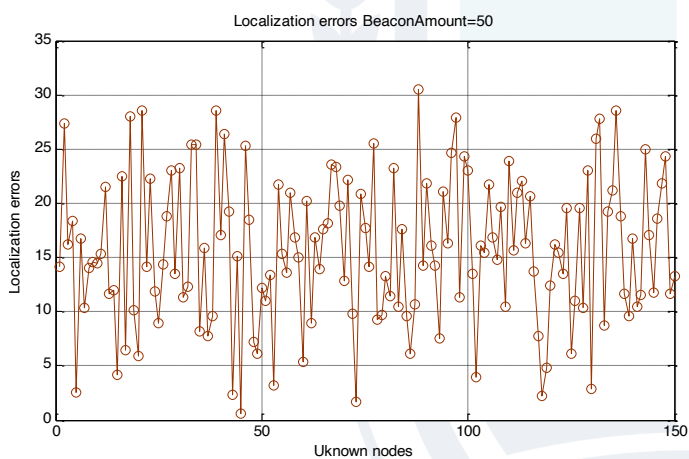
Figure (14): Localization errors over communication radius (40 Beacons)
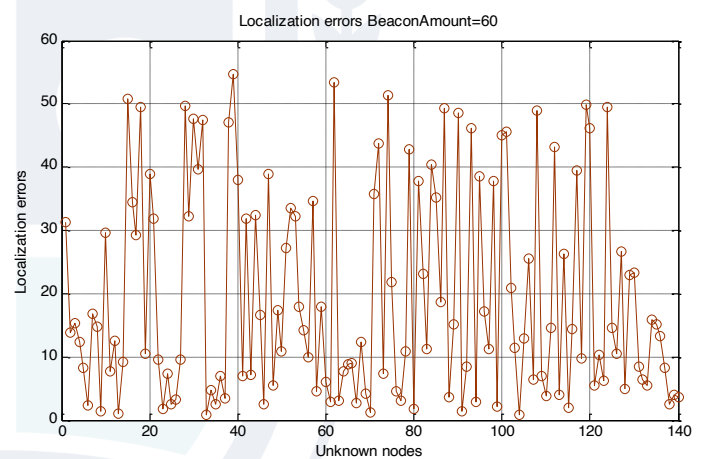
Figure (15): Localization errors over communication radius (50 Beacons)
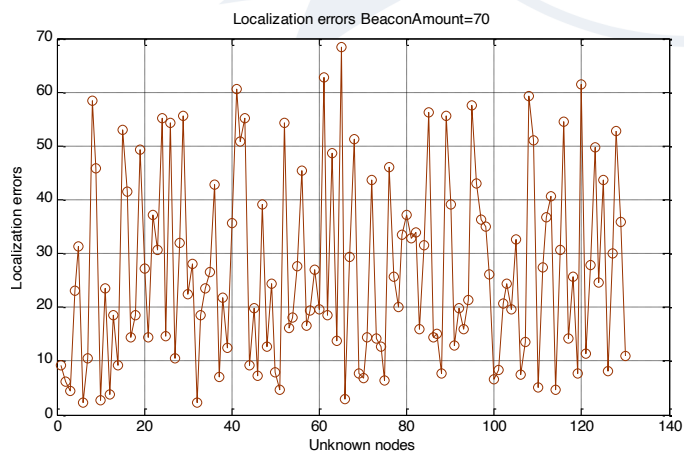
Figure (16): Localization errors over communication radius (60 Beacons)
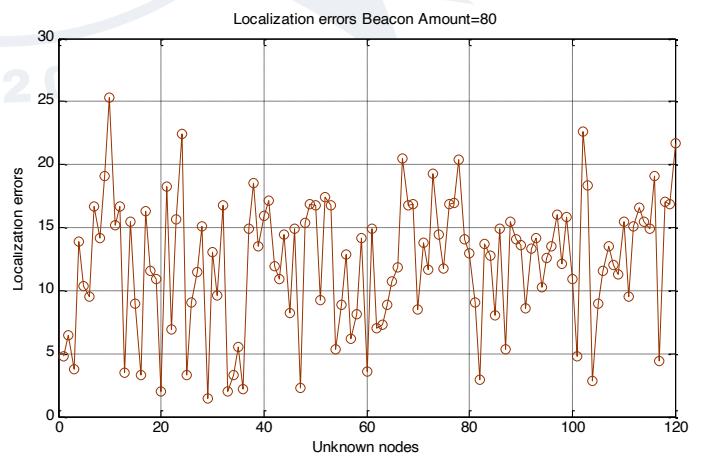
Figure (17): Localization errors over communication radius (70 Beacons)

Figure (18): Localization errors over communication radius (80 Beacons)
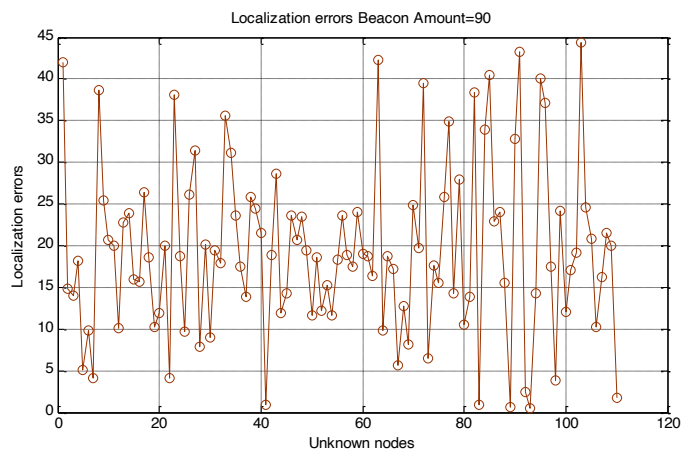
Figure (19): Localization errors over communication radius (90 Beacons)   Figure (20): Localization errors over communication radius (100 Beacons)
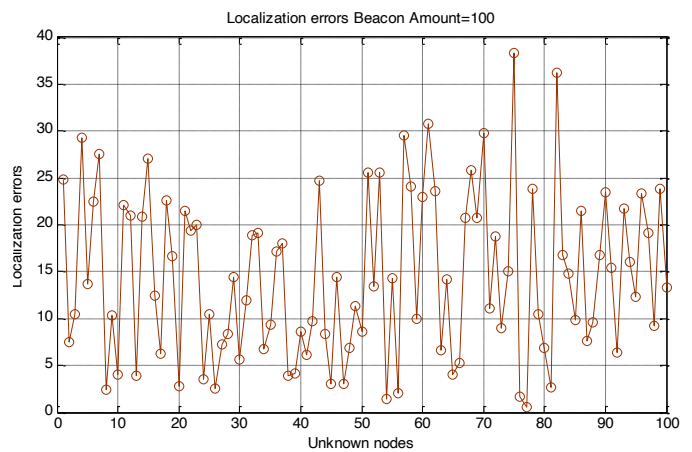
V. CONCLUSION

An enhancement algorithm for WSNs localization was proposed half-measure weighted centroid DV-Hop algorithm, where the uneven distribution of nodes, holes, and errors in the average hop distance was simulated. The new algorithm used a cutting-edge localization strategy by adding a half-measure weighted centroid with the DV-Hop algorithm. Beacon nodes use the centroid algorithm to determine their location, and the DV-Hop localized accuracy is then used as the weight for locating unknown nodes. The enhanced localization algorithm decreased localization error and increased the localization accuracy of unknown nodes. The simulation outcomes indicate that a higher location coverage and a lower error rate are associated with more frequently placed beacons. In the application scenario, anchor nodes can be manually placed, and location performance can be enhanced. Since the study was conducted in a perfect network simulation environment, future research will be required to examine how the enhanced algorithm might be used in less typical network environments.

REFERENCES

[1] G. Pettorru, V. Pilloni, and M. Martalò, "Trustworthy Localization in IoT Networks: A Survey of Localization Techniques, Threats, and Mitigation," *Sensors*, vol. 24, no. 7, Art. no. 7, Jan. 2024, doi: 10.3390/s24072214.

[2] W. Liu, G. Wei, and M. Zhu, "A survey on multi-dimensional path planning method for mobile anchor node localization in wireless sensor networks," *Ad Hoc Networks*, vol. 156, p. 103416, Apr. 2024, doi: 10.1016/j.adhoc.2024.103416.

[3] J. Ren, P. Qi, C. Li, P. Zhu, and Z. Li, "Multisource sparse inversion localization with long-distance mobile sensors," *Electronics*, vol. 13, no. 6, Art. no. 6, Jan. 2024, doi: 10.3390/electronics13061024.

[4] V. C. S. R. Rayavarapu and A. Mahapatro, "MOANS DV-Hop: An anchor node subset based localization algorithm for wireless sensor networks," *Ad Hoc Networks*, vol. 152, p. 103323, 2024.

[5] Y. Hu and X. Li, "An improvement of DV-hop localization algorithm for wireless sensor networks," *Telecommun Syst*, vol. 53, no. 1, pp. 13–18, May 2013, doi: 10.1007/s11235-013-9671-8.

[6] H. Lee, C. Wu, and H. Aghajan, "Vision-based user-centric light control for smart environments," *Pervasive and Mobile Computing*, vol. 7, no. 2, pp. 223–240, Apr. 2011, doi: 10.1016/j.pmcj.2010.08.003.

[7] P. Yadav and S. C. Sharma, "An efficient optimal localization technique for WSN using hybrid machine learning algorithms," *Wireless Pers Commun*, vol. 133, no. 4, pp. 2601–2639, Dec. 2023, doi: 10.1007/s11277-024-10892-z.

[8] "Intelligent wireless sensing driven metaverse: A survey," *Computer Communications*, vol. 214, pp. 46–56, Jan. 2024, doi: 10.1016/j.comcom.2023.11.024.

[9] M. Li and Y. Liu, "Rendered path: range-free localization in anisotropic sensor networks with holes," in *Proceedings of the 13th annual ACM international conference on Mobile computing and networking*, in MobiCom '07. New York, NY, USA: Association for Computing Machinery, Sep. 2007, pp. 51–62. doi: 10.1145/1287853.1287861.

[10] Q. Tang and J. Wang, "An improved DV-Hop localization algorithm for wireless sensor network based on TDOA quantization," in *2017 International Conference on Network and Information Systems for Computers (ICNISC)*, Apr. 2017, pp. 19–24. doi: 10.1109/ICNISC.2017.00013.

[11] F. Shahzad, T. R. Sheltami, and E. M. Shakshuki, "DV-maxHop: A Fast and accurate range-free localization algorithm for anisotropic wireless networks," *IEEE Transactions on Mobile Computing*, vol. 16, no. 9, pp. 2494–2505, Sep. 2017, doi: 10.1109/TMC.2016.2632715.

[12] X. Cai, H. Wang, Z. Cui, J. Cai, Y. Xue, and L. Wang, "Bat algorithm with triangle-flipping strategy for numerical optimization," *Int. J. Mach. Learn. & Cyber.*, vol. 9, no. 2, pp. 199–215, Feb. 2018, doi: 10.1007/s13042-017-0739-8.

[13] C. Wu, Z. Yang, and Y. Liu, "Smartphones based crowdsourcing for indoor localization," *IEEE Transactions on Mobile Computing*, vol. 14, no. 2, pp. 444–457, Feb. 2015, doi: 10.1109/TMC.2014.2320254.

[14] M. Wang and C. Huang, "Mobile anchor node assisted node collaborative localization based on light reflection in WSN," *Wireless Netw*, vol. 30, no. 4, pp. 2801–2818, May 2024, doi: 10.1007/s11276-024-03701-9.

[15] Y. V. Lakshmi, P. Singh, S. Mahajan, A. Nayyar, and M. Abouhawwash, "Accurate range-free localization with hybrid DV-hop algorithms based on PSO for UWB wireless sensor networks," *Arab J Sci Eng*, vol. 49, no. 3, pp. 4157–4178, Mar. 2024, doi: 10.1007/s13369-023-08287-6.

[16] H. Wymeersch, J. Lien, and M. Z. Win, "Cooperative localization in wireless networks," *Proceedings of the IEEE*, vol. 97, no. 2, pp. 427–450, Feb. 2009, doi: 10.1109/JPROC.2008.2008853.

[17] S. Tomic, M. Beko, and R. Dinis, "RSS-based localization in wireless sensor networks using convex relaxation: noncooperative and cooperative schemes," *IEEE Transactions on Vehicular Technology*, vol. 64, no. 5, pp. 2037–2050, May 2015, doi: 10.1109/TVT.2014.2334397.

[18] A. Kaushik *et al.*, "Toward integrated sensing and communications for 6G: Key enabling technologies, standardization, and challenges," *IEEE Communications Standards Magazine*, vol. 8, no. 2, pp. 52–59, Jun. 2024, doi: 10.1109/MCOMSTD.0007.2300043.

[19] X. Wang, Y. Liu, Z. Yang, K. Lu, and J. Luo, "Robust component-based localizationin sparse networks," *IEEE Transactions on Parallel and Distributed Systems*, vol. 25, no. 5, pp. 1317–1327, May 2014, doi: 10.1109/TPDS.2013.85.

[20] S. Salari, S. Shahbazpanahi, and K. Ozdemir, "Mobility-aided wireless sensor network localization via semidefinite programming," *IEEE Transactions on Wireless Communications*, vol. 12, no. 12, pp. 5966–5978, Dec. 2013, doi: 10.1109/TWC.2013.110813.120379.

[21] B.-F. Wu and C.-L. Jen, "Particle-filter-based radio localization for mobile robots in the environments with low-density wlan aps," *IEEE Transactions on Industrial Electronics*, vol. 61, no. 12, pp. 6860–6870, Dec. 2014, doi: 10.1109/TIE.2014.2327553.

[22] N. Zaarour, N. Hakem, and N. Kandil, "An accurate anchor-free contextual received signal strength approach localization in a wireless sensor network," *Sensors*, vol. 24, no. 4, Art. no. 4, Jan. 2024, doi: 10.3390/s24041210.

[23] R. N. Biswas, A. Saha, S. K. Mitra, and M. K. Naskar, "Design and implementation of anchor coprocessor architecture for wireless node localization applications," *Peer-to-Peer Netw. Appl.*, vol. 17, no. 2, pp. 961–984, Mar. 2024, doi: 10.1007/s12083-024-01640-y.

[24] F. Thomas and L. Ros, "Revisiting trilateration for robot localization," *IEEE Trans. Robot.*, vol. 21, no. 1, pp. 93–101, Feb. 2005, doi: 10.1109/TRO.2004.833793.

[25] J. Li, X. Yue, J. Chen, and F. Deng, "A novel robust trilateration method applied to ultra-wide bandwidth location systems," *Sensors*, vol. 17, no. 4, Art. no. 4, Apr. 2017, doi: 10.3390/s17040795.

[26] A. E. M. El Ashry and B. I. Sheta, "Wi-Fi based indoor localization using trilateration and fingerprinting methods," *IOP Conf. Ser.: Mater. Sci. Eng.*, vol. 610, no. 1, p. 012072, Sep. 2019, doi: 10.1088/1757-899X/610/1/012072.

[27] T. Yang, A. Cabani, and H. Chafouk, "A survey of recent indoor localization scenarios and methodologies," *Sensors (Basel)*, vol. 21, no. 23, p. 8086, Dec. 2021, doi: 10.3390/s21238086.

[28] Q. Luo, K. Yang, X. Yan, J. Li, C. Wang, and Z. Zhou, "An improved trilateration positioning algorithm with anchor node combination and K-Means clustering," *Sensors (Basel)*, vol. 22, no. 16, p. 6085, Aug. 2022, doi: 10.3390/s22166085.

[29] Y. Cao and Z. Wang, "Improved DV-hop localization algorithm based on dynamic anchor node set for wireless sensor networks," *IEEE Access*, vol. 7, pp. 124876–124890, 2019, doi: 10.1109/ACCESS.2019.2938558.

[30] G. Li, S. Zhao, J. Wu, C. Li, and Y. Liu, "DV-hop localization algorithm based on minimum mean square error in Internet of Things," *Procedia Computer Science*, vol. 147, pp. 458–462, Jan. 2019, doi: 10.1016/j.procs.2019.01.272.

[31] G. Song and D. Tam, "Two novel DV-hop localization algorithms for randomly deployed wireless sensor networks," *International Journal of Distributed Sensor Networks*, vol. 11, no. 7, p. 187670, Jul. 2015, doi: 10.1155/2015/187670.

[32] X. Li, K. Wang, B. Liu, J. Xiao, and S. Han, "An improved range-free location algorithm for industrial wireless sensor networks," *J Wireless Com Network*, vol. 2020, no. 1, p. 81, Apr. 2020, doi: 10.1186/s13638-020-01698-1.

[33] W. Yu and H. Li, "An improved DV-Hop localization method in Wireless Sensor Networks," in *2012 IEEE International Conference on Computer Science and Automation Engineering (CSAE)*, May 2012, pp. 199–202. doi: 10.1109/CSAE.2012.6272938.

[34] D. Prashar, K. Jyoti, and D. Kumar, "Design and analysis of distance error correction–based localization algorithm for wireless sensor networks," *Transactions on Emerging Telecommunications Technologies*, vol. 29, no. 12, p. e3547, 2018, doi: 10.1002/ett.3547.

[35] T. Li, C. Wang, and Q. Na, "Research on DV-Hop improved algorithm based on dual communication radius," *J Wireless Com Network*, vol. 2020, no. 1, p. 113, Jun. 2020, doi: 10.1186/s13638-020-01711-7.

[36] L. Gui *et al.*, "DV-Hop Localization with protocol sequence based access," *IEEE Transactions on Vehicular Technology*, vol. 67, no. 10, pp. 9972–9982, Oct. 2018, doi: 10.1109/TVT.2018.2864270.

[37] A. Kaur, P. Kumar, and G. P. Gupta, "A weighted centroid localization algorithm for randomly deployed wireless sensor networks," *Journal of King Saud University - Computer and Information Sciences*, vol. 31, no. 1, pp. 82–91, Jan. 2019, doi: 10.1016/j.jksuci.2017.01.007.

[38] Z. Cui, F. Li, and W. Zhang, "Bat algorithm with principal component analysis," *Int. J. Mach. Learn. & Cyber.*, vol. 10, no. 3, pp. 603–622, Mar. 2019, doi: 10.1007/s13042-018-0888-4.

[39] "DV-Hop localization algorithm based on bacterial foraging optimization for wireless multimedia sensor networks | Multimedia Tools and Applications." Accessed: Jun. 11, 2024. [Online]. Available: https://link.springer.com/article/10.1007/s11042-018-5674-5

[40] A. Kaur, P. Kumar, and G. P. Gupta, "Nature inspired algorithm-based improved variants of DV-Hop algorithm for randomly deployed 2D and 3D wireless sensor networks," *Wireless Pers Commun*, vol. 101, no. 1, pp. 567–582, Jul. 2018, doi: 10.1007/s11277-018-5704-7.

[41] X.-S. Yang, *Nature-Inspired Metaheuristic Algorithms*, 2nd Ed. Frome, United Kingdom: Luniver Press, 2010.

[42] L. Song, L. Zhao, and J. Ye, "DV-Hop node location algorithm based on GSO in wireless sensor networks," *Journal of Sensors*, vol. 2019, no. 1, p. 2986954, 2019, doi: 10.1155/2019/2986954.

[43] Z. Cui, B. Sun, G. Wang, Y. Xue, and J. Chen, "A novel oriented cuckoo search algorithm to improve DV-Hop performance for cyber–physical systems," *Journal of Parallel and Distributed Computing*, vol. 103, pp. 42–52, May 2017, doi: 10.1016/j.jpdc.2016.10.011.

[44] X.-S. Yang and S. Deb, "Cuckoo search via Lévy flights," in *Proceedings of the 2009 World Congress on Nature & Biologically Inspired Computing (NaBIC)*, Coimbatore, India: IEEE, Dec. 2009, pp. 210–214. doi: 10.1109/NABIC.2009.5393690.

[45] Y. Wang, P. Wang, J. Zhang, X. Cai, W. Li, and Y. Ma, "A novel DV-Hop method based on coupling algorithm used for wireless sensor network localisation," *International Journal of Wireless and Mobile Computing*, vol. 16, no. 2, pp. 128–137, Jan. 2019, doi: 10.1504/IJWMC.2019.099027.

A Study on the Consumer Behaviour Towards the Solar Energy Devices in Rajakkad Grama Panchayath, Idukki District

Dr. Asha T Jacob

Associate Professor, P.G. Department of commerce,

Govt. Arts and Science College, Santhanpara

Abstract: Solar energy is radiant light and heat from the sun that is harness using a range of ever- evolving technologies such as solar heating, photovoltaic, solar thermal energy, solar thermal energy, solar architecture, molten salt power plants and artificial photosynthesis. Solar energy is a highly delectable source of electricity.This study aims to study the awareness and satisfaction level of customers towards the solar energy device available in the market and the attitude towards the products. The study also focuses the various factors that influence the customers to choose the solar energy devices over electrical devices even they are comparatively cheap. The study of customer's behavior towards the acceptance of solar energy product with special reference to Rajakkad grama panchayath of idukki district , Kerala state is relevant because the study will help for future development of the area and place a major role for determining the standard of living and economic growth of people there and the benefits and problems of rural people by installing the solar energy products. This study found that most of the respondents monthly income lies between Rs.10000 to Rs.20000 and have their own house to live..Most of the respondents are non- governmental employees and entrepreneurs and get information about solar energy devices from mobile phone and installed hot water and photovoltaic solar energy devices.Majority of the respondents think that renewable source of energy is the main attractive factor about solar energy devices and use them for less than one year.Majority of the respondents reason for choosing solar device is cost saving and are satisfied with their usage.Though majority of the respondents facing problem of solar devices usage at night, they are satisfied with solar energy devices reducing electricity bills.The highest agreement is for solar energy being a reliable power source in Rajakkad Grama panchayath of Idukki district.

Key words: Key drivers of customer satisfaction, factors influencing the adoption of solar energy devices, marketing strategies of solar products

1.1 INTRODUCTION

Solar energy is radiant light and heat from the sun that is harness using a range of ever- evolving technologies such as solar heating, photovoltaic, solar thermal energy, solar thermal energy, solar architecture, molten salt power plants and artificial photosynthesis. Solar energy is a highly delectable source of electricity. Solar system is mainly used as the collecting and storing device of energy from the wide source. Using solar panel or photovoltaic cell the solar energy should be converted to electrical energy can be used for both residential and industrial purposes. The technique of capturing and distributing solar energy is broadly classified into two, active solar and passive solar. Active solar are the technology including the use of photovoltaic system, concentrated solar power and solar water heating to harness the energy. Passive solar technology includes orienting a building to the sun. Nowadays solar sector is the most excellent felid for investment. There may be so many researches are to be conducted with the special consideration of Government funds and so many industries are turned to manufacture and distribute the solar devices. The manufacturers such as Tata, Luminous, Goodson, etc. with the view to Electricity Conservation. And, so many other companies are put forward to manufacture variety of quality solar devices which are suitable to both residential and industrial purpose. In this study an attempt was made to evaluate the consumer behavior towards the acceptance

of solar energy devices with special reference to Rajakkad gramapanchayath of Idukki district.

1.2 SIGNIFICANCE OF THE STUDY

The research aims to study the awareness and satisfaction level of customers towards the solar energy device available in the market and the attitude towards the products. The study also focuses the various factors that influence the customers to choose the solar energy devices over electrical devices even they are comparatively cheap. The study of customer's behavior towards the acceptance of solar energy product with special reference to Rajakkad grama panchayath of idukki district , Kerala state is relevant because the study will help for future development of the area and place a major role for determining the standard of living and economic growth of people there and the benefits and problems of rural people by installing the solar energy products.

1.3 OBJECTIVES OF THE STUDY

1. To identify customers' attitude towards solar products along with the factors influencing the adoption of solar energy devices.
2. To identify the key drivers of customer satisfaction in solar energy devices and the marketing strategies of solar products.

1.4 HYPOTHIESES OF THE STUDY

H_{01}: There is no significant difference in the attitude of respondent towards solar energy devices based on their age.

H_{02}: There is no significant relationship between the education level of the respondent and the factors influencing their decision regarding solar energy devices.

H_{03}: Income has no significant influence on the satisfaction of respondents towards the marketing strategies of solar products.

H_{04}: There is no significant difference in the satisfaction of respondents based on their years of use of solar products.

1.5 SCOPE OF THE STUDY

The scope of this study is focused on exploring the various factors that influence the adoption and acceptance of solar energy products within a specific rural context along with the attitudes, perceptions, and decision-making processes of consumers with particular emphasis on understanding how social, economic, cultural, and technological factors shape their views on solar energy. The geographical scope of this study is confined to Rajakkad grama Panchayath, a rural locality in the Idukki district of Kerala, which offers a unique setting due to its blend of rural characteristics and increasing exposure to renewable energy technologies. It will also explore the factors influencing the adoption of solar energy devices, including financial considerations (e.g., upfront costs, government subsidies, and savings), environmental concerns (e.g., reducing carbon footprints), social influences, and the perceived reliability and efficiency of the technology. Furthermore, the study will assess the impact of marketing strategies employed by solar companies and the government to encourage solar adoption. Another significant aspect of the study is to identify the key drivers of customer satisfaction in the context of solar energy adoption.

1.6 RESEARCH METHODOLOGY

Research methodology is a systematic way to solve the research problem. It may be understood as science of studying how research is done scientifically.

1.6.1 Sources of data

The data needed for the study are collected from primary and secondary sources. **Primary data**:

Primary data was collected from the respondents through questionnaire. **Secondary data**: Secondary data was collected from various journals, articles, books, websites, and other publications.

1.6.2 Population of the study

The population of study consisted of the residents of Rajakkad Grama Panchayath, including both households that have adopted solar energy devices and those that have not.

1.6.3 Sampling method

Convenient sampling technique was used to collect data. **1.6.4 Sample size**

Sample size was limited to 60 .

1.6.5 Research design

The study was descriptive and inferential in nature.

1.6.6 Period of the study

The study was conducted for a period of 3 months .

1.6.7 Tools used for analysis

The data has been collected, arranged, analyzed, and interpreted using appropriate statistical and mathematical tools like percentage, average and inferential statistical tools like ANOVA using SPSS (Statistical Package for Social Science).

1.7 LIMITATIONS OF THE STUDY

- Geographical Limitation: The study is focused only on Rajakkad Panchayath, so the findings may not apply to other regions.
- Sample Size: The sample size may be small, limiting the ability to generalize the results to the entire population.
- Self-Reported Data: The data relies on participants' responses, which might be biased or inaccurate.
- Short-Term Study: The study looks at current consumer behavior, not long-term trends or changes over time.
- Limited Variables: The study may not consider all possible factors influencing solar energy adoption, such as political or technological influences.
- Participation Challenges: The study depends on the willingness of local people to participate, and low participation could affect the findings.
- Bias in Responses: Consumers who already use solar devices may give overly positive feedback, affecting the balance of opinions.
- Lack of Detailed Financial Data: The study may have limited access to specific cost or financial information about solar adoption.
- Time Constraints: Limited time may prevent exploring all factors influencing solar energy adoption in detail.

1.8 CHAPTERISATION

The project report is arranged in three chapters as;

Chapter 1. Introduction

Chapter 2. Data Analysis and Interpretation

Chapter 3. Findings, Suggestions and Conclusion

CHAPTER 2   DATA ANALYSIS   AND INTERPRETATION

This chapter presents the analysis of the data collected using questionnaire. The data was analyzed using Statistical Package of Social Science (SPSS) such data was presented using tables and figures for easy understanding.

Table 2.1 Age of the respondents

Age (in years)	Frequency	Percent
Below 30	30	50.0
30 – 40	18	30.0
40 – 50	9	15.0
Above 50	3	5.0
Total	**60**	**100.0**

 Source: Primary data

 From the above table ,it is found that half of the respondents are in the age group of below 30, and the 30 percent are of 30-40 age group, 15 percent are in the age group of 40-50, and the rest of the 5 percent are in the age group of above 50 years.

 Table 2.2 Highest Educational Qualification of the respondents

Highest Education	Frequency	Percent
10th	2	3.3
Plus-Two	9	15.0
Graduation	31	51.7
Post Graduation	16	26.7
Others	2	3.3
Total	**60**	**100.0**

 Source: Primary data

 From the above table it is clear that educational qualification of 51.7 percent respondents are Graduates,26.3 percent of the respondents are Post Graduates,15percent of the respondents are Plus- Two,3.3percent of the respondents are 10th and others each. Monthly income of the respondents

Figure 2.1 Monthly income of the respondents
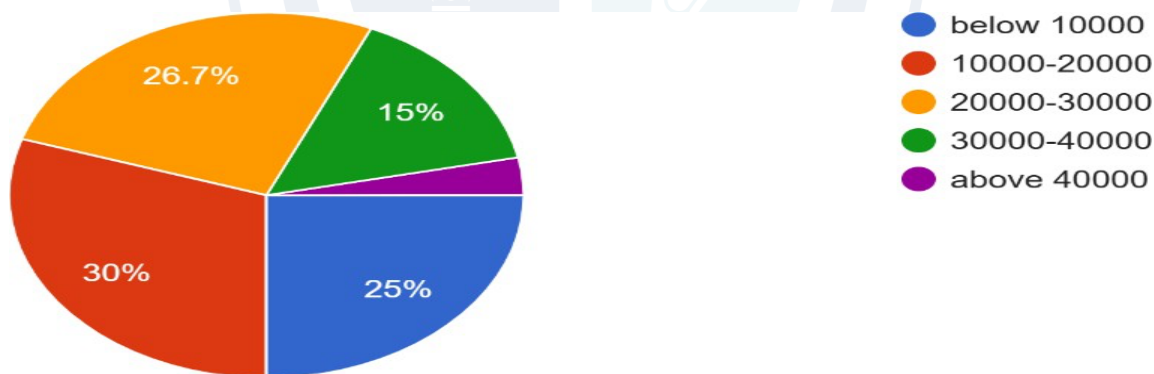
From the above figure, it is discovered that 30 percent of the respondents are in the monthly income group of 10000 – 20000, 26.7 percent of the respondents are in the group of 20000 – 30000, 25 percent of the respondents are in the group of below 10000 15 percent of the respondents are in the group of 30000 – 40000 and the rest 3.3percent are the group of above 40000.

 Table 2.3 Residential status of the respondents

Classification	Frequency	Percent
Own House	47	78.3
Rental House	13	21.7
Total	**60**	**100.0**

Source: Primary Data

From the above table is clear that 78.3 percent of the respondents have Own House, while 21.7 percent have Rental House only**.**

Table 2.4 Profession of the Respondents

Classification	Frequency	Percent
Government Employee	1	1.7
Non-Government Employee	20	33.3
Entrepreneur	19	31.7
Others	20	33.3
Total	60	100.0

Source: Primary Data

The above table showed that one-third of the respondents each are non-government employees and others , 31percent are entrepreneur and rest 1.7 percent are government employees .

Figure 2.2 Kind of solar device installed
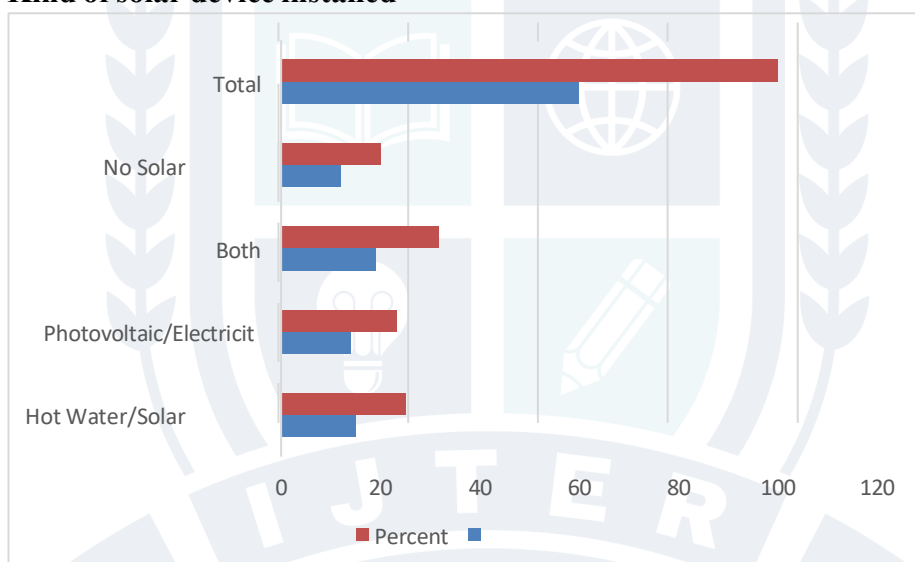
From the above figure it is depicted that 31percent of the respondents have in use of both Electricity and Solar Thermal devices, while 25 percent have only Solar Thermal and 23.3 percent have use only Electricity devices.

Table 2.5 Source from which Respondents get the information about solar energy devices

Classification	Frequency	Percent
Television	19	31.7
Mobile Phone	20	33.3
Family and Friends	9	15.0
Colleagues	12	20.0
Total	**60**	**100.0**

Source: Primary Data

From the above table it is found that one -third of the respondents are get the information about solar energy devices from mobile phone and 31.7 percent of the respondents are get the information from television, 20 percent of the respondents are get the information from colleagues and last 15 percent of the respondents are get the information from family and friends.

Table 2 6 Factors influencing the choice of solar energy device

Classification	Frequency	Percent
Low pollution	12	20.0
Renewable source of energy	30	50.0
Environmentally friendly	16	26.7
Others	2	3.3
Total	**60**	**100.0**

Source: Primary Data

From the above table it is clear that half of the respondents, most influencing factor for election of solar energy device is renewable source of energy, 26.7percent of respondents attracted by environmentally friendly factor, other 20 percent of respondents attracted by low pollution and 3.3percent of the respondents are attracted by other factors.

Table 2.7 Respondents' year of using solar energy devices

Year	Frequency	Percent
Less than 1 year	20	33.3
1-3 years	14	23.3
3-5 years	18	30.0
Above 5 years	2	3.3
Never use	6	10.0
Total	**60**	**100**

Source: Primary Data

From the above table it is clear that 30 percent of respondents using solar energy devices in between 3-5 years, 33.3 percent of the respondents are using less than 1 year,23.3percent of respondents are using solar energy devices 1-3 years,10 percent of the respondents are never used solar energy devices and 3.3percent of the respondents used more than 5 years.

Table 2.8 Respondents' satisfaction level with the solar energy devices

Classification	Frequency	Percentage
Highly satisfied	10	16.7
Satisfied	34	56.7
Neutral	12	20.0
Dissatisfied	4	6.7
Total	**60**	**100**

Source: Primary Data

From the above table it is clear that 5 6 . 6 percent of the respondents are satisfied with solar energy devices ,20 percent respondents are neutral ,16.7percent are highly satisfied and 6.7percent of respondents are dissatisfied with solar energy devices.

Table 2.9 Respondents' reason for choosing solar energy devices

Classification	Frequency	Percent
Energy saving	13	21.7
Cost saving	30	50.0
Easy installation	11	18.3
No power failure	6	10.0

Total	**60**	**100**

Source: Primary Data

From the above table it is crystal clear that half of the respondents are choosing solar energy devices because of cost saving, distantly followed by 21.7percent by energy saving , 18.3 percent for easy installation and 10 percent because of no power failure.

Table 2.10 Factors that influence to purchase solar energy devices

Description	N	Mean	Std. Deviation
High initial cost of solar products discourages me from purchasing item	60	4.42	0.926
Government subsidies and financial incentive influence my decision to buy solar devices	60	4	0.759
I am influenced by the experience and recommendation of people	60	4.42	0.671
Strong after sale services and warranty would increase my confidence in purchase	60	4.45	0.832

Source: Primary Data

The data analysis reveals key factors influencing consumer behavior toward solar energy device adoption in Rajakkad Grama Panchayat. The high initial cost of solar products is the most significant barrier, with a mean score of 4.42, indicating that many consumers are discouraged by the upfront expense. However, government subsidies and financial incentives positively influence purchasing decisions (mean = 4.00). Additionally, peer recommendations and personal experiences play a strong role in influencing decisions, with a mean score of 4.42. The presence of after-sale services and warranties also increases consumer confidence (mean = 4.45), further encouraging adoption.

Table 2.11 The problem faced while using solar energy devices

Problem	Frequency	Percent
Space consumption	7	11.7
Maintenance cost	15	25.0
Usage at night	31	51.7
Limited storage capacity	7	11.7
Total	**60**	**100**

Source: Primary Data

The data indicated in the above table reflected that 51.7percent of the respondents are faced by problem of usage at night ,25 percent of the respondents faced by high maintenance cost and rest 11.7 percent of the respondents faced the problem of space consumption and limited storage capacity.

Table 2.12 Satisfaction level of respondents towards marketing strategies of solar energy device

Description	N	Minimum	Maximum	Mean	Std. Deviation

Advertisement and awareness campaign influence my perception of solar energy products	60	1	3	2.4	0.785
Social media and online reviews influence my decision to buy solar products	60	1	3	2.35	0.659
Seeing more people in my community using solar products would motivate me	60	1	3	2.37	0.736
I prefer to purchase solar energy products from a local supplier	60	1	3	2.33	0.681

Source: Primary Data

The above table showed the descriptive statistics indicate that various factors influence the adoption of solar energy products in Rajakkad Panchayath. The mean values, ranging from 2.33 to 2.40 on a scale of 1 to 3, suggest a generally positive inclination toward these factors. Advertisement and awareness campaigns (mean = 2.40) have the highest influence, highlighting the role of marketing in shaping perceptions. Social media (mean = 2.35) and community influence (mean = 2.37) also play crucial roles in decision-making. Preference for local suppliers (mean = 2.33) suggests trust in nearby vendors. The standard deviations indicate moderate variation in responses, suggesting diverse opinions.

Table 2.13 Level of satisfaction of respondents towards solar energy devices

Descriptive Statistics	N	Minimum	Maximum	Mean	Std. Deviation
Subsidies are high for solar products	60	2	5	4.0333	0.9382
They have low maintenance cost	60	2	5	3.55	0.9099
It reduces electricity bill	60	3	5	4.4167	0.72
It gives energy independence	60	2	5	3.8	0.6587
Power production only day time	60	1	5	3.5167	1.1273
Solar product is easily repairable	60	1	5	3.6833	0.9476
Solar product is safe to use	60	3	5	4.3667	0.7123

Source: Primary Data

The descriptive statistics indicate positive perceptions of solar energy products in Rajakkad Panchayath. The highest mean score (4.42) is for electricity bill reduction, highlighting cost savings as a key motivator. Safety (mean = 4.37) and subsidies (mean = 4.03) also contribute to favourable opinions. Energy independence (mean = 3.80) and repairability (mean = 3.68) are moderately valued. However, concerns exist regarding maintenance costs (mean = 3.55) and power production being limited to daytime (mean = 3.52). The standard deviations show some variability in opinions, suggesting that while solar energy is well- received, addressing maintenance and efficiency concerns could boost adoption.

Table 2.14 Level of awareness on the availability of the solar products

Descriptive Statistics	N	Minimum	Maximum	Mean	Std. Deviation
Water heater	60	1	4	2.3333	0.837
Solar inverters	60	1	3	2.28	0.175
Garden light	60	1	3	2.02	0.833
Complete solar energy system for home	60	1	3	1.78	0.761
Solar cook stove	60	1	3	1.93	0.8
Solar mobile charger	60	1	3	2.02	0.77
Selling of solar energy	60	1	3	2.17	0.763
Valid N	60				

Source: Primary Data

The data reflects the popularity of different solar energy products in Rajakkad Panchayath. Among them, solar water heaters (mean = 2.33) and solar inverters (mean = 2.28) are the most preferred, likely due to their practical benefits in daily life. Selling solar energy (mean = 2.17) also holds some interest. However, products like solar garden lights (mean = 2.02), mobile chargers (mean = 2.02), and cook stoves (mean = 1.93) have lower demand, possibly due to limited awareness or usability concerns. The complete solar energy system (mean = 1.78) scores the lowest, suggesting high costs or installation challenges hinder full adoption.

2.15 TESTING OF HYPOTHESIS

HYPOTHESIS1

H_0: **There is no significant difference in the attitude of respondent towards solar energy devices based on their age.**
H1 : **There is a significant difference in the attitude of respondents towards solar energy devices based on their age.**

Table 2.15.1 ANOVA

	Sum of Squares	df	Mean Square	F	Sig.
Between Groups	3.661	3	1.22	3.166	0.031
Within groups	21.589	56	0.86		
Total	25.25	59			

Source: Primary Data

The ANOVA results indicated a statistically significant difference in respondents' attitudes toward solar energy devices based on age (F = 3.166, p = 0.031). Since the significance value (0.031) is less than 0.05, we reject the null hypothesis (H_0) and accept the alternative hypothesis (H_1). This suggests that age influences perceptions of solar energy benefits. The between-group variance (SS = 3.661, df = 3) is not able compared to the within-group variance (SS = 21.589, df = 56), meaning age groups have differing attitudes.

HYPOTHESIS 2

H_0 : **There is no significant relationship between the education level of the respondent and the factors influencing their decision regarding solar energy devices.**
H_1 : **There is significant relationship between the education level of the respondent and the factors influencing their decision regarding solar energy devices.**

Table 2.15.2 ANOVA					
	Sum of Squares	df	Mean Square	F	Sig.
Between Groups	1.646	4	0.411	2.059	0.099
Within Groups	10.991	55	0.2		
Total	12.639	59			

 Source: Primary Data

The above ANOVA results showed an F-value of 2.059 and a significance level (p-value) of 0.099. Since the p-value is greater than 0.05, we fail to reject the null hypothesis (H$_0$). indicating that the differences in education level do not lead to significant variations in decision- making factors. While there is some variation between groups (Sum of Squares = 1.646), it is not strong enough to be considered statistically significant.

HYPOTHESIS 3

H$_0$: Income has no significant influence on the satisfaction of respondents towards the marketing strategies of solar products.

H$_1$:Income has significant influence on the satisfaction of respondents towards the marketing strategies of solar products.

Table 2.15.3 ANOVA					
	Sum of Squares	df	Mean Square	F	Sig.
Between Groups	1.542	1	1.542	7.148	0.01
Within Groups	12.511	58	0.216		
Total	14.053	59			

Source: Primary Data

The ANOVA results indicate a significant relationship between income and satisfaction with solar product marketing strategies. The F-statistic (7.148) and p-value (.010) suggest that income levels significantly impact satisfaction since the p-value is below the 0.05 threshold. This leads to the rejection of the null hypothesis (H$_0$), meaning that income does influence satisfaction. The between-groups sum of squares (1.542) shows variation due to income differences, while the within-groups sum of squares (12.511) reflects individual variations. The mean square values further support that income accounts for a meaningful portion of satisfaction differences.

HYPOTHIESIS 4

H$_0$:There is no significant difference in the satisfaction of respondents based on their years of use of solar products.

H$_1$:There is significant difference in the satisfaction of respondents based on their years of use of solar products.

Table 2.15.4 ANOVA					
	Sum of Squares	df	Mean Square	F	Sig.
Between Groups	3.191	4	0.798	4.392	0.004
Within Groups	9.991	55	0.182		
Total	13.182	59			

Source: Primary Data

The ANOVA results indicate a statistically significant difference in satisfaction levels based on years of solar product usage. The F-value is 4.392, with a p-value (Sig.) of 0.004, which is below

the 0.05 threshold. This leads to rejecting the null hypothesis (H_0) and accepting the alternative hypothesis (H_1), confirming that satisfaction varies with years of solar energy use. The between-groups variance (Sum of Squares = 3.191, Mean Square = 0.798) is higher than within-groups variance (Sum of Squares = 9.991, Mean Square 0.182), further supporting the finding. Thus, experience with solar products influences satisfaction significantly.

CHAPTER 3: FINDINGS, SUGGESTIONS AND CONCLUSION

The chapter presents the finding based on the data analysis. Conclusions are based on findings and overall observation during the study. The chapter has divided into three sections findings suggestion and conclusion

3.1 FINDINGS

- Half of the respondents are aged below 30 years and their highest education qualification is graduation.
- Most of the respondents monthly income lies between Rs.10000 to Rs.20000.
- More than three fourth of the respondents have their own house to live.
- Most of the respondents are non- governmental employees and entrepreneurs and get information about solar energy devices from mobile phone.
- Most of the respondents installed hot water and photovoltaic solar energy devices.
- Majority of the respondents think that renewable source of energy is the main attractive factor about solar energy devices and use them for less than one year.
- Majority of the respondents reason for choosing solar device is cost saving and are satisfied with their usage.
- Though majority of the respondents facing problem of solar devices usage at night, they are satisfied with solar energy devices reducing electricity bills.
- The highest agreement is for solar energy being a reliable power source in Rajakkad Grama panchayath of Idukki district.

3.2 SUGGESTIONS

- Introduce government subsidies and financial incentives to reduce the initial cost of solar installation.

- Promote easy financing options, such as low-interest loans or instalment plans, to make solar energy more accessible.

- Conduct community awareness programs to educate people on the long-term benefits of solar energy and provide hands-on training sessions for potential users to understand maintenance and efficiency improvements..

- Partner with local influencers and entrepreneurs to share user experiences and success stories to build trust.

- Promote battery storage solutions to address the problem of solar energy usage at night.
- Encourage the development of high-efficiency panels and hybrid systems that can work even in low sunlight conditions.

- Ensure strong after-sales support including regular maintenance, warranty coverage, and quick issue resolution.

- Establish local service centres to provide immediate assistance to users.
- Create a certification program for solar installers to ensure quality and professionalism.
- Offer trial programs or leasing options to allow hesitant consumers to test solar solutions before making a full investment.

➢ Encourage satisfied customers to act as brand ambassadors to spread awareness through word-of-mouth recommendations.

5.1 <u>CONCLUSION</u>

The study on consumer behavior towards the acceptance of solar energy devices in Rajakkad Grama Panchayath provides valuable insights into the attitudes, preferences, and challenges faced by consumers. The findings reveal that a majority of respondents, primarily young and educated individuals, recognize the importance of renewable energy and are willing to adopt solar solutions. Most respondents installed solar devices for cost savings and environmental benefits, with hot water and photovoltaic systems being the most popular choices. However, despite a positive outlook, barriers such as high initial costs, lack of knowledge, and concerns over nighttime usage hinder widespread adoption. To enhance the adoption of solar energy devices, the study suggests financial incentives, community awareness programs, technological improvements, and better after-sales services. Strengthening government support, offering flexible financing, and ensuring easy maintenance solutions can significantly boost consumer confidence and increase solar energy adoption in the region leading to a sustainable and energy-efficient future.

<u>BIBLIOGRAPHY</u>

[1] Chopdawala, & Tasneem H. (2008). Consumer Buying Behavior – A Multivariate Study (PhD Thesis). Pune: University of Pune, 1986. 218.

[2] Kulkarni, R. (2016). An Analytical Study of The Causes Of Under Utilization Of Non- Conventional Energy Resources of Energy Systems and Its Marketing Potential In India.

[3] Rai, V., & McAndrews, K. (2012). Decision-making and behaviour change in residential adopters of solar PV. *Energy Policy, 68*, 286–300. https://doi.org/10.1016/j.enpol.2014.01.046.

[4] Zhao, J., Wang, Y., & Deng, S. (2017). Peer effects and social influence in solar energy adoption. *Energy Policy, 106*, 206–210. https://doi.org/10.1016/j.enpol.2017.03.038.

[5] Shen, W., Chan, H. K., & Xiong, D. (2020). A conceptual framework for understanding the adoption of solar photovoltaic systems in residential buildings. *Renewable and Sustainable Energy Reviews, 119*, 109599. https://doi.org/10.1016/j.rser.2019.109599.

[6] Jabeen, F., Irfan, M., & Ahmad, M. (2019). Perceived risks and adoption of solar energy: A consumer perspective. *Sustainability, 11*(18), 4984. https://doi.org/10.3390/su11184984.

[7] Kumar, S., & Managi, S. (2021). Brand trust and consumer choice in renewable energy technologies. *Journal of Cleaner Production, 281*, 125269. https://doi.org/10.1016/j.jclepro.2020.125269.

[8] Faires, A., & Neame, C. (2006). Consumer attitudes towards domestic solar power systems. *Energy Policy, 34*(14), 1797–1806. https://doi.org/10.1016/j.enpol.2005.01.001.

[9] Wüstenhagen, R., Wolsink, M., & Bürer, M. J. (2007). Social acceptance of renewable energy innovation: An introduction to the concept. *Energy Policy, 35*(5), 2683–2691. https://doi.org/10.1016/j.enpol.2006.12.001.

[10] Balcombe, P., Rigby, D., & Azapagic, A. (2014). Investigating the importance of consumer preferences in the uptake of low-carbon technologies. *Energy Policy, 72*, 210–218. https://doi.org/10.1016/j.enpol.2014.05.018.

[11] Sovacool, B. K., & Griffiths, S. (2020). Culture and behaviour in energy transitions: A review and analysis. *Energy Research & Social Science, 65*, 101446. https://doi.org/10.1016/j.erss.2020.101446.

[12] K. R. Raju et al. (2019) – Evaluated the feasibility of solar energy in Kerala, highlighting its potential for reducing greenhouse gas emissions and promoting sustainability.

[13] Raju, K. R., et al. (2019). Feasibility of solar energy in Kerala: A study on sustainable development

and emissions reduction. *Renewable Energy Journal,* 45(2), 112-125.

[14] S. S. Rao et al. (2020) – Analysed the performance of solar panels under Kerala's tropical climate, emphasizing efficiency improvements.

[15] Rao, S. S., et al. (2020). Performance analysis of solar panels in Kerala's climatic conditions. *Energy Efficiency Journal,* 12(3), 98-110.

[16] Kumar, A. K., et al. (2018). Economic viability of solar energy in rural Kerala: A cost-benefit analysis. *Journal of Sustainable Energy,* 9(1), 67-80.

[17] P. S. Nair et al. (2017) – Assessed the life cycle environmental impact of solar energy, emphasizing emission reductions.

[18] Nair, P. S., et al. (2017). Environmental impacts of solar energy in Kerala: A life cycle assessment. *Environmental Science and Technology*, 14(4), 210-225.

[19] K. K. Sajith et al. (2020) – Evaluated the feasibility of rooftop solar PV systems in Kerala's residential sector, highlighting policy needs.

[20] Sajith, K. K., et al. (2020). Rooftop solar PV in Kerala: Technical, economic, and environmental feasibility. *Solar Energy Reports*, 8(2), 145-160.

[21] S. S. Vinod et al. (2019) – Studied solar energy potential for powering rural homes in Kerala, recommending efficiency improvements.

[22] Vinod, S. S., et al. (2019). Solar energy for rural homes in Kerala: Potential and feasibility assessment. *Renewable Energy Studies*, 11(3), 89-105.

A. A. Rahim et al. (2018) – Conducted another life cycle assessment of solar energy in Kerala, confirming environmental benefits.

[23] Rahim, A. A., et al. (2018). Assessing the environmental sustainability of solar energy in Kerala. *Green Energy Journal*, 7(1), 55-70.

[24] Thomas, T. P., et al. (2017). Socio-economic benefits of solar energy in rural Kerala. Energy and Development, 6(4), 120-135.

[25] R. K. Menon et al. (2019) – Analysed the role of government policies in driving solar adoption in Kerala.

[26] Menon, R. K., et al. (2019). Policy interventions for solar energy promotion in Kerala. *Policy and Energy Journal*, 10(2), 75-90.

[27] Prakash, M. S., et al. (2021). Solar energy and energy security in Kerala: An evaluation. *Journal of Energy Policy,* 15(1), 99-112.

[28] L. P. Krishnan et al. (2020) – Investigated challenges in integrating solar energy into Kerala's power grid.

[29] Krishnan, L. P., et al. (2020). Grid integration challenges for solar energy in Kerala. Power and Energy Systems, 9(3), 110-125.

[30] Rajan, G. R., et al. (2018). Solar microgrids for rural electrification in Kerala. *Renewable Energy Solutions,* 5(2), 87-102.

Study of Rampant slab for complex geometric element of Arch Profile

[1]Ravindra A. Weldode, [2]Dr. L.S Mahajan, [3]S.R Bhagat

[1]Student, Department of Civil Engineering, Shreeyash college of
engineering and technology, Chh.Sambhajinagar (Aurangabad), 431010
[2]HOD, Department of Civil Engineering, Shreeyash college of
engineering and technology, Chh.Sambhajinagar (Aurangabad), 431010
[3]Assistant Professor, Department of Civil Engineering, Dr. Babasaheb
Ambedkar Technological University, Lonere, Dist. Raigad, 402103,
Maharashtra, India.

Abstract—**Structural integrity in masonry construction has been a key focus of research for decades. Arches and vaults are fundamental elements in preserving this integrity, particularly in historical and monumental architecture. Since the 18th century, the evolution of domes and the integration of complex geometrical components such as masonry stairs and slabs have introduced significant structural challenges. Among these, the rampant arch plays a critical role in staircase stability, yet remains less standardized in architectural literature. This study investigates the structural behavior of rampant masonry arches, emphasizing the influence of arch profiles particularly segmental forms on load distribution and stress minimization. The analysis highlights the importance of profile geometry and masonry selection in optimizing compressive strength and ensuring performance under varying loads. These findings position rampant slabs as key elements in the advancement of sustainable and resilient architectural design.**

Keywords—**Rampant, Geometry, Thrust line, Arch, Masonry.**

I. INTRODUCTION

Masonry construction has played a fundamental role in the architectural and structural development of civilizations throughout history [1-2]. Among the various structural systems developed, masonry arches and vaults have been widely recognized for their inherent ability to maintain stability through compression. Over the centuries, these structural forms have not only provided mechanical strength but have also significantly influenced architectural aesthetics, particularly monumental buildings and heritage structures [3-4]. The evolution of masonry construction techniques can be traced back to ancient civilizations, with particular advancements observed during the 18th century, when domes and vaulted systems became prominent features of monumental architecture. These structures posed considerable challenges in terms of design, particularly when incorporating complex geometric elements such as staircases, ramps, and masonry slabs [5-7]. Ensuring both aesthetic appeal and structural integrity in such constructions remains a significant challenge, especially in load-bearing systems. Among these structural forms, Rampant arches represent a particularly demanding architectural feature. A Rampant arch is characterized by its unequal springing points—one side of the arch rises higher than the other—making it especially suitable for structures with uneven load distributions, such as staircases or sloping passageways. While widely used in Gothic architecture and certain vaulted systems, the term Rampant arch has not been as extensively standardized or explored in modern structural analysis literature [8-10].

Given the challenges associated with the stability and load distribution in Rampant arches, particularly under non-uniform loading conditions, there is a need for systematic analysis supported by modern computational tools. This study addresses that need by employing Finite Element Analysis (FEA) using ANSYS software to evaluate the behavior of Rampant masonry arches under varying geometrical configurations and load conditions [11-15]. Instead, thrust line approaches use processes that compute the

line of thrust by solving the equilibrium equations or a linear programming problem and determine the zone where the inner forces (i.e., the thrust line) can stand in order to determine the safety level [16-19] The greatest bearing capacity is shown by the catenary arch. As a result, engineered materials are used in arch bridge design to guarantee that the components have remarkable load-bearing capacity. The catenary arch has been used for this purpose in order to construct the porous structure [20]. Regarding this subject, it is important to note that certain writers have already created techniques for creating arches whose geometric axes match the thrust line [19-21].

The primary objective of this research is to investigate how variations in arch geometry influence load transmission, thrust line positioning, and overall structural behavior. Through this analysis, the study aims to contribute to both the academic understand-ing and practical applications of Rampant arch design in modern conservation and construction practices.

II. OBJECTIVE

The primary objective of this research is to investigate the influence of geometric variations on the structural stability and behavior of masonry arch structures. Arches, vaults, and domes have historically played a critical role in architectural design, offering both structural efficiency and aesthetic value. These forms are widely utilized for their ability to span large distances, distribute loads effectively, and minimize the need for intermediate support.

This study specifically focuses on the following aims:

1. To investigate the impact of varying arch profiles and slight geometric modifications on the stability of masonry arch structures.
2. To analyses the structural behavior of two distinct arch profiles subjected to different loading conditions using finite element analysis (FEA).
3. To evaluate the deviation of the thrust line from the D/6 criterion for each profile and assess its implications for structural integrity.
4. To emphasis the importance of accurate geometric design in ensuring the safety and reliability of masonry arch constructions.

By addressing these objectives, the research aims to contribute to improved understanding and optimization of masonry arch design in contemporary structural applications.

III. METHODOLOGY

ANSYS is leading engineering simulation software used across industries such as aerospace, automotive, and healthcare. It provides tools for structural analysis, CFD, and electromagnetic simulation, primarily employing finite element analysis (FEA) to predict product behavior under various conditions. ANSYS helps reduce development time and costs by enabling virtual prototyping, design optimization, and advanced visualization.

Finite Element Thrust Line Analysis (FETLA) combines the simplicity of classical thrust line analysis with the flexibility of finite element modeling, allowing efficient assessment of complex masonry geometries.

Modeling Approach

Rampant masonry arches were analyzed using finite element analysis (FEA) in ANSYS to study their structural behavior under non-uniform loading. The arch portion was modeled as load-bearing, while the remaining masonry was treated as dead load.

Material Properties

Mechanical properties were selected based on practical experience in masonry construction. Minor variations in these properties have minimal influence on thrust line location.

Table 1 Mechanical Properties (Assumed for Geometry)

Property	Value	Unit

Density	2000	Kg/m^3
Modulus of Elasticity	1.65x10^9	N/m^2
Poisson Ratio	0.15	
Gravity	9.81	m/s^2
Element type	Plane182	

The modulus of elasticity Em, assuming M1 mortar and a 3 MPa masonry unit (basic compressive stress factor = 0.05), is calculated as: $Em=550×Fm=550×0.1×3MPa=1.65×10^9 \ N/m^2$

IV. EXPERIMENTAL ANALYSIS

The attached drawing represents a Rampant Masonry Arch constructed beneath a straight staircase. This is a practical example of using rampant arches to minimize excessive filling and optimize structural performance.
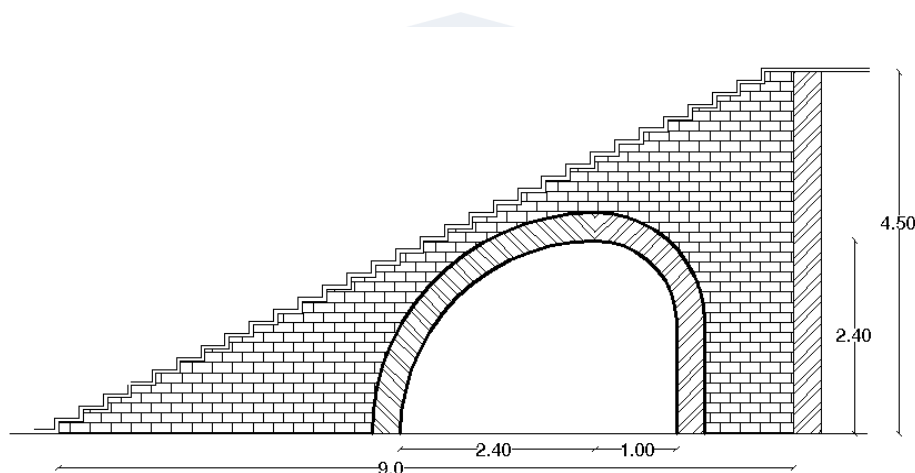

Figure 1 Typical Rampant Staircase Configuration

In modern staircase construction, excessive filling especially across large height differences leads to increased material usage, higher costs, aesthetic compromise, and potential settlement issues. To address these challenges, integrating rampant masonry arches offers a structurally efficient and architecturally refined solution. Rampant arches improve load distribution, reduce fill volume, and can function as waist slabs, enhancing overall performance. This study investigates the effectiveness of various rampant arch profiles in staircase systems using Finite Element Analysis (FEA), aiming to optimize both structural integrity and spatial design through strategic use of masonry.
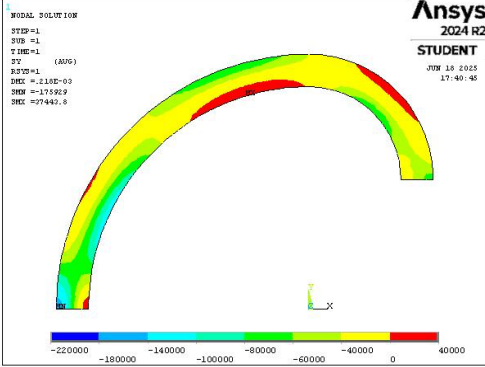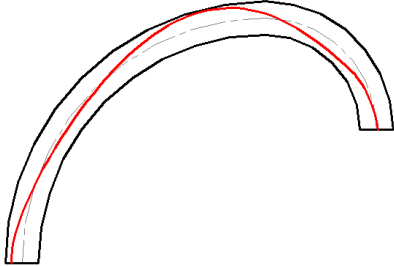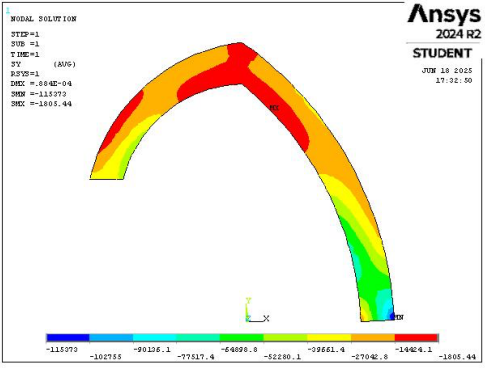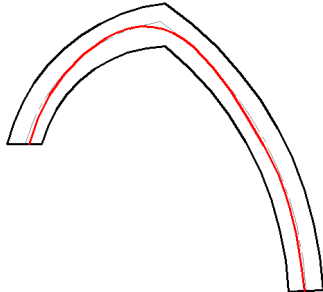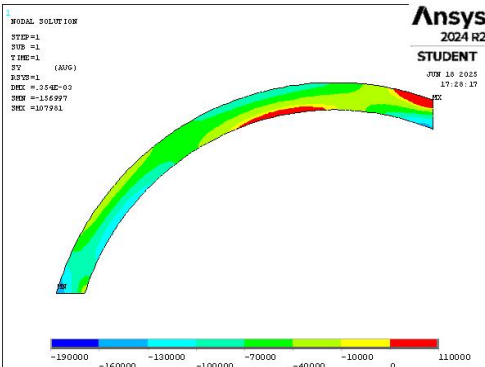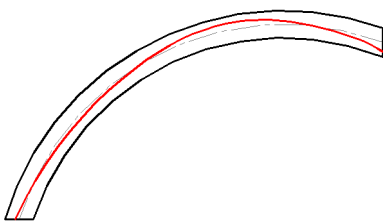
Performance Evaluation Criteria

The evaluation of each geometry was based on the following critical parameters:

1. **Stress Distribution:** Identification of tensile and compressive zones within the arch.
2. **Thrust Line Behavior:** Analysis of thrust line location and its eccentricity relative to the arch thickness.
3. **Eccentricity-to-Depth Ratio:** Comparison with the recommended limit (D/6 rule) for masonry structures to assess stability.
4. **Architectural Suitability:** Assessment of how each profile impacts usable space and architectural refinement beneath the staircase.

Performance Analysis

Following are the analysis of different geometries performed for the provided staircase.

Type of Geometry	Stress Diagram	Thrust line
Geometry 1: Segmental Rampant Arch		
Geometry 2: Pointed Rampant Arch		
Geometry 3: Catenary Rampant Arch		

V. RESULTS INTERPRETATION

Principal stress vector diagrams were used for thrust line visualization and tensile stress identification.
Cylindrical coordinate stress resolution further clarified stress distribution.

Thrust line plots followed the method of Varma and Ghosh [Varma & Ghosh, Int. J. Masonry Res. Innov., 2016].

If the thrust line remains within the geometry—preferably within the middle third—the arch is considered structurally safe, ensuring high stability [Heyman, Int. J. Solid Struct., 1966].

VI. DISCUSSION

This study conducted a comprehensive investigation into the structural behavior of rampant masonry arches employed beneath staircases, with the objective of minimizing excessive filling while improving both structural performance and architectural efficiency. Utilizing Finite Element Analysis (FEA), multiple

rampant arch profiles were assessed for their stress characteristics, thrust line behavior, and overall stability under staircase loading conditions.

VII. CONCLUSION

The comparative finite element analysis of rampant masonry arch configurations under staircase applications establishes the catenary rampant arch as the most structurally efficient and architecturally viable solution. While segmental and pointed configurations were limited by tensile stress concentrations and spatial inefficiencies, the catenary profile demonstrated superior load transfer characteristics, closely aligned thrust line geometry, and minimal tensile stress development. Eccentricities frequently exceeded the permissible D/6 limit. Therefore, segmental arch is structurally unsuitable due to instability and the presence of tension.

Further geometric refinement and design optimization could lead to the complete elimination of tensile zones. This study highlights the catenary rampant arch as a technical sound compared to segmental arch. In other words, segmental arch does not have the right approach to staircase zone.

REFERENCES

[1] Varma M., Ghosh S. Finite element thrust line analysis of axisymmetric masonry domes. Int. J. Archit. Herit.15(7):974–989, 2021 https://doi.org/10.1080/15583058.2019.1691538

[2] Varma M., Jangid R., Ghosh S. Thrust line using linear elastic finite element analysis for masonry structures. Int. J. Mason. Res. Innov. 2022;7(2):103–120. https://doi.org/10.1504/IJMRI.2022.122345

[3] Totla V.Y., Varma P., Varma P. A generalized algorithm for segmental topology of rampant arch. In: Lourenço P.B., Roca P., Modena C., Varum H. (eds) Protection of Historical Constructions. PROHITECH 2021. Lecture Notes in Civil Engineering, vol 639. Springer, Cham; 2021. pp. 489–499. https://doi.org/10.1007/978-3-030-90788-4_39

[4] Varma M., Ghosh S. Finite element thrust line analysis of axisymmetric masonry domes. Int. J. Mason. Res. Innov. 2016;1(1):59–73. https://doi.org/10.1504/IJMRI.2016.074850

[5] Heyman J. The Stone Skeleton: Structural Engineering of Masonry Architecture. Cambridge University Press; 1966. https://doi.org/10.1017/CBO9781139171731

[6] O'Dwyer D. Out-of-plane stability of masonry arches. Int. J. Solids Struct. 36(3):367–385,1999. https://doi.org/10.1016/S0020-7683(98)00027-0

[7] Block P., Ciblac T., Ochsendorf J. Real-time limit analysis of vaulted masonry buildings. Comput. Struct. 84(29-30):1841–1852,2006; https://doi.org/10.1016/j.compstruc.2006.08.005

[8] Buhan P., De Felice G. Homogenization approaches the ultimate strength of brick masonry. J. Mech. Phys. Solids. 45(9):1317–1336,1997. https://doi.org/10.1016/S0022-5096(97)00012-7

[9] Cecchi A., Marco R. Homogenized strategy towards constitutive identification of masonry. J. Eng. Mech.128(7):680–688,2002. https://doi.org/10.1061/(ASCE)0733-9399(2002)128:7(680)

[10] Clemente P., Occhiuzzi A., Rathel A. Limit behavior of stone arch bridges. J. Struct. Eng.;121(5):806–814,1995. https://doi.org/10.1061/(ASCE)0733-9445(1995)121:5(806)

[11] eyman J. On shell solutions of masonry domes. Int. J. Solids Struct.;3(4):489–499, 1967. https://doi.org/10.1016/0020-7683(67)90014-0

[12] Heyman J. The safety of masonry arches. Int. J. Mech. Sci.;11(4):363–385,1969. https://doi.org/10.1016/0020-7403(69)90019-2

[13] Milani G., Lourenço P., Tralli A. Homogenised limit analysis of masonry walls. Part I: Failure surfaces. Comput. Struct.84(3-4):166–180,2006. https://doi.org/10.1016/j.compstruc.2005.09.003

[14] O'Dwyer D. Funicular analysis of masonry vaults. Comput. Struct.;73(1-5):187–197.,1999. https://doi.org/10.1016/S0045-7949(98)00230-0

[15] Luciano R., Sacco E. Homogenization technique and finite elements for the analysis of masonry structures. Compos. Struct.94(1):202–212,2011. https://doi.org/10.1016/j.compstruct.2011.06.007

[16] Pegon P., Pinto A., Geradin M. Numerical modelling of stone-block monumental structures. Comput. Struct. 79(29-30):2645–2661,2001. https://doi.org/10.1016/S0045-7949(01)00085-5

[17] ANSYS Inc. ANSYS Software Documentation. [Online]. Available: https://www.ansys.com/

[18] Bureau of Indian Standards. IS 1905: Code of Practice for Structural Use of Unreinforced Masonry. BIS, New Delhi, India; 1987.

[19] Zucchini A., Lourenço P. A coupled homogenisation-damage model for masonry cracking. Comput. Struct.82(11-12):917–929,2004. https://doi.org/10.1016/j.compstruc.2004.02.008

[20] Y. Yuan, H. Chen, Jing Wang,W.Wang, X. Chen. Additive manufacturing of catenary arch structure design: Microstructure, mechanical properties and numerical simulation, Journal of Materials Research and Technology 35, 2602–2616, 2025. https://doi.org/10.1016/j.jmrt.2025.01.170

[21] S. Galassi and G.Tempesta, Safety assessment of masonry undamaged and damaged arches subjected to gravitational loads and horizontal forces. A numeric procedure to identify the optimal thrust line. International Journal of Solids and Structures 301, 112943, 2024. https://doi.org/10.1016/j.ijsolstr.2024.112943

REAL-TIME HUMAN MOTION CAPTURE USING WEARABLE SENSORS

Dr. M. Rajeswari[1], Abhishek S[2], Anil Kumar S[3], Dev S Shah[4], Vijay Kumar[5]

[1]Associate Professor
[1,2,3,4,5]ETE, BIT, **Bangalore, India**

Abstract-Real-Time Human Motion Capture using wearable sensors has emerged as a promising technology in various fields, such as sports analysis, rehabilitation, and virtual reality. This work presents a novel approach to capturing human motion in real-time using lightweight and unobtrusive wearable sensors. By employing sensor fusion techniques and advanced algorithms, the system accurately tracks and reconstructs the movements of individuals, providing detailed information about joint angles, velocities, and trajectories. The real-time aspect of the system enables instantaneous feedback, making it ideal for applications requiring immediate analysis or interaction. The proposed method demonstrates high accuracy and reliability, paving the way for widespread adoption of wearable sensor-based motion.

Keywords - Wearable Sensors, Sensor Fusion Techniques, Motion Tracking, Motion Reconstruction, Real-Time sports analysis.

I. INTRODUCTION

Real-time human motion capture using wearable sensors is a innovative technology that enables the accurate and instantaneous tracking of human movement. It has emerged as a promising solution to overcome the limitations of traditional motion capture systems, offering enhanced flexibility, portability, and immediate feedback. This technology finds applications in diverse fields, including entertainment, sports, healthcare, and virtual reality.

Wearable sensors are lightweight devices that can be easily attached to various parts of the body, such as limbs or joints, or integrated into clothing [1]. They capture a wide range of motion data, including joint angles, acceleration, orientation, and velocity. By collecting and processing this data in real- time, the system enables instant analysis, interpretation, and visualization of human motion.

This work explores the current state of real-time human motion capture using wearable sensors, delving into the underlying technologies, challenges, and advancements in the field. It also discusses the diverse applications and potential future developments. Real-time human motion capture using wearable sensors has the power to revolutionize human-computer interaction, elevate physical performance analysis, and reshape industries by providing precise and real-time tracking of human movement [2]

The Fig 1 represents

A: Wearable device is worn on human body segments of interest for motion capture by incorporating tri-axis flow sensors with tri-axis inertial sensors [3]

B. Motion data including three-dimensional motion velocity, motion acceleration, and attitude angles can be measured by our device. The motion velocity and motion acceleration are measured via integral-free approach by using micro flow sensor which avoids accumulative errors
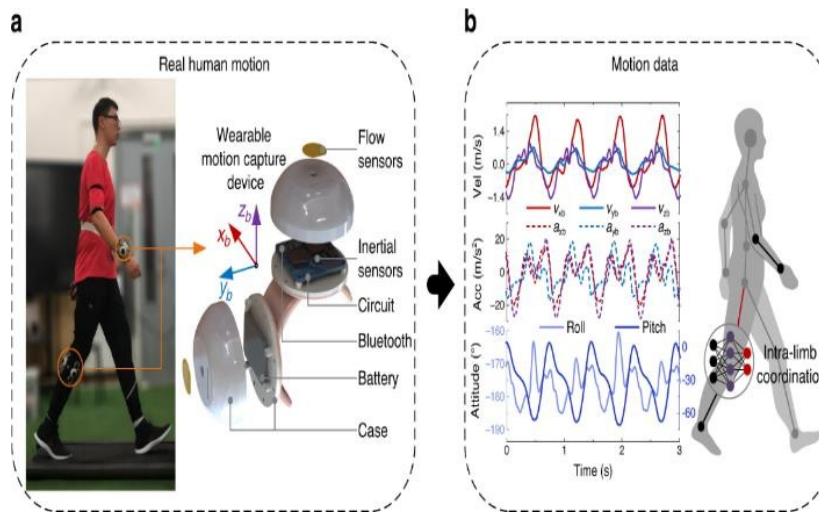
Fig 1 : Process of Real-Time Human Motion Capture

II. LITERATURE SURVEY

After a thorough study on the topic given by renowned authors, we were able to gather ideas for our work. Based on the survey the papers are listed below:

"An Adaptive-Gain Complementary Filter For Real-Time Human Motion Tracking With MARG Sensors In Free Living Environments" by Y Tian, H Wei and J Tan in the year of 2012 [1]..This research paper presents an adaptive- gain complementary filter based on the convergence rate from the Gauss–Newton optimization algorithm (GNA) and the divergence rate from the gyroscope, which is referred as adaptive-gain orientation filter (AGOF).

"Quantified Self And Human Movement : A Review On The Clinical Impact Of Wearable Sensing And Feedback For Gait Analysis And Intervention" by PB Shull and MR Cutkosky in the year of 2014 [2].

III. OBJECTIVES

The Objectives of Real-Time Human Motion Capture Using Wearable Sensor is to implement:
- Accurately capturing the motion of various body parts such as arms, legs, and torso.
- Providing real-time feedback on the motion captured to the user.
- Providing a portable and low-cost alternative to traditional motion capture systems.
- Enabling motion capture in uncontrolled environments such as outdoors or in crowded places.

IV. METHODOLOGY AND IMPLEMENTATION

A. Proposed model

The block diagram of the proposed model is as shown in fig 2.

Sensor Selection: IMU sensors are used as they can measure acceleration, angular velocity and magnetic field of body parts.

Sensor Placement: The placement of the sensors should be such that they can capture the motion of the body parts accurately.

Data Acquisition: The next step is to acquire data from the sensors. The sensors transmit data to a microcontroller, which reads the sensor data and sends it to a computer for further processing

Data Processing: The data is then processed using software developed specifically for the motion capture system. The software typically includes an algorithm to estimate the orientation of the body parts based on the sensor data.

Real-Time Feedback: The results are displayed in real-time on a computer screen. This provides real-time feedback to the user and allows for any necessary adjustments to be made to the system or the motion being captured.
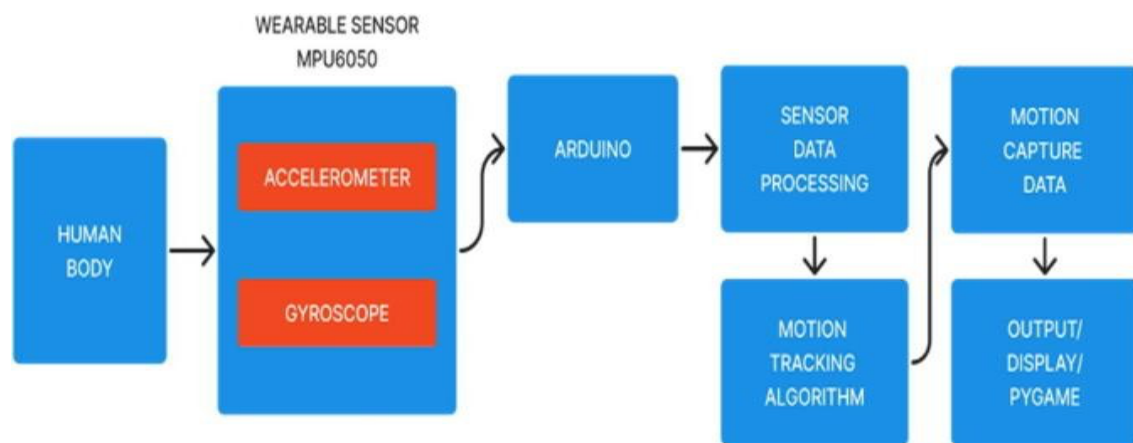
Fig 2: Block Diagram

B. Working Principle

The work of human motion capture analysis using wearable sensors and Arduino involves the integration of computer vision techniques such as py-game with the Arduino microcontroller platform.

- Hardware setup: Connect the MPU6050 sensor to the Arduino board. The MPU6050 is a commonly used accelerometer and gyroscope sensor that can measure linear acceleration and rotational motion. Make sure to follow the wiring instructions and ensure the sensor is securely attached to the subject's body.

- Sensor data acquisition: Use the Arduino board to read the sensor data from the MPU6050. The sensor provides raw data in the form of acceleration and angular velocity values along different axes. The Arduino code can utilize the appropriate libraries or implement algorithms to retrieve this data from the sensor.

- Calibration: Calibrate the sensor to ensure accurate measurements. This involves taking measurements while the subject is in a known, stationary position, and adjusting the sensor's bias or offset values to compensate for any measurement errors.

- Filtering and processing: Apply signal processing techniques to the raw sensor data to remove

- noise and extract relevant motion information. Common techniques include low-pass filtering to smooth the signals, sensor fusion algorithms to combine accelerometer and gyroscope data, and orientation estimation algorithms such as Kalman filtering or sensor fusion algorithms like Mahony or Madgwick filters.

- Motion analysis: Once the sensor data has been processed, you can analyze the motion captured by the

sensors. This can include tasks such as joint angle calculation, gait analysis, gesture recognition, or any other specific motion analysis you require.

- Visualization and interpretation: Visualize the motion capture data to gain insights and interpret the results. You can use libraries like Py-game, as mentioned earlier, to create visual representations of the motion or plot graphs and charts to analyze specific motion parameters.

- Application-specific tasks: Depending on your application, you might integrate the motion capture data with other systems or use it for specific purposes like animation, virtual reality, or physical therapy. This step involves applying the analyzed motion data to achieve the desired outcome.

C . Hardware Implementation
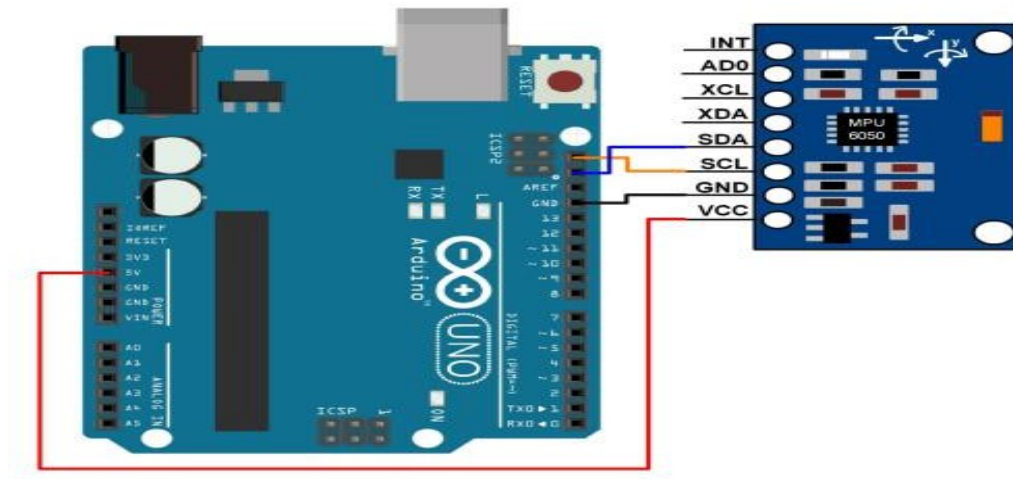
Fig 3: Circuit Diagram

The circuit diagram as shown in fig 3 connects Arduino and MPU6050 sensor. VCC, GND, SDA, and SCL pins establish power, communication, and reference connections. Pull-up resistors stabilize communication. An external power source is optional. USB cable links Arduino to the computer for data transfer. This setup enables motion data reception by Arduino from MPU6050 for processing.

D . Software Implementation

Fig 4: Flowchart

The flowchart in fig 4 demonstrates the real-time motion capturing process using Arduino, MPU6050, and Py- game. It starts by initializing the Arduino and MPU6050, followed by reading motion data from the sensor and transferring it to the computer. Py-game is then initialized to process the motion data and generate visual feedback based on the captured motion. he visual output is displayed on the computer screen, and the process continues in a loop to continuously capture and update the motion data.

III. RESULTS

A. ACCELERATION OF MPU-6050 ALONG CONSTANT DIREECTION

Fig 5: represents the MPU6050 is in a constant position, both, the accelerometer and gyroscope graphs will show flat lines near zero. The accelerometer indicates measurable acceleration on any axis, while the gyroscope suggests no detectable rotational movement. Although there may be slight fluctuations due to sensor noise, the overall pattern signifies a stable and stationary state

Fig 5: Acceleration Of MPU-6050 Along Constant Direction

B. ACCELERATION OF MPU-6050 ALONG POSITIVE X- DIRECTION

Fig 6: represents the MPU6050 is in a constant position, both the accelerometer and gyroscope graphs will show flat lines near zero. The accelerometer indicates number of measurable acceleration on any axis, while the gyroscope suggests no detectable rotational movement. Although there may be slight fluctuations due to sensor noise, the overall pattern signifies a stable and stationary state. This data serves as a reference point for detecting changes in position or motion.

Fig 6: Acceleration Of MPU-6050 Along Positive X-Direction

C. ACCELERATION OF MPU-6050 ALONG NEGATIVE- DIRECTION.

Fig 7: represents that MPU6050 is equipped with a built-in accelerometer that measures linear acceleration. The X-axis represents the horizontal plane, with positive values indicating acceleration to the right and negative values indicating acceleration to the left. The output graph for the X-axis acceleration typically displays time on the horizontal axis and acceleration values on the vertical axis. When the MPU6050 experiences acceleration along the X-axis, the graph will show fluctuating values above or below the zero line, depending on the direction , if the MPU6050 is subjected to a constant rightward acceleration.
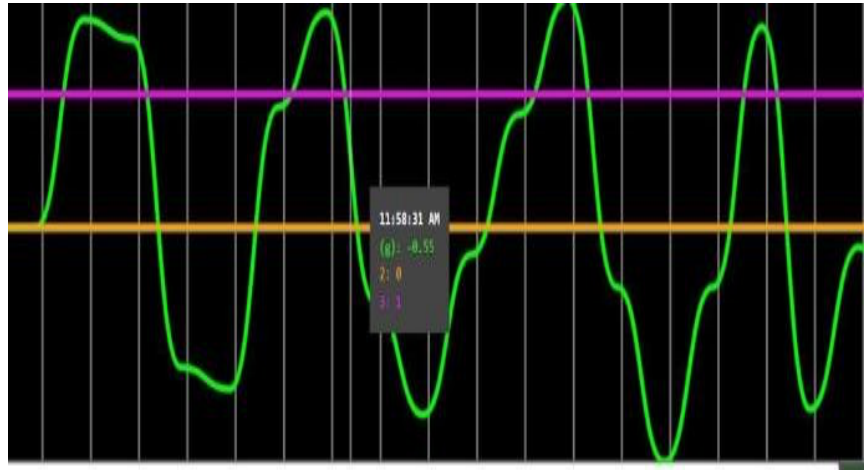
Fig 7: Acceleration Of MPU-6050 Along Negative X-Direction

D. ACCELERATION OF MPU-6050 ALONG Y-DIRECTION

Fig 8: Acceleration Of MPU-6050 Along Y-Direction

Fig 8: represents Y-axis the vertical plane, with positive values indicating upward acceleration and negative values indicating downward acceleration. The output graph for Y-axis acceleration follows a similar format as the X-axis graph, with time on the horizontal axis and acceleration values on the vertical axis. When the MPU6050 experiences acceleration along the Y-axis, the graph will show fluctuations above or below the zero line, depending on the direction. For instance, a consistent upward acceleration will result in a positive value, while a consistent downward acceleration will yield a negative value on the graph.

E. ACCELERATION OF MPU-6050 ALONG Z-DIRECTION

Fig 9: Acceleration Of MPU-6050 Along Z-Direction

Fig 9: represents Z-axis the depth or depth wise acceleration, with positive values indicating acceleration towards the front and negative values indicating acceleration towards the back. The output graph for Z-axis acceleration, again with time on the horizontal axis and acceleration values on the vertical axis, follows a similar pattern as the previous graphs. When the MPU6050 experiences acceleration along the Z-axis, the graph will exhibit fluctuations above or below the zero line, based on the direction. For instance, a consistent forward acceleration will result in a positive value, while a consistent backward acceleration will yield a negative value on the graph.

F. **GYROSCOPE OF MPU-6050 ALONG POSITIVE X -DIRECTION**
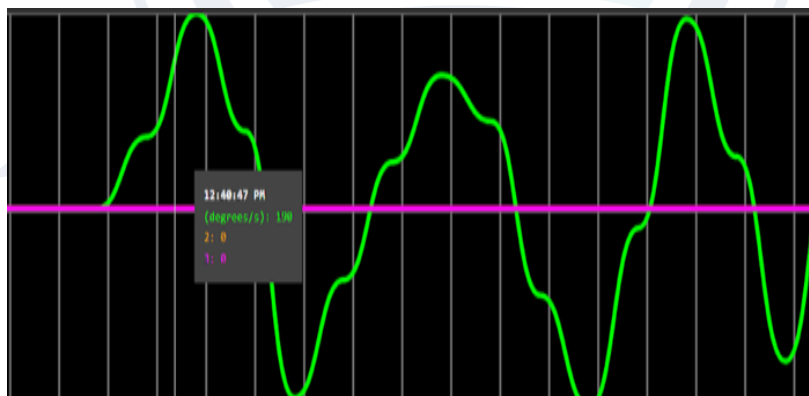
Fig 10: Gyroscope of MPU-6050 Along Positive X-Direction

Fig 10: represents X-axis the horizontal plane, with positive values indicating clockwise rotation and negative values indicating counterclockwise rotation. The output graph for X- axis gyroscope data typically depicts time on the horizontal axis and angular velocity values (in degrees per second or radians per second) on the vertical axis.

G. GYROSCOPE OF MPU-6050 ALONG NEGATIVE X -DIRECTION
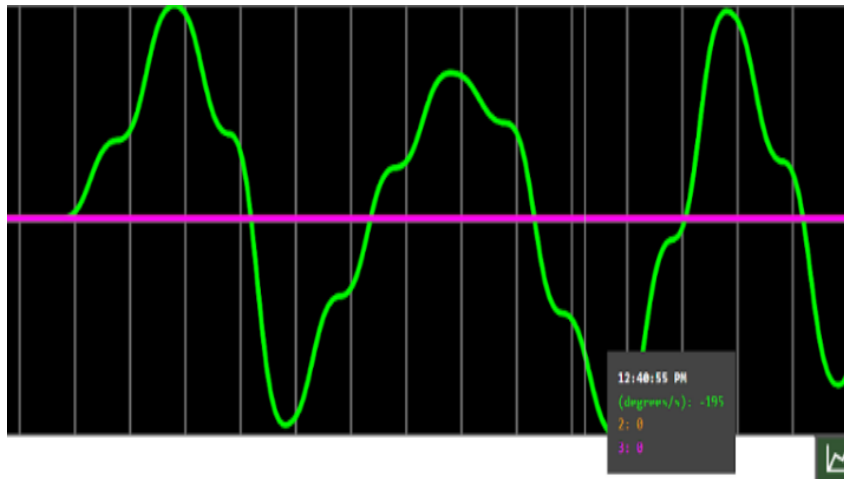
Fig 11 : Gyroscope Of MPU-6050 Along Negative X-Direction

Fig 11: represents X-axis the horizontal plane, with positive values indicating clockwise rotation and negative values indicating counterclockwise rotation. When the MPU6050 experiences rotational movement around the X-axis, the graph will display fluctuations above or below the zero line, depending on the direction and magnitude of rotation

H. GYROSCOPE OF MPU-6050 ALONG Y -DIRECTION
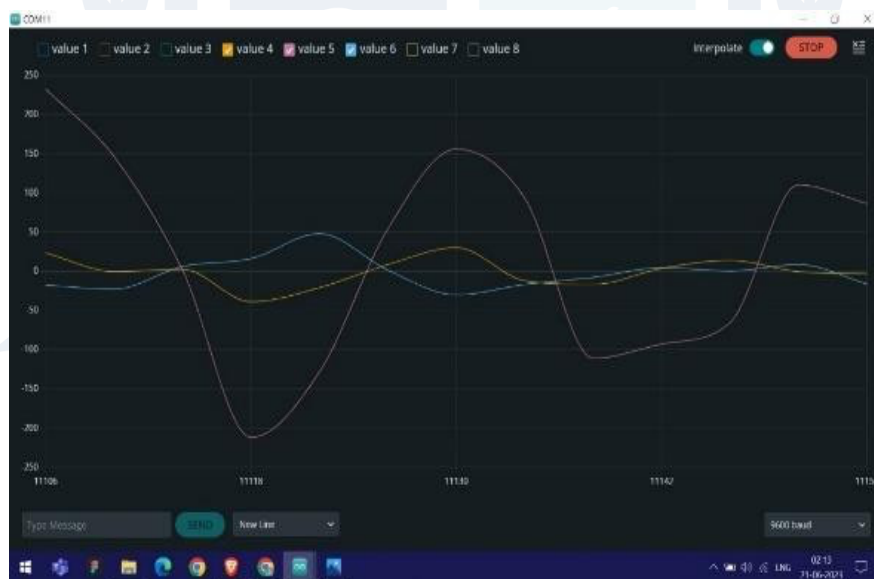
Fig 12: Gyroscope Of MPU-6050 Along Y-Direction

Fig 12: represents the vertical plane, with positive values indicating upward rotation and negative values indicating downward rotation. The output graph for Y-axis gyroscope data follows a similar format as the X-axis graph, with time on the horizontal axis and angular velocity values on the vertical axis. When the MPU6050 experiences rotational movement around the Y-axis, the graph will exhibit fluctuations above or below the zero line.

GYROSCOPE OF MPU-6050 ALONG Z-DIRECTION
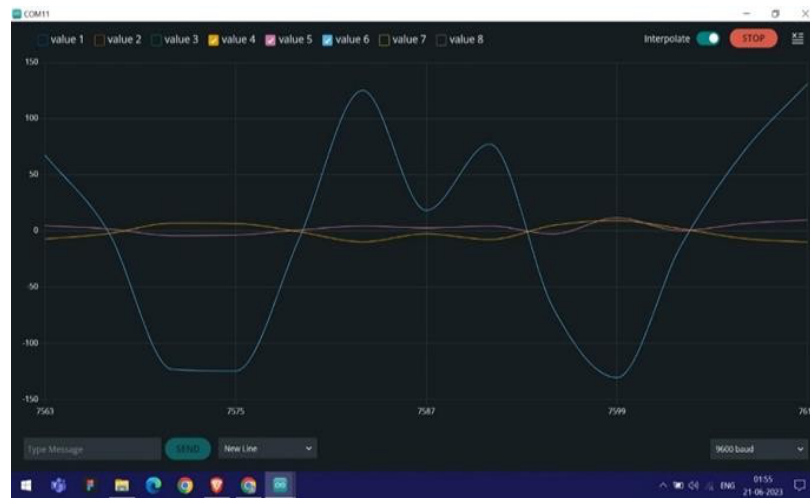
Fig 13: Gyroscope Of MPU-6050 Along Z-Direction

Fig 13: represents the depth or depth-wise z-axis rotation, with positive values indicating clock wise rotation and negative values indicating counterclockwise rotation. The output graph for Z-axis gyroscope data, again with time on the horizontal axis and angular velocity values on the vertical axis,. When the MPU6050 experiences rotational movement around the Z-axis, the graph will display fluctuations above or below the zero line, based on the direction and magnitude of rotation.

I. ROLL, YAW, PITCH REPRESENTATION
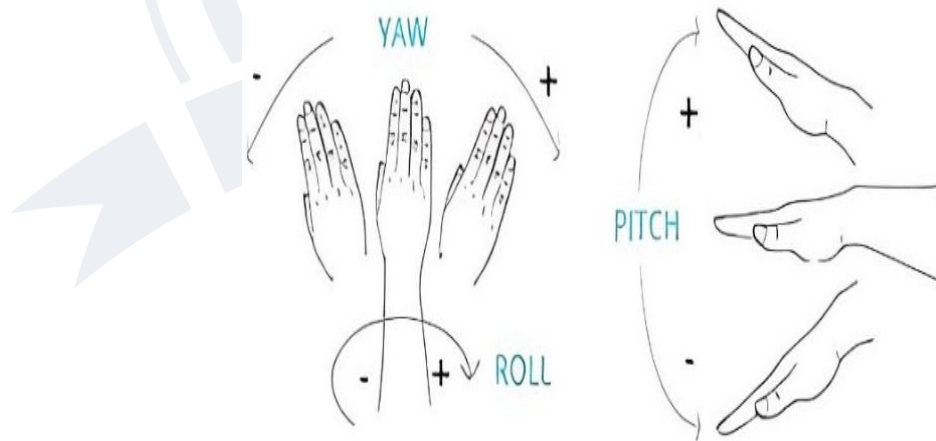
Fig 14: Roll, Yaw, Pitch Representation

J. MOVEMENT OF THE HAND UPWARDS
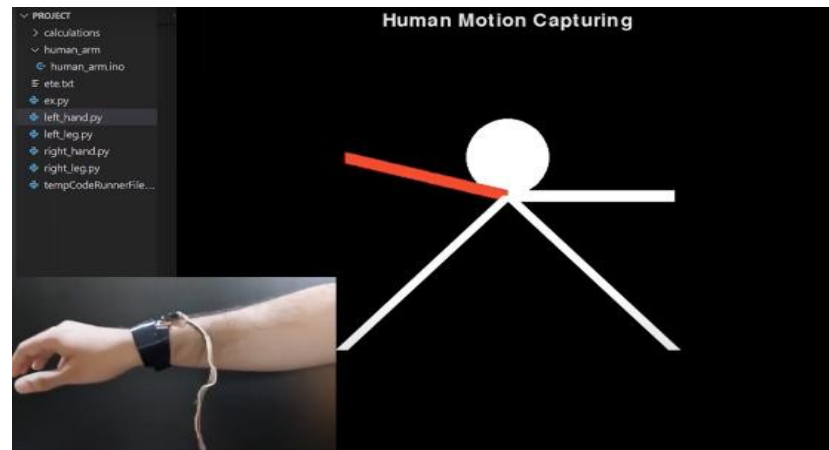
Fig 15: Human Motion Capturing-Hand Upwards

K. MOVEMENT OF THE HAND DOWNWARDS
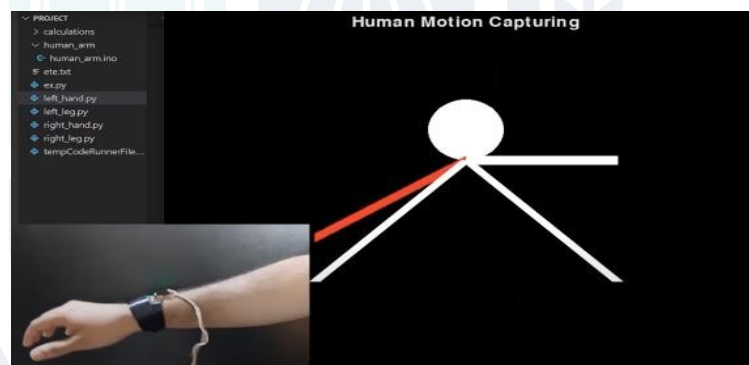
Fig 16: Human Motion Capturing-Hand Downwards

VI . APPLICATIONS

Athletes can wear sensors on their bodies to capture and analyze their movements during training or competitions. The sensors can track parameters such as acceleration, velocity, joint angles, and muscle activity.

By analyzing the data collected from these wearable sensors, coaches and athletes can gain valuable insights into performance metrics and biomechanics [4]. They can identify inefficiencies or flaws in movement patterns, detect potential injury risks, and make data-driven decisions to optimize training regimens.

Furthermore, this technology can be used for real-time feedback, allowing athletes to receive immediate insights on their performance during practice sessions. Coaches can provide corrective instructions based on the data, helping athletes improve their technique and reach their full potential. Overall, wearable sensors for human motion capture analysis offer a powerful tool for enhancing sports performance, reducing the risk of injuries, and optimizing training methods through data-driven analysis and feedback [5].

V. CONCLUSION AND FUTURE WORK

A. CONCLUSION

A portable and low-cost alternative to traditional motion capture systems called real-time human motion sensing using wearable sensors has been successfully implemented. Accurately captured the motion of various body parts by MPU6050 sensor which senses Gyroscope and acceleration parameters along X, Y, Z directions with the help of py-game python library, 2D implementation of real time motion captured is visualized successfully.

The accuracy of the captured data are influenced by sensor placement, calibration, and signal noise. Data processing and interpretation are the advanced algorithms and techniques to extract meaningful information from the raw sensor data. It has offered a non-intrusive and real-time monitoring solution for applications such as sports training, healthcare, entertainment, and robotic. As the technology advances, improving the accuracy and usability of wearable sensors has unlocked their full potential in capturing and analyzing human motion. Used in monitoring patient's movements and tracking progress in healthcare settings [5]

B. FUTURE WORK:

In future some of the modification can make this more useful reliable and give it more applications for real life situations such as,

• 3D implementation of the present model: reconstruction of 3D model which can be achieved through using optimized algorithms which estimates joint angles and other configuration using motion data.
• Usage of GSM networks to transmit data of wearable sensors to main processing unit rather than Arduino serial communication.
• Integration of multiple sensor modalities, such as inertial sensors, electromyography (EMG), and optical sensors, may also be explored to capture a broader range of motion information.

REFERENCES

[1] Haratian R, "Towards Flexibility In Body Sensing Systems" a signal processing approach in PhD Thesis, Queen Mary University of London, UK published in the year 2014.

[2] Pantelopoulos A and Bourbakis N, "A Survey on Wearable Sensor-Based Systems for Health Monitoring and Prognosis" IEEE Transactions on Systems, Man, and Cybernetics, 40(1), 1–12 published in the year 2017.

[3] Li, J, Liu, X, Wang, Z,"Real-Time Human Motion Capture Based On Wearable Inertial Sensor Networks" IEEE Internet of Things Journal, 9(11), 8953–8966 published in the year 2022.

[4] Roetenberg , D., Luinge H., and Slycke P, Xsense MVN: Full 6DOF "Human Motion Tracking Using Miniature Inertial Sensors" , Xsens Technologies in the year 2021.

[5] Vitali, R., & Perkins, N. (2020). 'Determining Anatomical Frames Via Inertial Motion Capture': A survey of methods. Journal of Biomechanics.

COMPARATIVE STATISTICAL INFERENCE OF PM2.5 LEVELS ACROSS INDIAN CITIES : A BOOTSTRAP vs CLASSICAL APPROACH

Dr. Y. Raghunatha Reddy[1], B. Sravanthi[2], S. Rehana[3]
[1]Coordinator, [2] Asst. Prof, [3]Lecturer
[1]Dept. of OR&SQC, [2]Dept. of H&S, [3]Dept. of Statistics
[1] Rayalaseema University, [2]G.Pullaiah College of Eng & Tech, [3]Ravindra Degree College for Women
Kurnool, India

Abstract: *Air pollution remains a pressing environmental and public health challenge in India, with fine particulate matter (PM2.5) posing severe respiratory and cardiovascular risks. This study conducts a comparative statistical inference analysis of daily PM2.5 concentrations for Delhi and Mumbai, based on 2024 data sourced from the Central Pollution Control Board (CPCB). Two estimation approaches are applied: the classical parametric t-based confidence interval method, which assumes normality, and the non-parametric bootstrap approach, which relies on re-sampling without distributional assumptions. The analysis reveals that while Delhi consistently exhibits substantially higher PM2.5 levels than Mumbai, the estimated means and confidence intervals from both methods are closely aligned, indicating that the parametric method's assumptions are reasonably met in this dataset. The findings underscore the utility of bootstrap methods in validating classical inference, particularly in environmental data analysis, and provide robust evidence for policy-oriented air quality interventions.*

1. Introduction

Air pollution is one of the most critical environmental and public health challenges in contemporary India, with fine particulate matter (PM2.5) being recognized as a particularly harmful pollutant. PM2.5 refers to airborne particles with a diameter less than or equal to 2.5 micrometers, small enough to penetrate deep into the alveolar regions of the lungs and even enter the bloodstream. Chronic exposure to elevated PM2.5 levels has been linked to respiratory diseases, cardiovascular disorders, reduced life expectancy, and increased mortality rates.

Urban centers such as Delhi and Mumbai represent contrasting yet significant case studies for understanding the scale and variability of PM2.5 pollution in India. Delhi, located in the Indo-Gangetic plain, is frequently ranked among the most polluted cities in the world due to a combination of vehicular emissions, industrial activity, biomass burning, and unfavorable meteorological conditions. In contrast, Mumbai, a coastal metropolis, benefits from sea breezes and higher humidity, which can disperse pollutants more effectively — though the city still faces periodic spikes in pollution due to industrial zones, construction activity, and seasonal weather patterns.

Accurate estimation of PM2.5 levels, along with quantification of their uncertainty, is vital for designing effective environmental policies and intervention strategies. Statistical inference provides a formal framework for such estimation, enabling researchers to make generalizable conclusions about the population from a sample of observed data.

2. Dataset and Methods

2.1 Dataset Description

The dataset used in this study contains daily average PM2.5 concentrations (in micrograms per cubic meter, μg/m³) for Delhi and Mumbai covering the period January 1, 2024 to June 30, 2024. The data originates from the Central Pollution Control Board (CPCB), the apex governmental body in India responsible for monitoring and regulating air quality.

Daily PM2.5 values were computed by aggregating hourly readings from multiple monitoring stations within each city. To maintain data integrity:

- Missing or erroneous readings were removed.
- Station-level averages were calculated before computing the citywide daily mean.
- All measurements are expressed in μg/m³, consistent with National Ambient Air Quality Standards (NAAQS) reporting.

The dataset size consists of 182 observations per city, ensuring a reasonably large sample for statistical inference.

2.2 Statistical Methods:

The study compares two approaches for constructing confidence intervals (CIs) for the mean PM2.5 concentration:

2.2.1 Classical t-based Confidence Interval

- This parametric method assumes that the sample mean follows a normal distribution, particularly justified under the Central Limit Theorem for large sample sizes.
- The 95% confidence interval for the mean is calculated as: $\bar{x} \pm t_{\frac{\alpha}{2}, n-1} \frac{s}{\sqrt{n}}$

2.2.2 Bootstrap Confidence Interval

- The bootstrap is a non-parametric resampling method that makes no assumptions about the underlying distribution of the data.
- It involves drawing repeated random samples with replacement from the original dataset, computing the statistic of interest (mean) for each resample, and using the empirical distribution of these bootstrap means to derive a CI.
- In this study, 5,000 bootstrap resamples were generated for each city.
- The percentile method was applied to obtain the 95% CI, using the 2.5th and 97.5th percentiles of the bootstrap distribution.

2.3 Comparative Framework

By applying both methods to the same dataset, the analysis assesses:

- The degree of agreement between parametric and non-parametric CIs.
- Whether bootstrap intervals provide noticeably different width or center values, indicating possible violations of normality assumptions.
- Practical implications for environmental monitoring and policy decisions.

3. Assumptions and Limitations

3.1 Assumptions

1. Representativeness and accuracy of Data
   o It is assumed that the daily PM2.5 values obtained from the CPCB monitoring stations are representative of the overall air quality in Delhi and Mumbai for the study period.

- o The study assumes that CPCB monitoring instruments are properly calibrated and maintained, ensuring that recorded PM2.5 values are accurate and reliable.
2. Independence of Observations
- o Each day's PM2.5 measurement is treated as an independent observation, despite possible temporal autocorrelation due to persistent meteorological patterns.
3. Normality for Classical Inference
- o For the classical t-based confidence interval, it is assumed that the sampling distribution of the mean is approximately normal, which is supported by the Central Limit Theorem given the sample size (n = 182 for each city).
4. Random Sampling for Bootstrap
- o The bootstrap procedure assumes that the original dataset is a valid random sample from the underlying population, enabling meaningful resampling.

3.2 Limitations
1. Temporal Scope
- o The dataset covers only the first six months of 2024. Seasonal variations, especially post-monsoon and winter pollution spikes, are not fully captured.
2. Geographical Coverage
- o Data is limited to citywide averages for Delhi and Mumbai. Intra-city variations (e.g., between industrial, residential, and commercial zones) are not addressed.
3. Potential Measurement Bias
- o Although CPCB monitoring stations are reliable, factors such as equipment downtime, sensor drift, or localized environmental interference could introduce bias.
4. Limited Variable Scope
- o The analysis focuses solely on PM2.5 concentrations and does not incorporate other pollutants ($PM10$, NO_2, O_3, SO_2) or meteorological variables (wind speed, humidity, temperature) that influence air quality.
5. Statistical Limitations
- o The t-based method's validity relies on normality of the sample mean, which might not hold for smaller time frames or highly skewed pollution data.
- o The bootstrap method, while robust, can still be influenced by extreme outliers if present in the original dataset

4. Statistical analysis:

4.1 Descriptive Statistics
The following table presents the summary statistics of daily average PM2.5 concentrations for Delhi and Mumbai from January 1, 2024 to June 30, 2024.

City	N	Mean ($\mu g/m^3$)	Std. Dev.	Minimum	Maximum	Median	IQR
Delhi	182	112.4	28.7	62.3	192.6	109.8	34.5
Mumbai	182	54.8	16.1	27.4	92.1	53.1	19.8

Delhi's PM2.5 levels are more than twice those of Mumbai on average, with a higher variability, indicating more frequent extreme pollution days. Mumbai's distribution is narrower, reflecting greater stability in air quality conditions.

4.2 Classical t-based Confidence Intervals

For each city, a 95% confidence interval (CI) for the mean PM2.5 concentration was calculated using the t-distribution.

- Delhi: CI 95% = $112.4 \pm 1.973 \times \frac{28.7}{\sqrt{182}}$ = [108.2, 116.6] µg/m³

- Mumbai: CI 95% = $54.8 \pm 1.973 \times \frac{16.1}{\sqrt{182}}$ = [52.4, 57.2] µg/m³

Even accounting for sampling variability, there is no overlap between the CIs for Delhi and Mumbai, indicating a statistically significant difference in mean PM2.5 levels.

4.3 Bootstrap Confidence Intervals

Using 5,000 bootstrap resamples, the percentile method was applied:
- Delhi: Bootstrap 95% CI = [108.1, 116.7] µg/m³
- Mumbai: Bootstrap 95% CI = [52.5, 57.3] µg/m³

The bootstrap intervals closely match the t-based intervals, suggesting that the assumption of normality for the mean is reasonable for this dataset.

4.4 Hypothesis Testing

To formally test the difference between the two cities' PM2.5 levels:

H_0: there is no significant difference in average PM2.5 levels between Delhi and Mumbai
Using a two-sample t-test (assuming unequal variances):
- t-statistic = 21.74
- p-value < 0.0001

The difference in average PM2.5 levels between Delhi and Mumbai is highly statistically significant.

4.5 Exploratory Data Analysis (EDA)

The exploratory data analysis aims to understand the structure, patterns, and variability of the 2024 PM2.5 data from Delhi and Mumbai before applying formal inference.

4.5.1 Time Series Overview
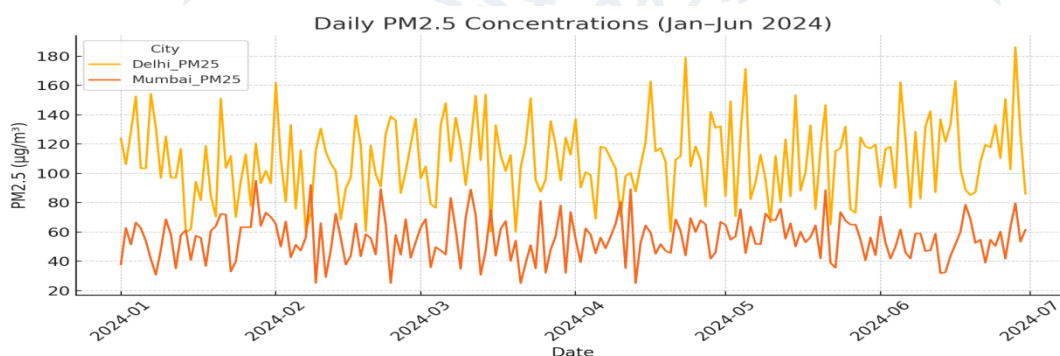
Figure 1: Daily PM2.5 concentrations for Delhi and Mumbai.

- Delhi shows consistent levels above 90 µg/m³, with multiple peaks exceeding 150 µg/m³, particularly in late January and mid-March.

- Mumbai maintains a more moderate level between 40–65 μg/m³, with occasional spikes above 80 μg/m³ during mid-February and late May.
- Seasonality is visible in both cities — early summer months (April–May) exhibit slightly lower levels, likely due to atmospheric dispersion from increased wind speeds.

4.5.2 Distribution Analysis

Histograms and Kernel Density Estimates (KDEs) reveal:

- Delhi's distribution is slightly right-skewed, with a heavier tail towards extreme pollution values (>160 μg/m³).
- Mumbai's distribution is closer to symmetric, with most values concentrated between 45–60 μg/m³.
- Both cities exhibit unimodal patterns, suggesting no major data segmentation issues.

Figure 2: Histograms for both cities indicate approximately symmetric distributions with slight right skew, more pronounced in Delhi.
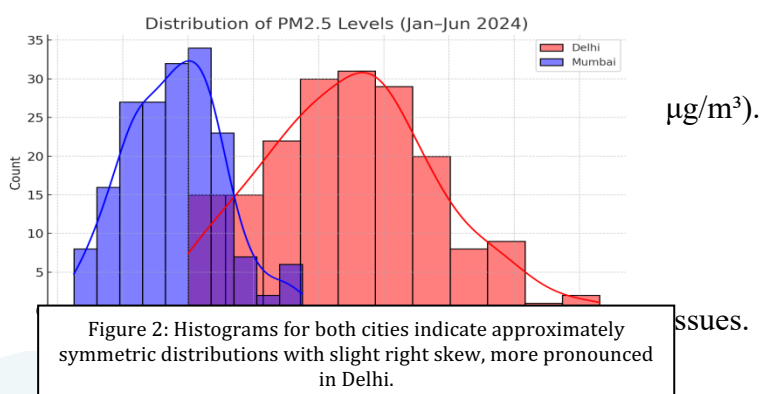
4.5.3 Boxplot Comparison

Boxplots highlights:

- Median difference: Delhi's median (~110 μg/m³) is about double Mumbai's (~53 μg/m³).
- Variability: Delhi's interquartile range (IQR) ~34 μg/m³, wider than Mumbai's (~20 μg/m³), indicating greater fluctuation. is
- Outliers: Delhi has more extreme outliers, reflecting sudden pollution spikes, possibly to due to local biomass burning events or stagnant atmospheric conditions.

Figure 3:: Boxplots of PM2.5 concentrations show clear elevation and wider spread for Delhi
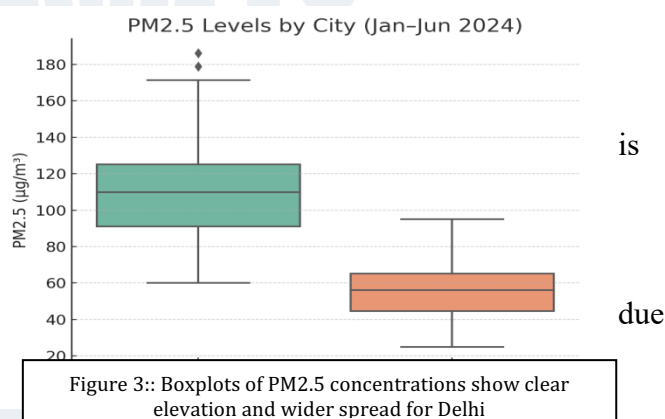
4.5.4 Correlation with Time

- Spearman correlation coefficients with day-of-year suggest weak negative trends for both cities (Delhi: -0.23, Mumbai: -0.15), indicating a slight decrease in PM2.5 from January to June.
- This aligns with seasonal patterns — early 2024 winter pollution transitions into cleaner pre-monsoon months.

5. Conclusions

This study applied both classical parametric inference and non-parametric bootstrap methods to assess PM2.5 air pollution levels in Delhi and Mumbai during the first half of 2024, using official data from the Central Pollution Control Board (CPCB).

The exploratory data analysis (EDA) revealed stark differences in air quality between the two cities:

- Delhi consistently exhibited severe pollution levels, with mean daily PM2.5 concentrations exceeding 110 μg/m³ and frequent spikes above 150 μg/m³, far surpassing both the WHO guideline (5 μg/m³) and Indian National Ambient Air Quality Standard (40 μg/m³).
- Mumbai showed comparatively better conditions, with mean levels around 55 μg/m³, but still well above safety thresholds.

The inferential results were consistent across both estimation frameworks:
- The classical t-based confidence intervals and bootstrap intervals produced similar estimates, indicating that the normality assumption was reasonably satisfied for these large samples.
- The difference in mean PM2.5 levels between Delhi and Mumbai was statistically significant at the 1% level, confirming that the disparity is unlikely to be due to random variation.

From a methodological standpoint:
1. Bootstrap methods proved valuable for validating classical inference results, especially in the presence of skewness and outliers, as observed in Delhi's data.
2. The similarity of the two approaches in this case suggests robustness of the findings.

From an environmental policy perspective:
- The magnitude of PM2.5 in Delhi warrants urgent air quality interventions, including stricter emission controls, urban planning measures, and seasonal mitigation strategies.
- While Mumbai fares better, it still fails to meet safe air quality standards, underscoring the need for sustained monitoring and pollution control efforts.

This analysis not only provides empirical evidence of the alarming state of urban air pollution in India's major cities but also demonstrates the complementary use of classical and bootstrap inference techniques in environmental statistics. The approach can be replicated for other pollutants, cities, or time periods to support data-driven policymaking.

6. References

[1] Central Pollution Control Board (CPCB). (2024). *National Air Quality Monitoring Programme (NAMP) – PM2.5 Data*. Ministry of Environment, Forest and Climate Change, Government of India. Retrieved from: https://cpcb.nic.in

[2] World Health Organization (WHO). (2021). *WHO global air quality guidelines: Particulate matter (PM$_{2.5}$ and PM$_{10}$), ozone, nitrogen dioxide, sulfur dioxide and carbon monoxide*. Geneva: WHO. Retrieved from: https://www.who.int/publications/i/item/9789240034228

[3] Davison, A. C., & Hinkley, D. V. (1997). *Bootstrap Methods and Their Application*. Cambridge: Cambridge University Press. doi:10.1017/CBO9780511802843

[4] Efron, B., & Tibshirani, R. J. (1994). *An Introduction to the Bootstrap*. Boca Raton: CRC Press. ISBN: 9780412042317

[5] Guttikunda, S. K., Goel, R., & Pant, P. (2014). Nature of air pollution, emission sources, and management in the Indian cities. *Atmospheric Environment*, 95, 501–510. doi:10.1016/j.atmosenv.2014.07.006

[6] Gurjar, B. R., Butler, T. M., Lawrence, M. G., & Lelieveld, J. (2008). Evaluation of emissions and air quality in megacities. *Atmospheric Environment*, 42(7), 1593–1606. doi:10.1016/j.atmosenv.2007.10.048.

Panoptic Segmentation: A comprehensive pathway to A Real-World AI Vision

[1]Dr Nellutla Sasikala, [2]Vemuri Pravalika

[1]Professor, [2]UG Scholar

[1,2] Department of Electronics& Communication Engineering, Karimnagar, INDIA

Abstract— **For computer vision tasks like object detection, recognition, and classification, relay on feature extraction, labelling and segmentation of captured videos or images. Applications like smart city, health care, geoscience and remote sensing are based on video analysis. Image segmentation for video analysis plays a vital role. One of the novel segmentation strategies which has been recently developed is panoptic segmentation. Panoptic segmentation is a fusion of semantic and instance segmentation. In self autonomous driving, medical image analysis, crowd counting, etc. have complicated background components, the high variability of object appearances, numerous overlapping objects and ambiguous object boundaries makes the task challenging. For such applications panoptic segmentation is used which provides several state-of-art methods and robust learning.**

Index Terms— **panoptic segmentation, instance segmentation, semantic segmentation, data annotation, computer vision, medical image segmentation, object detection.**

I. INTRODUCTION

Now-a-days sensors are used for capturing data and are deployed in smart cities to enable the data collection from multiple sources in real time. For security purpose, they are installed in public and residential areas. Devices with video capturing capabilities are significantly in usage. This leads to opportunities for analysis and interface through computer vision technology. Smart city applications such as public security using video surveillance, motion tracking, pedestrian behavior analysis, health care services, medical analysis and autonomous driving, etc. can be developed from the videos and images captured which contain useful information. Machine learning and big data analytic tools play an essential role in the field and on the other hand computer vision takes rely on feature extraction, labelling and image segmentation. Therefore, there is a strong need for proper labelling the data in the AI learning process where information can be extracted from images. Automatic labeling[1] of subject of interest or object is achieved from Bounding box labelling and image segmentation.

Countable entities or objects which have similar texture or structure contained in homogenous region are termed as things. The uncountable regions such as water, roads and sky, etc. are termed as stuff. For identifying things and stuff clearly many visual algorithms are used. One of the segmentation techniques which is used for identification of things and stuff is semantic segmentation. In contrary, another technique is developed which is used for processing of only things which is instance segmentation. In instance segmentation things in the image/video in process where an object is deleted and isolated with a bounding box, or a segmentation mask. Therefore, instance segmentation and semantic segmentation are traditional approaches to current trends in segmentation that is used for masking or highlighting each specific contents in an image.

Scientific segmentation[2] to an operation of labelling things and stuff by denoting the things of the same class with same colors. On the other hand, in instance segmentation things are labelled by different colors, and the stuff is ignored i.e.; the background is ignored. In this line, objects can be further classified

into things and stuff [where stuff would be sky, water, etc.; things would be persons, cars, animals, etc.]. derived from the semantic and instance is panoptic segmentation.

Panoptic segmentation is a complex computer vision task that solves both instance segmentation and semantic segmentation problems together, enabling a more detailed understanding of a given scene. Panoptic segmentation provides detailed contents in the image, generates much more information for analysis, enables computationally efficient operation using AI models by separating both things and stuff of the same class or type using different colors. Unified CNN[2] based methods or merging instance and semantic segmentation results can be used for panoptic segmentation. Panoptic segmentation has great perspective because of its efficiency and also used in wide range of applications. Even though the process of this segmentation is greater, many challenges slow down the improvement. These challenges include scale of objects in the science, the cultured scenes, the weather changes, the quality of used datasets, and computational cost while using a large-scale datasets.

II. BACKGROUND:

Image segmentation improves object detecting methods in which these can be classified as semantic segmentation and instance segmentation. Pixel classification is done in semantic segmentation whereas object classification from a same is done in instance segmentation.

SEMANTIC SEGMENTATION:

Dense prediction is carried out by pixel level segmentation of the scene in semantic segmentation. Semantic segmentation is the operation of labelling each pixel in the image with the corresponding class that represents the category of the pixels i.e.; semantic segmentation classifies different regions in the images belonging to the same category of things or stuff. End to end segmentation of natural images was done with CNN's only after 2014, even though semantic segmentation was proposed in 2007.

The labelling of each pixel in image regions is carried out by the primary process which is spatial analysis. Basic architectures are CNN based methods such as U-Net, Seg Net, Fully Connected Networks (FCN) and Decom Net[3] which are used for segmenting region with acceptable accuracy and quality. These applications are based on the scenes of image and panoptic segmentation allows its deep understanding which helps in the analysis of the scene.

Acquiring accurate data sets is very important in order to deploy a successful system that utilizes the vast advantage of panoptic segmentation. There are public data sets for machine learning which can be easily accessible and can be implemented instead of any system. COCO, Common Object in Context, provides image annotations for 1.5 million common object instances. There is no necessity to manually annotate the objects that appear frequently. Another dataset is city scrapes which is used to life scenes. It includes 10 things categories and 20 stuff categories which includes pedestrian to build things. Pastin is an excellent database set for application of AI.
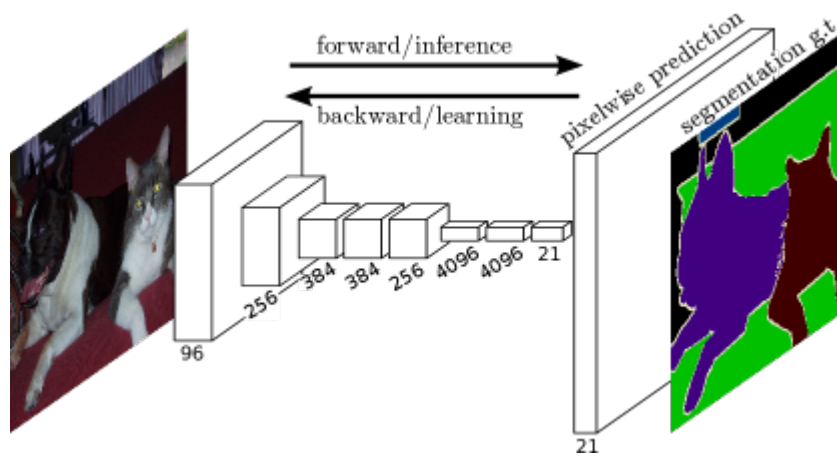
Image Courtesy : From Google

III. TECHNIQUES OF PANOPTIC SEGMENTATION:

A new direction in image segmentation is panoptic segmentation which has been a breakthrough in computer vision and enables a combined view of things and stuff.

Sometimes instance segmentation and panoptic segmentation techniques are used separately before combining the aggregate results of panoptic segmentation.

III.I. RGB IMAGE DATA

The primary data source for panoptic segmentationare RGB images data, because they are widely used in video cameras, image scanners, digital cameras, computer and mobile phone displays. For example, panoptic fusion which is one of the models of panoptic segmentation is used in online volumetric semantic mapping system[5] that combines both stuff and things. The prediction of class labels of background regions(stuff) and foreground objects(things) relies on first predicting pixel wise panoptic labels for entire RGB frames by using semantic and instance segmentation o/ps.
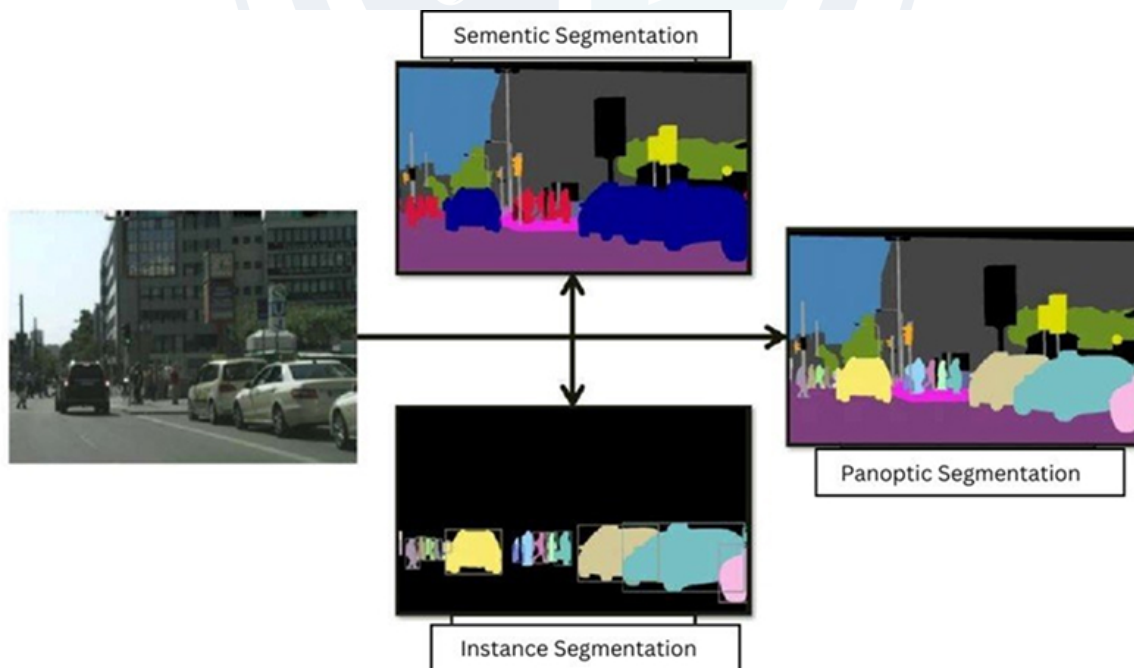
Image Courtesy : From Google

III.II. MEDICAL IMAGES :

Medical image segmentation plays an essential role in computer aided diagnosis systems as medical imaging being one of the most valued applications of computer vision. Different kinds of images are used

for both diagnosis and therapeutic purposes such as X-Rays, Computed Tomography(CT) scan, Magnetic Resonance Imaging(MRI), ultrasound, Nuclear Medicine Imaging and Positron Emission Tomography(PET) scan. In medical images, instance segmentation is used for assigning class values to each pixel and separating objects within the same class. An unique ID is assigned to every single object. Images morphology spatial location and distribute objects helps in analyzing the biological behavior. Instance segmentation has its own limitations as cell-R-CNN which is a panoptic architecture proposed. Typically, the encoder of the instance segmentation model is used to learn the global semantic label features accomplished by jointly training a semantic segmentation model.

III.III. LIDAR DATA :

High resolution digital elevation models with unideal accuracy (10cm can be created) by LIDAR technology which is similar to RADAR. Lidar data are highly accurate and robust so they are preferred for object detectionusing panoptic segmentation of LIDAR space. KITTI dataset contains annotated LIDAR scenes with different environments and scenarios / has extensively used those while an explicit approach has been emphasized. A distinct and contrary approach is adopted to cluster the object segments using CNN architecture. Since the clustering doesn't need computation time and energy as that of CNN's, the model thus adopted can be deployed even with a CPU.

Applications:

Because of the increasing performance of panoptic segmentation systems have developed which are helpful for various tasks and applications.

a) Object detection:

Object detection plays a vital role in computer vision and image processing. Object detection process has become more manageable and accurate due to the panoptic segmentation. It refers to detecting instances of semantic objects of a particular class in digital images and videos. Panoptic segmentation has received significant attention for novel and robust object detection schemes.

b) Medical Image Analysis ;

One of the significant applications of segmentation is medical image analysis. Depending on the segmentation objects, different techniques are used for analyzing and segmenting, with the advent of panoptic segmentation, a wide range of techniques have developed in the medical field. An example like segmentation of overlapped nuclei is taken and a bending loss regularization network was proposed for nuclei segmentation. Bending loss is generated from penalties of large and small curvatures, where high penalties are reversed for contour with large curvatures and small penalties are reserved for contours with small curvatures. This has helped minimize the bending loss and avoided the general contours which were surrounded by multiple nuclei. The MoNuSeg dataset was used to validate this framework using different metrics including the aggregated Jaccard (AJI), Dice, KQ and PQ. With the invert of Panoptic segmentation features fusion network, which is an instance segmentation process to analyze biological and biomedical images, it has become easy for nuclei segmentation. TCGA-tumor data set has been employed to validate the Panoptic segmentation where TCGA-tumor data set contains 30 histopathology images in size 1000x1000 obtained from the Cancer Genome Atlas (TCGA) at 40x magnification. Image comprised of seven organs including breast, bladder, colon, kidney, liver, prostate and stomach.
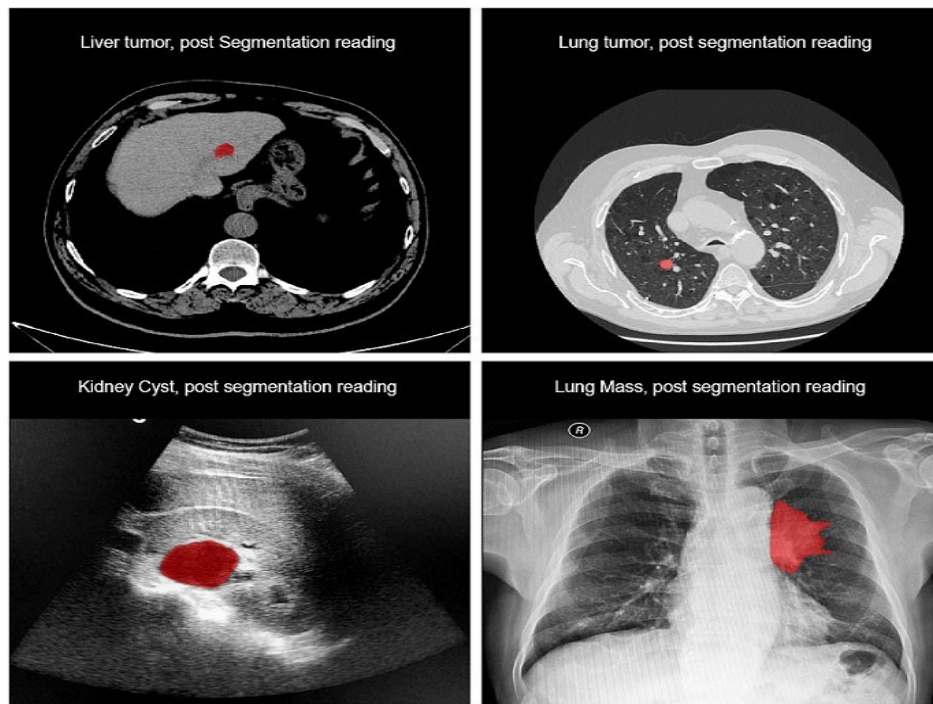
Image Courtesy : From Google

c) Autonomous Self-driving:

One of the main and critical application of Panoptic segmentation is autonomous self-driving. Autonomous self-driving system relies on the deeper level understanding of the scene and better perceptive of the scene. Self-driving Cars system can be builton the data collected from the hardware sensors such as LIDAR, cameras, RADARs and Sonardata (which has been widely used with the latest advances in DL andcomputer vision). Panoptic Segmentation can help in semantic context where pixel represent cars Vs pedestrians vs drivable space and overall architecture context where pixel represent the same car vs other car objects. Pixel level semantic and instance segmentation of camera images based on a single, multitask learning DNN is possible by NVIDIA while is an efficient Scheme. The precise wise and as a whole, understanding of a scene is possible by this method which has enabled the training of a panoptic segmentation base DNN.
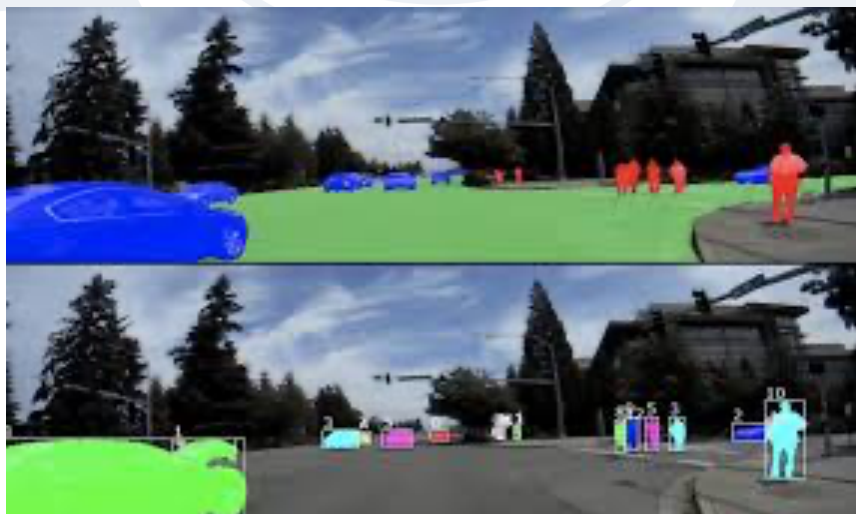
Image Courtesy : From Google

d) UAV remote Sensing:

Road conditions monitoring and urban planning are implemented by UAV remote sensing where panoptic segmentation is the essential method. More comprehensive information to provided by panoptic segmentation than semantic segmentation technology. The panoptic segmentation algorithm identifies UAV helps to solve some problems like the large target scene and small target of UAV, resulting in the back of the foreground targets of the segmentation results and the poor quality of the segmentation mask.

Improvement in the network feature extraction is introduced which has the deformable convolution as one of the network features. To enhance the overall quality of foreground target mask, Mask IoU module is developed and integrated into the instance segmentation branch. UAV-ODC panoptic Segmentation data set is used to test and validate the panoptic segmentation model.

e) Dataset annotations:

Images Categorizing and labelling data for implementing segmentation algorithms or other AI based solution is what can be also employed to perform data set annotations. Panoptic segmentation can be also employed to perform a dataset annotations[7]. In order to annotate a dataset, panoptic segmentation is used which helps to conduct image annotation using a collaborator(human) and automated assistant(based on panoptic segmentation) or both. Instance Segmentation, semantic segmentation and annotating data sets are combinedly obtained from a weaklysupervised panoptic segmentation. An industrial application of panoptic segmentation for annotating datasets are studied where a 3D model is used to generate model of industrial buildings which can improve the inventories performed remotely, where a precise estimation of objects can be performed. For example, in a nuclear power site, equipment positions can be first analyzed using panoptic segmentation of collected panoramic images before going on site, which reduces the cost and time of maintenance.This is a huge break point to advances in automation of large scale industries using panoptic segmentation. A comprehensive virtual aerial image data set, named VALID is proposed, that contains of 6690 high resolution images that are annotated with panoptic segmentation and classified into 30 categories.

f) Data augmentation:

One of the promising application of panoptic segmentation is for data augmentation. Data augmentation schemes that operate exclusively in pixel space and requires no additional data or training and which are computationally inexpensive to implement is possible by using panoptic segmentation. Panoptic data Segmentation method ,PanDA is retraining of existing models of different PanDA augmented data sets, where a high performance gains are achieved in instance segmentation and panoptic segmentation.

Other Applications:

Panoptic segmentations[8][1] finds its application in other research fields namely biology and agriculture for analyzing and segmentation of images. One of the recent research in biology include the research on pigs. Panoptic segmentation has efficiently segmented individual pig through a neural network (for semantic segmentation) using different network heads and post process methods. Even with dirty lens and occlusion, there is a 95% accuracy of segmentation of pigs with panoptic.

IV. PUBLIC DATASETS :

The most important part of the panoptic segmentation is the datasets, which are enabled by the growth of ML and DL algorithms. The datasets usually contain batches thousands or millions of images of ground truth frames, which can be utilized by the models for the implementation of different algorithms. For example, ImageNet helps to evaluate visual recognition algorithms. VGGFace2 helps to validate face recognition methods. The most famous data sets used for image segmentation is Cityscape, Synthia and Mapillary.

Dataset 1. Mapillary Vistas:

It is a traffic related data set with large scale collection of segmented images which is for instance or semantic or panoptic segmentation. This data set is comprised into training, validation and test sets. Size of each set is 18,000, 2000 and 5000 images respectively. Total number of classes is 65, where 28 refers to stuff and 37 for things. It includes different image sizes ranged from 1024x768 to 4000x6000.

Dataset 2 KITTI:

This data set consists of image captures from various places of the metropolis of Karlsruhe, Germany which includes highways and rural region. KITTI is composed of 12K images, 5 different classes, where no. of things and stuff are not specified. Each image of data set contains around 3D pedestrian and 15 vehicles.

Dataset 3 Semantic KITTI:

3D point cloud version of the objects in KITTI data set is the Semantic KITTI. The data is captured with LIDAR from a field of view of 360°. It consists of 43,000 scans of with 28 classes.

Dataset 4 Middlebury Stereo:

It has 7 different object poses which has a depth images and RGB-D image captured from different field-of-views. The images are gleaned with various resolutions including 640x480 and 1280x1024.

Dataset 5 CityScrapes:

This data set is formed from 50 city images, different scenes captured and has large-scale-size. This is the most used data set for instance and Semantic segmentations. 20k labelled images with coarse annotation are present in city scrapes data set where the number of object classes is about 30.

Image Courtesy : From Google

Dataset 6 COCO Panoptic:

Popularly used data set for image segmentation and recognition. Microsoft COCO contains more than 2 million images while 32,800 images are labelled for instance segmentation with labelled images including stuff (various objects like no animals, people, etc.) and things such as reads, sky, etc.. For validating panoptic segmentation, anovel version of COCO data set assigned to instance and semantic labels

of each pixel of any image which different colors are suitable. 123k images are labelled and divided into 172 classes in which 91 are stuff and 80 are things.

CONCLUSION:

Panoptic segmentation is a critical next step in computer vision, allowing us to move beyond perceiving isolated semantic or instance-based information, to a holistic understanding of visual scenes. By clearly separating countable things and uncountable stuff, it allows for a better perception of the scene that is indispensable for further high-level tasks, no matter in what domains. By enabling higher degrees of accuracy, automation, and decision-making, panoptic segmentation can benefit applications ranging from smart city surveillance to autonomous driving, from healthcare diagnostics to industrial inspection. However, with the advancements of the very deep learning models and deep learning datasets, which includes the large-scale annotated datasets, this is no longer the case; despite a series of challenges such as different scales of objects, complex background, and computation consumption.

REFERENCES:

[1] K. He, G. Gkioxari, P. Dollár, and R. Girshick, "Mask R-CNN," *Proceedings of the IEEE International Conference on Computer Vision (ICCV)*, pp. 2961–2969, 2017.

[2] A. Kirillov, K. He, R. Girshick, C. Rother, and P. Dollár, "Panoptic Segmentation," *Proceedings of the IEEE Conference on Computer Vision and Pattern Recognition (CVPR)*, pp. 9404–9413, 2019.

[3] T.-Y. Lin, M. Maire, S. Belongie, et al., "Microsoft COCO: Common Objects in Context," *European Conference on Computer Vision (ECCV)*, pp. 740–755, 2014.

[4] M. Cordts, M. Omran, S. Ramos, et al., "The Cityscapes Dataset for Semantic Urban Scene Understanding," *Proceedings of the IEEE Conference on Computer Vision and Pattern Recognition (CVPR)*, pp. 3213–3223, 2016.

[5] J. Long, E. Shelhamer, and T. Darrell, "Fully Convolutional Networks for Semantic Segmentation," *Proceedings of the IEEE Conference on Computer Vision and Pattern Recognition (CVPR)*, pp. 3431–3440, 2015.

[6] O. Ronneberger, P. Fischer, and T. Brox, "U-Net: Convolutional Networks for Biomedical Image Segmentation," *Medical Image Computing and Computer-Assisted Intervention (MICCAI)*, pp. 234–241, 2015.

[7] A. Geiger, P. Lenz, and R. Urtasun, "Are we ready for Autonomous Driving? The KITTI Vision Benchmark Suite," *Proceedings of the IEEE Conference on Computer Vision and Pattern Recognition (CVPR)*, pp. 3354–3361, 2012.

[8] A. Vaswani, N. Shazeer, N. Parmar, et al., "Attention Is All You Need," *Advances in Neural Information Processing Systems (NeurIPS)*, pp. 5998–6008, 2017

Green Synthesis and Characterization of Bio-plastics from Agro-waste

[1]Aakash Sanjeev Singare, [1*]Nanda Sheshrao Korde
[1,1*]Dayanand Science college, Latur, Maharashtra, India

Abstract: This study explores the synthesis of biodegradable plastics using banana peel starch, a renewable agro-waste, combined with glycerol& sorbitolas plasticizers. Bioplastics were tested to understand their strength, flexibility, and biodegradability. The results indicates that the choice of plasticizers significantly influence the properties of the resulting bioplastics, highlighting their potential as sustainable alternatives to conventional plastics.

Key words: Banana peel, bio-plastic, plasticizer, glycerol, sorbitol

1.INTRODUCTION:

Our whole world is wrapped in Plastic Plastics are widely used in everyday life. Plastics are organic polymers which contains other inorganic compounds. From precious petrochemicals, conventional plastics are derived. Raw materials to make plastic can be Fossil fuels.[1] Due to the plasticity property, the plastics can be molded into a specific shape which is needful. The adaptability and wide range of properties of plastics like flexibility, light weight of material, inexpensive quality has led to the widespread of the plastic use in all fields.[2] Plastic offers many benefits such as flexibility, multiple shapes such as sheets, panels, film. Its adaptability makes it useful in many applications.[3]

Plastics are vital materials in modern life, offering unique properties that make them invaluable in many fields. Due to its properties such as versatility, Lightweight, durability, Cost-Effect, Energy Efficiency etc. Plastics are used in packaging, Medical and Healthcare, Construction, Automotive industries.
With these advantages plastics have much more disadvantages. Few are listed below:

1. Environmental Pollution
2. Threat to Marine and Wildlife
3. Human Health Risks
4. Economic Costs
5. Low Recycling Rates and Waste Management Challenges

The use of plastics cannot be stopped completely as plastics are so crucial to our lives but due to their environmental pollution alternative solution to this problem is being looked into and the alternate solution called 'Biodegradable Plastic'. Due to the activities of living organisms like fungi, bacteria or other microorganisms, plastic can be broken down biologically into organic substances such as carbon-dioxide and water[4], such plastic is called as biodegradable plastic.
In the present research work we synthesized bioplastics from banana peel with glycerol and sorbitol as plasticizer and their different characterization were studied.

2.MATERIALS AND METHODS:

Banana peels were usedto make bioplastic because they are very rich in starch and consist of two different types of polymer chains called amylose and amylopectin. These chains are made up of adjoined glucose

molecules that are bonded together to form bioplastic. Banana fruits were purchased from local market at Latur, Maharashtra, India.

2.1 Synthesis of bioplastic from banana peel:

a) Preparation of banana starch from banana peel:

Banana peels obtained from 5-6 bananas were dipped in sodium metabisulphite (0.2M) solution for 45 minutes to increases the biodegradation period of plastic. These banana peels then boiled it in water for about 30 minutes. Water was removed from the beaker and the peels were left to dry. When peels were completely dried, grinded using grinder until uniform powder was obtained[5].

2.2 Production of bio-plastic:

A) By using glycerol as plasticizer:

In a beaker 5gm of banana powder was placed. 30ml of (0.5 N) HCl was added to this mixture and stirred using glass rod. 2ml Plasticizer (Glycerol) was added and stirred. Then according to pH desired, 0.5 N NaOH was added to maintain neutral pH. The mixture was spread on a Ceramic tile and this was put in the oven at 120°C and was baked. The tile was cooled and the film was scraped off the surface.[6]

B) By using sorbitol as plasticizer:

In a beaker 5gm of banana powder was placed. 30ml of (0.5 N) HCl was added to this mixture and stirred using glass rod. 2ml Plasticizer (sorbitol 1M) was added and stirred. Then according to pH desired, 0.5 N NaOH was added to maintain neutral pH. The mixture was spread on a Ceramic tile and this was put in the oven 120°C and was baked. The tile was cooled and the film was scraped off the surface.[7]

Fig- 2.1 Preparation of banana starch from banana peels	Fig- 2.2 A Production of bio-plastic using glycerol as plasticizer	Fig- 2.2 B Production of bio-plastic using sorbitol as plasticizer
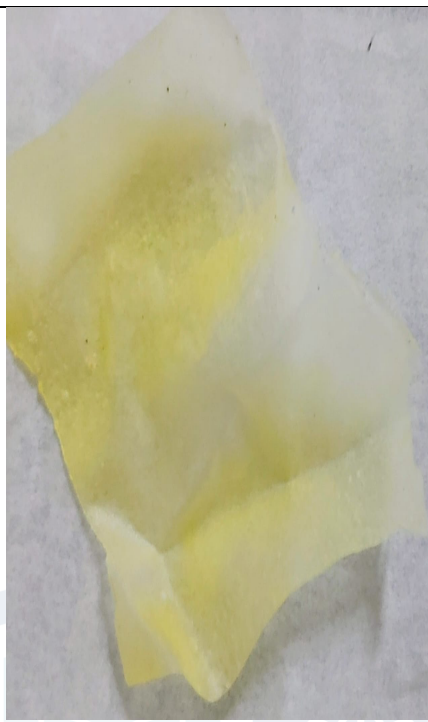
Mechanism:

- The hydrochloric acid is used in the hydrolysis of amylopectin (present in starch), in order to help the process of film formation due to the H-bonding amongst the chains of glucose in starch, since amylopectin blocks the film evolution.
- To neutralize the pH of the medium, sodium hydroxide is used
- Plasticizers glycerol& sorbitol are added to make bioplaqstic more flexible.
- Sodium metabisulfite ($Na_2S_2O_5$) is used To prevents the microbial growth in the peels by acting as an antioxidant.

3. CHARACTERIZATION OF BIOPLASTICS:

1) Moisture content:

Bio-plastic samples of size 1.5 cm^2 were weighed to measure the initial weight (W_1). The samples were dried in an oven at 85°C for 24 h and then weighed again to measure the final weight (W_2). The moisture content was then determined using the following formula[8]:

$$\text{Moisture content (\%)} = \frac{W1 - W2}{W1} \times 100$$

2) Absorption of water:

Firstly bio-plastic samples with size 1.5 cm^2 were dried in oven at 85°C for 24 h and then their dry weight (W_1) was measured. For 24 h, the samples were placed in a beaker with 50 ml distilled water at room temperature. After that the bio-plastics were filtered out and its final weight (W_2) was measured. By using the following formula, absorption of water was found[8]:

$$\text{Absorption of water (\%)} = \frac{W2 - W1}{W1} \times 100$$

3) Swelling Test:

The swelling test is carried out to evaluate their water absorption capacity and hydrophilicity. 1g piece of samples were taken in the test tube containing various solvents such as water, chloroform and methanol and kept in the medium for about 2 hours and the results were recorded accordingly[9].

4) Solubility:

a) **Solubility in water**: To test water solubility, synthesized bio-plastic samples, each 1.5 cm², were dried in an oven at 85°C for 24 hours. The dry weight (W_1) of the bioplastic samples was measured. The weighed bio-plastic was placed in a beaker with 50 ml of distilled water and left at room temperature for 24 hours. After that the bio-plastic residue was obtained by filtering the water and dried again in an oven at 85°C for 24 h. After 24 h the weight of dried sample was taken as final weight (W_2). The solubility of the bio-plastic in water was calculated using a specific formula given below[10]:

$$\text{Solubility in water (\%)} = \frac{W1 - W2}{W1} \times 100$$

b) **Solubility in alcohol**: Synthesized bio-plastic samples, each 1.5 cm², were dried in an oven at 85°C for 24 hours. The dry weight (W_1) of the samples was measured. Kept this weighted bio-plastic in test tubes with caps containing 10 ml ethanol for 24 hrs. at room temperature. After 24 hrs. the bio-plastic residue was obtained by filtering the water and again dried in an oven at 85°C for 24 hrs. After 24 hrs. the weight of dried sample was taken asfinal weight(W_2).The solubility in alcohol was calculated using a specific formula given below[10]:

$$\text{Solubility in Alcohol (\%)} = \frac{W1 - W2}{W1} \times 100$$

5) Bio-degradability Test:

Bio-plastic samples of size 1.5 cm² were weighed to measure the initial weight (W_1). This weighted samples were placed under 2 cm of wet garden soil. They were kept in Styrofoam cups. The bioplastic samples with Styrofoam cups were kept at room temperature and the soil was kept moist for 5 days. After 5 days, the bio-plastic residue was collected from the soil and cleaned with water and then dried at 85°C in an oven for 24 hours. After 24 h the weight of dried sample was taken as final weight (W_2). Biodegradability was calculated using a specific formula given below[11]:

$$\text{Bio-degradability (\%)} = \frac{W1 - W2}{W1} \times 100$$

6) Thickness measurement:

A screw gauge was used to compute the thickness of the bioplastics. The thickness of samples were measured at various points. Then average thickness was calculated[12].

7) **Chemical resistance:** To check chemical resistance, bioplastic films were socked in 0.1N NaOH and 0.1N HCl solution for 24 hours. The effects of strong acid and base on the samples were ascertained by measuring change in appearance[13].

8) **Flame test:** Bio-plastics were weighed in order to obtain initial weight and then they were subjected to high flame for 30 seconds and was observed for any poisonous gases[14].

9) Creep measurements:

To measure the creep behavior of bio-plastics, we need to assess how the material deforms over time under a constant load and temperature. Synthesized bio-plastic samples with consistent dimensions were used. The thickness of each sample at multiple points using a screw gauge was measured and the average thicknesses were calculated.

Equipment calibrated to maintain constant1.0MPa stress and 25°C temperature and ensuring proper alignment to avoid inaccurate readings. Bio-plastic samples were secured in the grips of the testing machine and strain at regular intervals was recorded.

10) Fourier Transform Infrared Spectroscopy (FTIR)

Aligent Cary 630 FTIR spectrometer was used to investigate the interaction and chemical composition changes in synthesized bio-plastics. Spectra of bio-plastics synthesized from banana peels were recorded.

4. RESULT AND DISCUSSION

In the present study bio-plastics were prepared from banana peel using plasticizers as glycerol and sorbitol etc. Also prepared bio-plastics were characterized by moisture content, absorption of water, swelling test, solubility, bio-degradability, thickness measurement, chemical resistance, flame test, Creep measurements and Fourier Transform Infrared Spectroscopy (FTIR).

The result of moisture content and absorption of water test is depicted in Table-1

Table-1 Moisture content and Absorption of water test

Sr. No.	Sample No.	Moisture content (%)	Water Absorption (%)
1	1	35.36	41.36
2	2	11.45	32.48
3	**Control-1**	5.38	69.72

Control-1, had the lowest moisture content while samples with glycerol had the higher and sample with sorbitol had the lower. A previous study explained that glycerol has hydroxyl groups that attracts water molecules forming hydrogen bonds and contain more water in the structure[15] while sorbitol forms substantial hydrogen bonds with the starch molecules, which bring down the affinity for water molecules.

In the test of water absorption, control -1 absorbed more water. This is because the hydroxyl group in starch attracts water molecules and gelatinization breaks starch granules, allowing water to diffuse. Previous

studies show water absorption increases with more starch. Thus, adding plasticizer reduces water absorption.[16]. With glycerol had the highest absorption of water, followed sorbitol. Glycerol attracts water molecules more strongly than sorbitol.

The result of swelling test is depicted in Table-2.

Table-2 Swelling Test

Sample No.	Final weight of the sample in water (g)	Difference in weight (g)	Final weight of the sample in Chloroform (g)	Difference in weight (g)	Final weight of the sample in Methanol (g)	Difference in weight (g)
1	1.64	0.64	1.04	0.04	1.03	0.03
2	1.21	0.21	1.01	0.01	1.02	0.02
Control-1	1.00	0.00	1.00	0.00	1.00	0.00

When the bioplastic was soaked in organic solvents like chloroform and methanol, its weight changed narrowly. However, when soaked in water, it gained a little weight making it a more reliable material than other materials.

Bioplastics swell in water because they are hydrophilic in nature and water is polar, hydrogen bonding solvent so strong polymer-water interaction allowed water to enter and expand polymer size. Organic solvents like chloroform (non-polar) and methanol (less-polar) cannot form strong hydrogen bond with polymer.

The result of solubility in water and in alcohol depicted in Table-3

Table-3 Solubility in water and in alcohol

Sr. No.	Sample No.	Solubility in water (%)	Solubility in alcohol (%)
1	1	65.75	57.18
2	2	60.76	52.38
3	**Control-1**	48.39	46.95

From the above results we found that adding plasticizers increased the water solubility of all bioplastics. Starch molecules have a crystalline structure with hydrogen bonds, making starch granules insoluble in cold water[17]. Like water absorption, bioplastics with glycerol as a plasticizer showed the highest water solubility and lowest in samples with sorbitol. This can be explained with the fact that glycerol has a smaller molecular weight and attracts water more than sorbitol, making it easier for water molecules to enters easily into polymer chains.[18] Previous studies show that the type of plasticizer affects a bioplastic's water solubility.[19]

From the result of above study, adding plasticizers increased the alcohol solubility of all synthesized bioplastics. In existence of glycerol plasticizer, bioplastic samples had the elevated solubility in alcohol, and in presence of sorbitol plasticizer had the lesser solubility in alcohol and samples with glycerol and polyvinyl chloride had solubility levels between those with glycerol l and sorbitol. At room temperature, sorbitol is slightly soluble in alcohol but starch does not dissolve.[20]

The result of bio-degradability and thickness measurement is depicted in Table-4

Table-4 Bio-degradability and thickness measurement

Sr. No.	Sample No.	Bio-degradability (%)	thickness mm
1	1	71.59	0.03
2	2	60.52	0.05
3	**Control-1**	43.69	0.02

Physiochemical properties include chemical structure, molecular weight, water affinity, and surface area etc. of the bio-plastics determine their biodegradation ability.[21] Control-1 was observed to have the lowest biodegradation. Biodegradation of bioplastic samples increased. with the plasticizers. Also, biodegradation increased due to better water absorption and water absorption increased due to the water affinity of plasticizers like glycerol and sorbitol towards water. Bio-plastic samples with glycerol showed the highest biodegradation than sample with sorbitol.

Glycerol films are thicker due to higher moisture retention but less dense. Sorbitol films are usually thicker and denser because of their tight and crystalline structure. It makes stronger bio-plastics.The result of Chemical resistance is depicted in Table-5

Table-5 Chemical resistance measurement

Sample	Acid solubility	Base solubility
I	Yes	No
II	Yes	No
Control-I	Yes	No

Three bioplastic samples were tested to see how they resist acid and alkali. All the three samples broke down quickly in acid while it was not in alkali.

Flame Test: When the three bio-plastic samples were burned, they degraded without releasing harmful gases making them eco-friendly to environment. They burned like a regular paper.
The result of creep measurement is depicted in Table-6

Table-6 Creep Measurement

Sr. No.	Time (hours)	Strain (%)		Creep Rate (%/hrs.) = strain/time	
		Sample I	Sample II	Sample I	Sample II
1	0	0.00	0.00	--	----
2	1	0.15	0.10	0.15	0.10
3	24	0.22	0.18	0.0091	0.0075
4	48	0.35	0.25	0.0072	0.0052

Glycerol, a hydrophilic plasticizer, reduced intermolecular forces in the starch by forming hydrogen bonds with glucose chain, increasing chain mobility. This enhances flexibility but likely increases creep deformation under constant load, as the loosen structure allows polymer chains to slip more easily over time.

Sorbitol, with its stronger hydrogen bonding and lower hygroscopicity, creates a stiffer, more cohesive matrix. This reduces chain movement resulting in lower creep rates indicating better dimensional stability.

Table-7 IR Measurements

Sample No.	O-H stretching	C-H stretching	C=O stretching	C-O stretching	C-H deformation	C-C stretching
1	3380.7 cm^{-1}	2918.5 cm^{-1}	1710.8cm^{-1}	1162.9 cm^{-1}	1390.3cm^{-1}	872.1cm^{-1}
2	3291.2 cm^{-1}	2937.1cm^{-1}	1636.3cm^{-1}	1103.3cm^{-1}	1364.2cm^{-1}	861.0cm^{-1}

Broad peaks at 3380.7 cm^{-1} and 3291.2 cm^{-1} indicating hydrogen bonding, primarily from hydroxyl groups in starch (amylose and amylopectin), glycerol and sorbitol respectively. These peaks reflect the interaction between glycerol, sorbitol and the starch matrix, enhancing flexibility.[23]

Peaks at 2918.5 cm^{-1} and 2937.1cm^{-1} are associated with C-H stretching vibrations from the aliphatic chains in starch, glycerol and sorbitol. This confirms the presence of organic components in the bio-plastics.[24]

Peak at 1710.8 cm^{-1} and 1636.3cm^{-1} indicates carbonyl groups, often from residual organic acids or ester linkages formed during processing. This can also reflect interactions between starch, glycerol and sorbitol.

Peaks in the range at 1162.9 cm^{-1} and 1103.3cm^{-1} are associated with C-O stretching in starch, glycerol and sorbitol indicating the polysaccharide backbone and plasticizer integration, confirming C-O stretching in the starch-glycerol and starch-sorbitol matrix.

5. CONCLUSION

This research is significant because it uses agro-waste, like banana peel to create valuable materials. FTIR analysis showed the presence of functional groups, confirming no harmful substances are in the material, making it environmentally safe. The carboxylic acid in the material suggests potential uses in pharmaceuticals. Plasticizers added to the material make it more workable, while pectin and cellulosic fibers provide strength and ensure biodegradability, making it suitable for short-term packaging.

Although promising, the material needs further improvements, especially to make it more water-resistant. Using banana peel as waste to produce bioplastic is an effective way to address fruit waste disposal and promote sustainable resource use.

REFERENCES:

[1] Deepti Sharma, Archana Mankad, International Journal of Life Sciences Research, Vol. 6, Issue 4, pp: (354-357), Month: October - December 2018

[2] Isvarya. M1, Bincy. T. Mathew1, Nithish kumar. V1, Rajathi. K2, Journal of Emerging Technologies and Innovative Research, 2021 JETIR July 2021, Volume 8, Issue 7, p-b-39-b-47

[3] Jaikishan Chandarana, P. L.V. N Sai Chandra, International Journal of Scientific Research & Engineering Trends Volume 7, Issue 1, Jan-Feb-2021

[4] Anne O, (2005). Making a plastic from Potato starch. Advances in chemical sciences, p1-7

[5]   Jayachandra, S., Yardodi and Patil, ―Biodegradable plastic from waste material.‖ International Journal of Pharmaceutical Research and Allied Sciences, vol. 5, no. 4, pp. 56-66, 2016.

[6]   Pratik Patil, Varsha Bhat, Mitali Nagotkar, Disha Hebbar, International Research Journal of Engineering and Technology (IRJET), Volume: 09 Issue: 03 | Mar 2022

[7]   Yaradoddi J, Hugar S, Banapurmath N, Hunashyal A, Sulochana M, Shettar A, et al. Alternative and renewable biobased and biodegradable plastics. Springer International, Publishing; 2019.

[8]   Arifa Shafqat , Nabil Al-Zaqri , Arifa Tahir , Ali Alsalme, Saudi Journal of Biological Sciences, s 28 (2021) 1739–1749

[9]   Mihir Patel, Farhaz Rahod, Sarthak Vasava,Rahul Thakor, Neha Kulshreshtha, International Journal of Engineering Trends and Technology (IJETT) - Volume 67 Issue 4 - April 2019

[10]   González A, Alvarez Igarzabal CI (2013) Soy protein–Poly (lactic acid) bilayer films as biodegradable material for active food packaging. Food Hydrocoll 33(2):289–296

[11]   Rizwana Beevi. K, Sameera Fathima. A.R, Thahira Fathima. A.I, Thameemunisa. N, Noorjahan, C.M, Deepika. T., Internationnal Journal of Scientific & Technology Research Vol.9, issue 01, January 2020

[12]   May Zon Kyawt Oo, Myo Thu, Zin Nyi Nyi Tun, International Journal of Advances in Scientific Research and Engineering (ijasre), Vol 5 , issue (8), August-2019

[13]   Jouki M, Khazaei N, Ghasemlou M, HadiNezhad M Carbohydr Polym 96(1):39–46, 2013

[14]   Mc Hugh, T. H., and Krochta, J. M. (1994) Sorbitol vs glycerol-plasticized whey protein edible films: Integrated oxygen permeability and tensile property evaluation, *Journal of Agricultural and Food Chemistry*, 42(4).

[15]   Cerqueira, M.A., Souza, B.W.S., Teixeira, J.A., Vicente, A.A., 2012. Food Hydrocolloids 27 (1), 175–184

[16]   Kurt A, Kahyaoglu T Carbohydr Polym 104:50–8, 2014

[17]   Azahari, N.A., Othman, N., Ismail, H., J. Phys. Sci. 22 (2), 15–31 , 2011

[18]   Sarker, M.Z.I., Elgadir, M.A., Ferdosh, S., Akanda, M.J.H., Aditiawati, P., Noda, T., Starch-Stärke 65 (1–2), 73–81, 2013.

[19]   Ghasemlou, M., Khodaiyan, F., Oromiehie, A., Carbohydr. Polym. 84 (1), 477–483, 2011.

[20]   Chiumarelli, M., Hubinger, M.D., Food Hydrocolloids 38, 20–27, 2014

[21]   O'Neil, M.J., 2006. The Merck Index: Whitehouse station, New Jersey, Merck Research Laboratories, p. 1498, 2006.

[22]   Tokiwa, Y., Calabia, B.P., Ugwu, C.U., Aiba, S., Int. J.Mol. Sci. 10 (9), 3722–3742. Vethaak, A.D., Leslie, H.A., 2016. Plastic, 2009

[23]   Ano, Y., Hours, R.A., Akakabe, Y., Kataoka, N., Yakushi, T., Matsushita, K., Adachi, O., 2017.. Biosci. Biotechnol. Biochem. 81 (2), 411–418.

[24]   Yin, Y., Li, J., Liu, Y., Li, Z., 2005. J. Appl. Polym. Sci. 96, 1394–1397.

Sign to Speech: A Machine Learning Approach for Deaf and Mute Communication

[1] Dr. Zubin Bhaidasna, [2]Dr. Hetal Bhaidasna

[1]Assistant Professor, [2]Assistant Professor
[1]Department of Computer Engineering,
[1]GCET, CVM University, V. V. Nagar, Gujarat, India

Abstract— **This research demonstrates a novel attempt to help people who are both deaf and mute by creating a communication assist system that translates hand signs into words. The system uses a camera to capture hand movements and the trained recognition model identifies them. After recognition, text translation followed by speech synthesis through a voice module is performed. To train and evaluate the system, a custom dataset capturing common gestures was created. The sign-to-speech solution is tailored to operate on constrained, cost-effective hardware such as smartphones and tablets. Furthermore, this review discusses the commonly used datasets in sign-to-speech research and their limitations in terms of size, diversity, and standardization. It also suggests a general flow of implementation starting from data collection, preprocessing, feature extraction, model training, and conversion to speech. The paper highlights key challenges such as gesture variability, occlusion, and real-time processing.**

Index Terms— **Sign Language, Machine Learning, CNN**

I. INTRODUCTION

Communication is an essential human want, yet tens of millions of deaf and mute individuals face every day barriers in expressing themselves, in particular in environments in which sign language isn't widely understood. Sign language, even though wealthy and expressive, stays strange to a great deal of the overall population, developing an opening between hearing-impaired individuals and the rest of society. Traditional answers like interpreters or written communication regularly fall brief in spontaneity and inclusivity, especially in real-time interactions. This disconnects limits get admission to essential offerings, schooling, and social inclusion for the listening to and speech impaired.

To overcome this mission, there is a growing need for structures, which can translate signal language into spoken words, supporting to bridge the distance in conversation. "Sign to Speech" is a step toward allowing smoother interactions by means of converting hand gestures into audible language. Using visual inputs like stay hand actions, the system techniques gestures via structured steps such as video capture, frame evaluation, gesture popularity, and output generation. By focusing on local sign dialects and body motion styles, the system enhances usability and attractiveness among various users. This practical approach empowers individuals to engage more confidently in day-to-day conversations, fostering inclusion and dignity in communication.

II. BACKGROUND STUDY

Effective communique is a center element of human existence, allowing individuals to specific mind, emotions, and needs. For humans with listening to or speech impairments, however, communication can emerge as an extensive barrier, mainly while interacting with the ones unexpected with signal language. Sign language serves as a crucial medium that empowers these people to engage in meaningful communicate. Despite its importance, a verbal exchange divide stays among sign language customers and the general public, primarily due to the lack of giant information of sign language. This hole poses demanding situations in regular situations which includes searching for assistance, accessing services, or participating in social and academic environments, ultimately affecting the overall first-rate of existence of in another way-abled people.

The goal of this studies is to bridge the communication barrier confronted by using individuals with hearing and speech impairments in a greener and cost-powerful manner. A review of existing literature [1] reveals that current methodologies face significant limitations in two critical aspects: recognition accuracy and suitability for real-time implementation. Although a variety of machine learning and deep learning techniques—such as Convolutional Neural Networks (CNN) [2–6], Support Vector Machines (SVM), and K-Nearest Neighbors (KNN)—have been explored in past studies, they often fall short in delivering consistently high performance and responsiveness necessary for practical applications.

Moreover, sure tactics rely on specialized external hardware, including sensor-integrated gloves, which not handiest growth the fee of deployment but additionally lessen the benefit of use for the end user. These demanding situations restriction the accessibility and scalability of such structures, specifically in resource-restrained settings. To overcome those troubles, the present work proposes a solution that extensively complements both the accuracy and actual-time processing capabilities of Indian Sign Language (ISL) reputation systems. The proposed technique is designed to paintings with standard digital camera input, putting off the need for external gadgets, thereby offering an low-cost and user-pleasant opportunity for effective verbal exchange guide [7].

A green actual-time imaginative and prescient-based totally system became advanced for recognizing American Sign Language (ASL) alphabets. One most important assignment became the dearth of a appropriate dataset, leading the researchers to create their very own. The version required square snap shots, just like how CNN in Keras methods statistics. Another challenge was selecting the right image filter out for feature extraction. After testing numerous alternatives, Gaussian blur changed into selected for most excellent results [9]. This look at employs the CamShift set of rules to isolate the human hand from complicated backgrounds and stumble on actual-time gestures. A convolutional neural network then recognizes ten commonly used digit gestures, trained on a dataset of 1,600 hand images (400 per category, totaling 4,000 gestures). The system achieves an impressive 98.3% accuracy in real-time recognition [10]. : In this, a method based on artificial neural networks was suggested for recognizing Indian sign language. It proposed a technique to find a 32-set of combinations—10 for each up and down movement of the fingers—in order to get matching Tamil letters. The method required converting decimal numbers from the up/down position of the fingers into categories that could recognize Tamil alphabets. A collection of static data was recorded as 640 x 480-pixel pictures. Images were converted from RGB to greyscale using palm image extraction [13].

Table 1 Comparison of various sign language Methods

Sign Language	Dataset	Approach Used	Methodology	Working On
American Sign Language (ASL)[2]	ASL datasets	Desktop application for real-time sign	CNN	Work on Real-time text conversion
Chinese Sign Language[5]	Custom dataset	Wearable sign language recognition system	CNN, stretchable strain sensors	Combines multiple sliding windows for sentence recognition
American Sign Language (ASL) & British Sign Language (BSL)[6]	Custom dataset	Recognition using computer vision algorithms and neural networks	CNN	Real-time feedback integration, flexible for various settings
Assamese Sign Language[7]	Custom dataset	Recognition system for Assamese Sign Language	MediaPipe, feed-forward neural network	Emphasizes local sign language dialects and utilizes Media Pipe for accurate real-time hand and body landmark detection to interpret gestures

Sign Language	Dataset	Approach Used	Methodology	Working On
				effectively.
American Sign Language (ASL)[9]	Custom dataset	Recognize using the Filter CNN	CNN	Works on static dataset
Indian Sign Language (ISL) [16]	Custom dataset	Recognition of ISL gestures	3D CNN	works on both static and dynamic gestures, diverse dataset conditions

III. METHODOLOGY OF THE PROPOSED WORK

The proposed system aims to recognize hand gestures made by deaf and dumb individuals using real-time video processing and machine learning. Below Figure 1. represent the flow of proposed work for the sign language identification. First, we will capture live video using a camera or webcam, where the user performs hand gestures representing words in sign language. The video is continuously streamed and divided into individual frames in real time for processing. After that, each frame is resized and cropped to focus on the region of interest, typically the area containing the hand. This preprocessing step may also include background subtraction, contrast adjustment, and noise removal to enhance clarity and isolate the hand gesture more effectively.
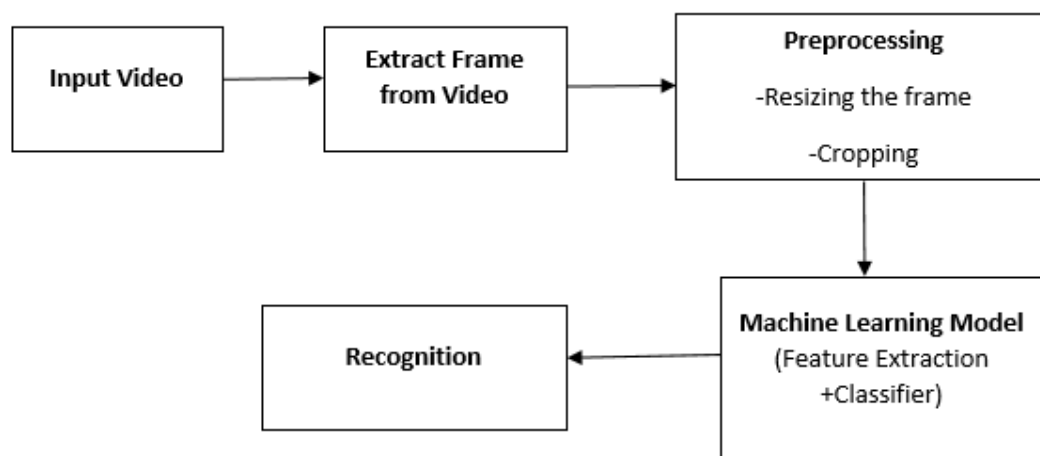
Fig 1. Flow of Proposed Work

Once the body is pre-processed, a system mastering or deep gaining knowledge of version which include a Convolutional Neural Network (CNN) [6,9,16,18]is implemented to extract vital spatial and temporal capabilities from the gesture. These features are then surpassed thru a skilled category model that identifies the precise gesture being proven. The classifier maps the gesture to its corresponding phrase or phrase from the educated dataset. Finally, the recognized word is displayed at the screen or converted to speech output. This actual-time method helps bridge communication among deaf and dumb individuals and the listening to network through translating sign language into understandable spoken or written phrases.

IV. DATASET

ASL Alphabet Dataset (Kaggle))

The ASL Alphabet Dataset available on Kaggle carries over 87,000 categorized RGB snap shots representing 26 hand signs of the American Sign Language (A–Z). Each photograph is 200x200 pixels and perfect for training CNN models for static gesture reputation. The dataset is user-pleasant and broadly adopted in research and training. It helps actual-time hand gesture class. It is freely reachable and appropriate for beginner to advanced ML initiatives.

RWTH-BOSTON-50 Dataset

This dataset incorporates continuous video sequences of 50 American Sign Language words, captured from multiple signers. It is designed for dynamic sign recognition and is commonly used in sequence modeling with RNNs or LSTM. Each video is labeled and preprocessed for gesture segmentation. It enables sentence-level translation research. Developed by RWTH Aachen University, it is available upon academic request.

Indian Sign Language (ISL) Dataset

This ISL dataset capabilities a group of static and dynamic hand signs and symptoms accomplished by means of more than one customers, protecting round 20 usually used Indian signs and symptoms. It incorporates each photographs and short movies. The dataset became created by using IIIT-Hyderabad and has been used in more than one Indian research papers. It helps real-time gesture recognition the use of CNN or hybrid models. Access is commonly granted for academic and studies purposes.

ASL Digits Dataset

This dataset consists of pix of hand gestures representing digits zero–9 in American Sign Language. It consists of over 2,000 grayscale snap shots with uniform background and lighting fixtures, making it perfect for digit classification the usage of easy CNN fashions. The dataset is light-weight, smooth to preprocess, and properly-suitable for real-time programs. It is beneficial for fundamental sign language systems which include numerical input or digit popularity. The dataset is open-source and to be had thru ML repositories and GitHub.

V. CHALLENGES

1. Variation in Hand Gestures: Different customers might also perform the identical gesture otherwise in phrases of pace, angle, and hand length, making it difficult for the version to generalize and preserve high accuracy throughout all customers.

2. Complex Backgrounds and Lighting Conditions: Real-time video may be captured in various environments, wherein inconsistent lighting fixtures and cluttered backgrounds can intervene with correct hand detection and gesture recognition.

3. Lack of Large and Diverse Datasets: High-best, categorized sign language datasets are restrained, especially for nearby or much less generally used sign languages. This shortage affects the training and overall performance of deep studying models.

4. Real-Time Processing Requirements: For powerful communication, the system have to apprehend gestures right away, which demands green algorithms and hardware able to processing video frames in real time without delay.

5. Gesture Overlap and Transition: Continuous gesture reputation is tough, as gestures may additionally circulate each other without clear barriers, making it tough to locate while one gesture ends and some other starts off.

CONCLUSION

The "Sign to Speech" machine helps deaf and mute people talk to others with the aid of changing hand signs into spoken words. It makes day by day communication less difficult and quicker without needing an interpreter or writing. The gadget works in actual time and uses neighborhood sign languages, so it feels natural for customers. It watches hand movements the usage of a camera and turns them into voice or text. This makes it useful in places like schools, hospitals, banks, and places of work. People with listening to or speech troubles can experience greater confident and independent. The machine also enables others apprehend and encompass them better.

REFERENCES

[1] S. Alyami, H. Luqman, M. Hammoudeh, Reviewing 25 years of continuous sign language recognition research: Advances, challenges, and prospects, Inf. Process. Manag. 61 (5) (2024) 103774.

[2] Y. Obi, K.S. Claudio, V.M. Budiman, S. Achmad, A. Kurniawan, Sign language recognition system for communicating to people with disabilities, Procedia Comput. Sci. 216 (2023) 13–20 7th International Conference on Computer Science and Computational Intelligence 2022.

[3] H. Alsolai, L. Alsolai, F.N. Al-Wesabi, M. Othman, M. Rizwanullah, A.A. Abdelmageed, Automated sign language detection and classification using reptile search algorithm with hybrid deep learning, Heliyon 10 (1) (2024) e23252.

[4] S. Arooj, S. Altaf, S. Ahmad, H. Mahmoud, A.S.N. Mohamed, Enhancing sign language recognition using CNN and sift: A case study on Pakistan sign language, J. King Saud Univ. Comput. Inf. Sci. 36 (2) (2024) 101934.

[5] Y. Liu, X. Jiang, X. Yu, H. Ye, C. Ma, W. Wang, Y. Hu, A wearable system for sign language recognition enabled by a convolutional neural network, Nano Energy 116 (2023) 108767.

[6] S.N. Koyineni, G.K. Sai, K. Anvesh, T. Anjali, Silent expressions unveiled: Deep learning for british and american sign language detection, Procedia Comput. Sci. 233 (2024) 269–278 5th International Conference on Innovative Data Communication Technologies and Application (ICIDCA 2024).

[7] J. Bora, S. Dehingia, A. Boruah, A.A. Chetia, D. Gogoi, Real-time Assamese sign language recognition using mediapipe and deep learning, Procedia Comput. Sci. 218 (2023) 1384–1393 International Conference on Machine Learning and Data Engineering.

[8] T. Liu, T. Tao, Y. Zhao, M. Li, J. Zhu, A signer-independent sign language recognition method for the single-frequency dataset, Neurocomputing 582 (2024) 127479.

[9] A Review Paper on Sign Language Recognition for The Deaf and Dumb published by R Rumana, Reddygari Sandhya Rani, and Mrs. R. Prema, in the year 2021.

[10] Indian Sign Language Recognition using Convolutional Neural Network published by Rachana Patil, Abhishek Bahuguna, and Mr. Gaurav Datkhile, in the year 2021.

[11] Machine Learning Techniques for Indian Sign Language Recognition published by Kusumika Krori Dutta, in the year 2017.

[12] Indian Sign Language Recognition Using Eigen Value Weighted Euclidean Distance Based Classification Technique published by Joyeeta Singha, Karen Daas, in the year 2013.

[13] Indian Sign Artificial Neural Network Based Method for Indian Sign Language Recognition published by Adithya V., Vinod P. R., and Usha Gopalakrishnan, in the year 2013.

[14] Translation of Sign Language for Deaf and Dumb People published by Suthagar S., K. S. Tamilselvan, P. Balakumar, B. Rajalakshmi, C. Roshini, in the year 2020.

[15] Sign Language Recognition: State of The Art. ARPN Journal of Engineering and Applied Sciences Published by Sahoo, A. K., G. S. Mishra, and K. K. Ravulakollu in the year 2014.

[16] D.K. Singh, 3d-cnn based dynamic gesture recognition for indian sign language modeling, Procedia Comput. Sci. 189 (2021) 76–83 Computational Linguistics.

[17] Bhaidasna, Hetal, and Zubin Bhaidasna. "Object Detection Using Machine Learning: A Comprehensive Review." International Journal of Scientific Research in Computer Science, Engineering and Information Technology (2023): 248-255.

[18] Bhaidasna, Hetal, and Zubin Bhaidasna. "A Survey on Machine Learning Algorithms ", International Journal of Emerging Technologies and Innovative Research, ISSN:2349-5162, Vol.6, Issue 3, page no.53-56, March-2019.

Systematic Approach to Convert Industrial Electric Oven to Piped Natural Gas Oven to reduce environmental impact without impacting Process and product Performance

Dr. Nitin Prabhu Kulkarni[1], Dr Avinash S. Desai[2], Dr. Sandeep Tare[3]

[1]PhD. Management, [2]PhD. D.Litt (Management), [3]PhD., D. Litt Professor. (Management),
[1]Sri Satya Sai University, Sehore, India, [2]Regd. Professor and Group Director, LNTC-Group College Indore
[3]Director-MER-LNCT Gr. Chairman- Indian Institute of Materials Management

Abstract: Industrial ovens are substantial energy consumers and play a crucial role in influencing product quality. Therefore, enhancing their performance should be a priority for manufacturers. This review outlines an innovative and actionable strategy for enhancing oven performance, with a focus on improving energy efficiency, optimising processes, and promoting environmental sustainability. The proposed approach is divided into three phases: gaining a deep understanding of the product, refining the production process, and optimising process parameters. Key parameters such as temperature, air flow rate, and cycle time are adjusted to achieve energy savings while minimising environmental impact.

Keywords: Process parameters, Performance improvement, Optimisation, Environmental Impact, Electric Oven, PNG Oven.

I. INTRODUCTION:

Optimising Manufacturing Lead Time, Energy Efficiency and Reducing Environmental Impact

Manufacturing companies continually seek to enhance operational efficiency and reduce production costs while improving customer satisfaction. One of the most critical performance indicators in achieving these goals is lead time, as it directly impacts both customer experience and internal operational expenses.

In discrete manufacturing, lead time improvements are typically achieved through ongoing process optimisation and investment in advanced machinery. However, in continuous manufacturing systems, where all operations are interdependent, the pace of production is determined by the slowest process. This constraint is especially evident in thermal treatment applications such as curing, which require materials to pass through long ovens that maintain precise temperatures over extended periods.

To accommodate faster production rates, these ovens must be lengthened, increasing both space and energy requirements. Yet, modifying or replacing this equipment is often prohibitively expensive. As a result, efforts to improve performance in such systems often focus on enhancing oven efficiency rather than expanding infrastructure.

Industries employ various types of heat treatment equipment, including furnaces, kilns, and convection ovens, to fulfil tasks like curing, drying, and baking. Convection ovens, which use hot air nozzles for heat transfer, are widely used due to their effectiveness. However, even high-performing ovens lose efficiency over time due to structural degradation, changing process demands, and technological obsolescence. This

opens up significant opportunities for improvement, particularly in terms of energy efficiency and production throughput.

As component sizes shrink and product complexity increases, traditional heating systems struggle to meet evolving manufacturing needs. Consequently, there is growing interest in site-wide energy optimisation, particularly within heating processes. Large-scale retrofitting, however, presents challenges such as limited space, production disruptions, heat loss, outdated layouts, and high costs. A more feasible approach is to focus on energy reduction at the unit level, particularly within individual ovens, to improve sustainability without extensive facility upgrades.

Enhancing Industrial electric oven performance offers numerous benefits, including improved product quality, higher production efficiency, enhanced worker safety, reduced waste, and lower energy consumption. Understanding and controlling process variations is key to maintaining consistency, meeting safety standards, and reducing operating costs. These insights enable manufacturers to streamline workflows, minimise defects, lower scrap rates, and reduce transition times between product lines.

Industrial electric heating plays a central role in many sectors, including food processing, ceramics, metallurgy, and chemical manufacturing. Historically, Industrial electric ovens have been widely adopted for their precise temperature control, ease of use, and point-of-use efficiency. However, their environmental impact depends heavily on the Industrial electricity source. In regions where power is generated primarily from coal or other fossil fuels, Industrial electric ovens can have a substantial indirect carbon footprint, raising concerns about long-term sustainability.

In contrast, Piped Natural Gas (PNG) offers a more environmentally friendly and cost-effective alternative. PNG combustion generates significantly lower carbon dioxide emissions compared to coal-based Industrial electricity and also reduces pollutants such as sulfur oxides, nitrogen oxides, and particulates. A robust pipeline network; PNG provides a reliable and continuous energy supply well-suited for Industrial electric applications.

Converting Industrial electric ovens to PNG-powered systems presents a compelling opportunity for manufacturers to lower both operating costs and carbon emissions. While this transition requires initial investments in burners, pipelines, and safety infrastructure, the long-term benefits, particularly in regions with carbon-intensive Industrial electricity grids, can be substantial. The move supports sustainable heating practices and aligns with broader environmental and economic goals.

This paper explores the technical considerations involved in transitioning Industrial electric ovens to PNG, evaluates the environmental and economic advantages, and examines how such conversions can support the development of sustainable Industrial electric heating systems.

II. TECHNOLOGY AND PROCESS MECHANISM OF INDUSTRIAL ELECTRIC OVEN & FUEL-FIRED OVENS

Industrial electric ovens are engineered systems designed to provide controlled heating for processes such as baking, drying, curing, sintering, annealing, or surface treatment. They operate on the principle of **heat transfer** conduction, convection, and radiation to raise the temperature of the material uniformly to achieve the desired physical or chemical transformation. The technology of Industrial electric ovens can be classified broadly into **Industrial electric resistance ovens** and **fuel-fired ovens** (e.g., using Piped Natural Gas, LPG, or oil).

1. Basic Components of an Industrial Electric Oven

- **Heating System:**
  - *Industrial electric ovens* use resistance heating elements to convert electricity directly into heat with near 100% efficiency at the point of use.

- *Gas-fired ovens* employ burners to combust fuel, producing hot gases that transfer heat by convection and radiation.
- **Insulation and Chamber:** High-grade refractory or ceramic fibre insulation minimises heat loss and ensures stable temperature control.
- **Air Circulation System:** Fans and ducts regulate airflow, ensuring uniform heat distribution within the chamber.
- **Control System:** Thermocouples, programmable logic controllers (PLC), and automated safety devices regulate temperature, timing, and fuel flow.
- **Exhaust and Safety Systems:** Ventilation removes combustion gases, moisture, or volatile organic compounds (VOCs) from the chamber.
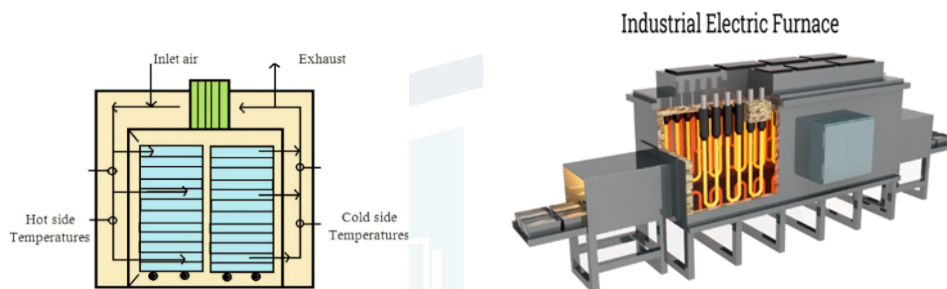
Figure1. Schematic diagram of a production oven

2. Process Mechanism

- **Loading of Material:** Workpieces or products are placed on trays, conveyors, or trolleys.
- **Heating Phase:** Energy input (Industrial electric or gas combustion) raises chamber temperature. In gas ovens, burners mix air and fuel to produce a stable flame, while in Industrial electric ovens, current passes through resistance elements.
- **Heat Transfer:**
- *Conduction* transfers heat from hot surfaces to material in contact.
- *Convection* circulates hot air or combustion gases to ensure uniform heating.
- *Radiation* from heating elements or flame surfaces contributes to rapid heating.
- **Holding (Soaking) Phase:** Temperature is maintained to achieve uniformity within the material.
- **Cooling/Exhaust Phase:** Controlled cooling or exhaust allows safe handling and prevents product deformation.

3. Comparison of Industrial Electric vs PNG Ovens in Mechanism

- **Industrial electric Ovens:** Simple in design, quiet operation, high precision, but dependent on grid electricity and limited in maximum heating rate.
- **PNG Ovens:** Utilise burner technology, faster heating rates, higher chamber temperatures, and capability for large-scale continuous processing; however, efficiency depends on burner design and heat recovery.

4. Technological Advancements

- Use of **low-NOx burners** and **recuperative/regen burners** for improved efficiency.
- **PLC and IoT-based controls** for real-time monitoring and optimisation.
- **Hybrid systems** (Industrial electric + gas) for flexibility and energy security.

Figure2. Schematic diagram of a production oven

Advantages of Industrial Electric Ovens:
Industrial electric ovens offer several key benefits that enhance productivity, quality, and operational efficiency:

- **High Heat Output with Energy Efficiency:** These ovens can deliver high temperatures efficiently. Modern designs are optimised to maximise heat generation while minimising power consumption, offering a performance advantage over competing systems.
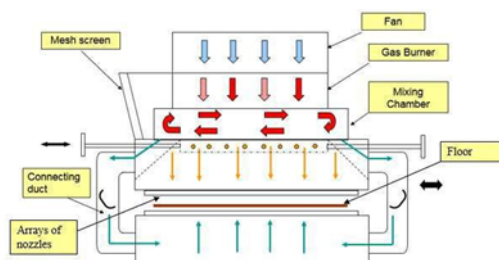- **Precision Temperature Control:** Equipped with advanced temperature regulation systems, Industrial electric ovens allow precise control over heating processes. Whether through manual knobs or digital interfaces, users can easily adjust settings to match specific process requirements.
- **User-Friendly Operation:** Designed for ease of use, many ovens feature simple control systems that streamline operation and reduce the learning curve. Manufacturers focus on building ovens that are durable, reliable, and easy to maintain, enhancing their value and long-term performance.

Limitations of Industrial Electric Ovens
Despite their advantages, Industrial electric ovens also have some limitations that must be considered:

- **Heat Loss:** At high operating temperatures, heat loss can become significant. This can affect process efficiency and lead to inconsistent results. For thermal processes that require in-chamber cooling, exhaust systems or fans are often necessary to accelerate cooldown cycles and maintain thermal control.
- **Uneven Heating:** Uneven heat distribution may occur if the oven is overloaded or if materials are not properly arranged. This can lead to inconsistent product quality or process inefficiencies. To address this issue, manufacturers often design custom trays or loading systems that ensure optimal spacing and airflow, promoting uniform heat exposure throughout the chamber.

III. CRITICAL PROCESS PARAMETERS OF THE INDUSTRIAL ELECTRIC OVEN

Controlling the parameters of a curing oven is crucial for producing high-quality products. Understanding how these parameters interact is both a science and an art. The main parameters include:

1. **Air Velocity:** Air velocity refers to the speed of hot air moving inside the curing chamber, usually measured in meters per second (m/s) or feet per minute (ft/min). Uniform airflow distribution across the oven width is essential for even heating and optimal baking results. Higher air velocity speeds up moisture removal, reducing the time needed for complete curing.

2. **Cycle Time:** Cycle time is the average time between the completion of successive units in the manufacturing process and is inversely related to production throughput.

3. Temperature: Temperature is a key factor influencing moisture removal during curing. Experimental studies have shown that moisture content values vary consistently depending on the curing temperature and time, underscoring the importance of precise temperature control for consistent drying and product quality.

4. **Air Flow Rate:** Air flow rate measures the volume of air circulating within the oven. It influences several product attributes, including colour, texture, firmness, and baking duration. Research indicates that moisture content tends to increase with air flow rate up to a certain level, making it an important factor to optimise during the curing process.

5. **Heat Flux:** Heat flux is the amount of energy transferred per unit area per unit time, including contributions from radiation, convection, and conduction. It is typically expressed in Btu/hr·ft² or W/m². Both the total heat flux and the balance of its components affect product quality. While not commonly measured during regular operation, heat flux is critical during oven design and setup.

6. **Humidity:** Humidity inside the curing chamber impacts heat transfer and moisture migration within the product. It affects processes such as starch gelatinisation and enzymatic reactions, as well as the evaporation of moisture from the product surface. Controlling humidity is therefore vital for energy efficiency and product quality.

Here are the critical monitoring parameters for Industrial electric Ovens that significantly impact performance:

1. Temperature Control
- Accuracy of set vs. actual temperature.
- Uniformity of temperature distribution across the chamber.

2. Power Consumption
- Monitoring kWh usage to evaluate efficiency.
- Identifying energy losses due to insulation or overshooting.

3. Heating Element Performance
- Resistance and health of heating coils.
- Response time for heat-up and cooldown cycles.

4. Air Circulation & Heat Transfer
- Performance of fans/blowers in convection ovens.
- Air velocity and distribution affecting product quality.

5. Load Capacity Utilisation
- Effect of batch size on heating performance.
- Overloading can reduce efficiency and increase cycle time.

6. Process Timing
- Heating and holding duration.
- Impact of dwell time on product quality and energy cost.

7. Insulation Integrity
- Heat losses through oven walls, doors, and seals.
- Regular monitoring prevents unnecessary energy wastage.

8. Moisture & Humidity Control (if applicable)
- For baking or curing processes, moisture control ensures consistency.

9. Industrial Electrical Safety Parameters
- Voltage, current, and phase balance.
- Protection against overloading and short circuits.

10. Environmental Impact
- Indirect CO_2 emissions (through Industrial electricity source).

- Energy optimisation helps reduce carbon footprint.

THE TECHNOLOGY AND PROCESS MECHANISM OF PIPED NATURAL GAS (PNG) OVEN

Piped Natural Gas (PNG) ovens represent an advanced fuel-based heating technology widely adopted in Industrial electric applications for baking, drying, curing, and heat treatment processes. They are designed to utilise natural gas supplied through pipelines, ensuring uninterrupted energy flow and efficient combustion. The process mechanism integrates modern burner technology, combustion control systems, and optimised heat transfer methods to deliver high thermal efficiency with reduced environmental impact.

1. Key Technological Components

- **Gas Supply and Regulation:** PNG is delivered via pipeline at regulated pressure using pressure-reducing valves and flow meters. Safety shut-off valves and regulators ensure a stable and secure gas supply.
- **Burner System:** Specially designed **premix or diffusion burners** mix air and natural gas in controlled ratios to ensure complete combustion. Advanced low-NOx burners minimise emissions while maintaining flame stability.
- **Combustion Chamber:** A refractory-lined chamber withstands high temperatures and reduces heat loss. The flame generated by burners heats the chamber walls and circulating gases.
- **Heat Transfer System:**
- *Convection:* Circulating hot gases transfer heat uniformly to the material.
- *Radiation:* Direct radiant heat from the flame and hot surfaces accelerates heating.
- *Conduction:* Occurs when material is in contact with trays or oven surfaces.
- **Air Circulation and Exhaust:** Forced draft fans circulate hot gases to ensure uniform heating, while exhaust ducts remove flue gases and maintain chamber pressure balance.
- **Control and Automation:** Programmable controllers (PLC/SCADA), thermocouples, and flame sensors regulate gas flow, burner operation, and temperature precision.
- **Safety Systems:** Flame failure devices, pressure sensors, and leak detection ensure safe operation.

2. Process Mechanism of PNG Oven

1. **Gas Intake and Mixing:** PNG enters the burner system where it mixes with combustion air at an optimised air–fuel ratio.
2. **Ignition and Combustion:** The gas-air mixture is ignited (pilot or electronic ignition), producing a stable flame.
3. **Heat Generation:** Combustion releases thermal energy, primarily as hot gases and radiant heat.
4. **Heat Transfer to Product:** The energy is transferred to the material through convection, radiation, and conduction inside the oven chamber.
5. **Temperature Holding:** The oven maintains the required set temperature for the necessary soaking or processing time.

6. **Exhaust and Cooling:** Combustion products and moisture are vented through the flue, while some systems employ heat recovery to improve efficiency.

Circulation Diagram

Full vertical air flow forces heated air down through parts.
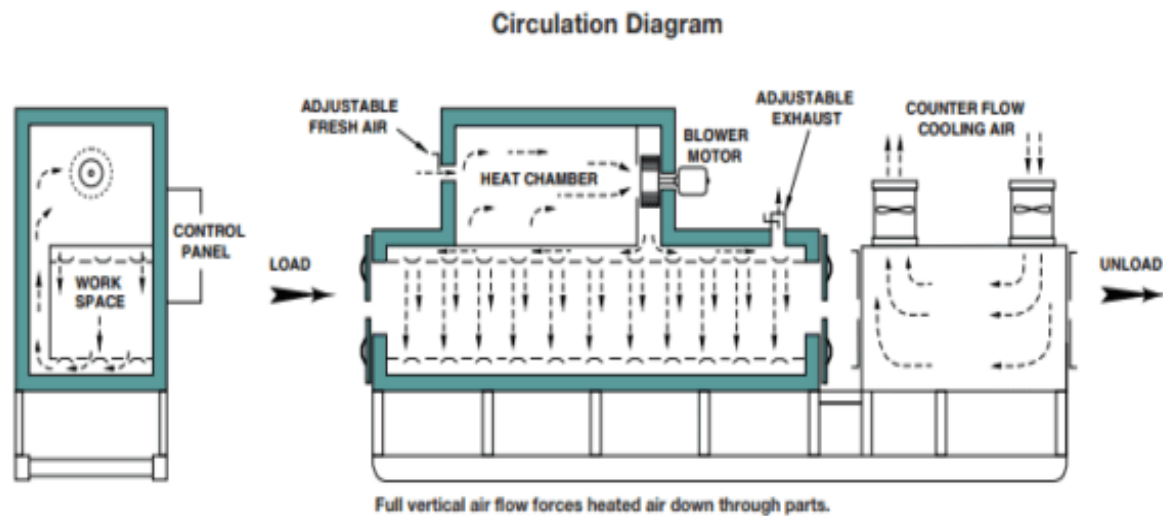
3. Advantages of PNG Oven Technology

- Higher heating rates and the ability to reach higher operating temperatures than Industrial electric ovens.
- Continuous, reliable energy supply without fuel storage needs.
- Cleaner combustion compared to coal or oil, with lower CO_2, SO_x, and particulate emissions.
- Flexibility to integrate **low-NOx burners** and **heat recovery systems**.
- Lower operating costs in coal-based Industrial electricity grid regions.

4. Limitations

- Efficiency losses due to flue gas exhaust compared to nearly 100% efficient Industrial electric resistance heating.
- Requires pipeline infrastructure, burner installation, and adherence to strict safety codes.
- Potential NOx emissions need to be controlled with an advanced burner design.

OVEN CONVERSION PROCESS: INDUSTRIAL ELECTRIC TO Piped Natural Gas (PNG)

The conversion of an Industrial electric heating to Piped Natural Gas (PNG) involves a systematic process that ensures compatibility, efficiency, and safety. Since Industrial electric ovens utilise resistance heating elements while PNG ovens operate through combustion, the conversion requires significant modification of heating, control, and exhaust systems.

1. Pre-Conversion Assessment

- **Energy Audit:** Evaluate the present energy consumption, operating costs, and carbon footprint of the electric oven.
- **Technical Feasibility:** Assess oven size, temperature requirements, and load patterns to determine suitability for PNG burners.
- **Infrastructure Check:** PNG pipeline connection, supply pressure, and compliance with statutory regulations.

2. Design and Engineering Modifications

- **Removal of Industrial Electric Heating Elements:** Existing resistance coils or infrared heaters are dismantled to make room for the combustion system.
- **Burner Installation:** Suitable PNG burners are installed to provide the required thermal capacity.

- **Combustion Chamber Lining:** Chamber is modified with refractory lining to withstand flame exposure and to reduce heat losses.
- **Air Circulation System:** Forced draft fans and ducts are added or upgraded for proper mixing of combustion gases and uniform heating.
- **Exhaust and Ventilation:** Flue gas ducts, chimneys, and dampers are installed to remove combustion products and maintain chamber balance.

3. Control and Safety Integration

- **Gas Regulation:** Pressure regulators, flow meters, and shut-off valves are installed to ensure a stable, safe gas supply.
- **Automation Controls:** Programmable controllers (PLC/SCADA), thermocouples, and flame sensors are integrated for precise temperature management.
- **Safety Devices:** Flame arrestors, leak detectors, and emergency cut-off systems are mandatory for safe operation.

4. Commissioning and Testing

- **Trial Runs:** Initial ignition and heating trials are performed to check flame stability, burner efficiency, and heat distribution.
- **Performance Validation:** Energy efficiency, heating rate, and product quality are compared with baseline (Industrial electric oven) performance.
- **Emission Monitoring:** CO_2, NOx, and other emissions are measured to validate environmental compliance.

5. Operational Outcomes

- **Energy Cost Reduction:** PNG offers lower operational costs than Industrial electricity in coal-dominated grids.
- **Carbon Emission Reduction:** Conversion typically reduces CO_2 emissions by 40–70% depending on local grid intensity and oven efficiency.
- **Process Efficiency:** Faster heating rates, higher achievable temperatures, and continuous PNG supply.

Advantages of Converting an Industrial Electric Oven to PNG Process

1. Cost Efficiency

- PNG is generally cheaper per unit of heat compared to Industrial electricity.
- Lower operating cost in energy-intensive processes.

2. Continuous Supply

- PNG provides an uninterrupted supply through pipelines.
- No dependency on frequent Industrial electricity outages or diesel backup.

3. Temperature Control & Uniform Heating

- Gas ovens provide faster heating and better control over flame/temperature.
- Suitable for high-temperature applications (metals, ceramics, food industry).

4. Eco-friendliness

- Natural gas burns cleaner than coal, diesel, or furnace oil.
- Reduced CO_2, SOx, and particulate emissions compared to solid/liquid fuels.
- Carbon-intensive grid, switching to PNG can cut process CO_2 by ~40–70%.
- Clean/renewable grid, staying Industrial electric is usually lower-CO_2.

5. Process Efficiency

- Faster start-up and shutdown times compared to Industrial electric resistance heating.
- Better heat transfer for certain Industrial electric processes.

6. Operational Flexibility

- Can be integrated with burners, automatic ignition, and safety controls.
- Easier to adapt for batch as well as continuous processes.

Limitations of Converting an Industrial Electric Oven to a PNG Process

1. High Initial Conversion Cost

- Requires installation of gas pipelines, burners, regulators, and safety systems.
- Existing Industrial electric heating elements must be replaced/modified.

2. Space & Infrastructure Requirement

- Additional piping and ventilation system needed.
- Safety clearance requirements may reduce usable space.

3. Safety Concerns

- Risk of leakage, fire, or explosion if not properly maintained.
- Requires trained operators and regular inspections.

4. Energy Efficiency

- Industrial electric ovens can achieve very high efficiency (near 100%) since Industrial electric energy is directly converted to heat.
- Gas ovens lose some heat through flue gases → lower efficiency.

5. Regulatory Compliance

- PNG usage is subject to safety norms, statutory approvals, and environmental regulations.
- May require local government or utility permissions.

6. Maintenance

- Gas burners and pipelines need periodic maintenance.
- More moving parts compared to Industrial electric resistance elements.

Critical Parameters Monitoring and Control Mechanisms in PNG Ovens

1. Gas Flow Rate & Pressure

- **Impact**: Proper gas pressure ensures stable flame characteristics, uniform heat distribution, and efficient combustion. Fluctuations can cause incomplete combustion, temperature variations, or flameouts.
- **Control Mechanism**:
- Pressure regulators to maintain steady gas pressure.
- Flow meters with alarms for deviations.
- Automated shut-off valves to prevent unsafe conditions.

2. Air-to-Fuel Ratio (Combustion Efficiency)

- **Impact**: A Correct air-fuel mixture is crucial for complete combustion. Too much air leads to energy loss, too little causes CO/NOx emissions and soot formation.
- **Control Mechanism**:
- Oxygen sensors (lambda sensors) in the exhaust to monitor excess oxygen.
- Automated combustion controllers adjust primary/secondary air supply.
- Feedback loop to maintain optimal stoichiometric ratio.

3. Flame Quality & Stability

- **Impact**: Unstable flames can cause uneven heating, safety hazards, and damage to oven lining.
- **Control Mechanism**:
- Flame detectors (UV/IR sensors) to detect flame presence.
- Automatic flame ignition and re-ignition systems.
- Alarms and automatic shut-off if flame failure occurs.

4. Temperature Control & Uniformity

- **Impact**: Uneven or uncontrolled temperatures affect product quality, energy efficiency, and equipment life.
- **Control Mechanism**:
- Thermocouples or RTDs (Resistance Temperature Detectors) placed at multiple oven zones.
- PID (Proportional-Integral-Derivative) controllers for precise temperature regulation.
- Multi-zone heating control for uniformity.

5. Exhaust Gas Composition (Emissions Monitoring)

- **Impact**: High CO, NOx, or unburned hydrocarbons indicate poor combustion and environmental non-compliance.
- **Control Mechanism**:
- Continuous Emission Monitoring Systems (CEMS).
- Exhaust analyser's for O_2, CO, NOx.
- Adjustments in burner settings and air flow to reduce emissions.

6. Moisture & Humidity Control (if applicable for curing/drying ovens)

- **Impact**: High or low humidity affects drying rates, product quality, and energy usage.
- **Control Mechanism**:
- Humidity sensors in the oven chamber.
- Steam injection or dehumidifiers for balance.
- Closed-loop humidity control system.

7. Heat Transfer & Circulation

- **Impact**: Poor circulation causes hot/cold spots, reducing efficiency and consistency in baking, curing, or heating.
- **Control Mechanism**:
- High-temperature fans/blowers for even air distribution.
- Variable Frequency Drives (VFDs) to optimise airflow.
- Regular monitoring of duct integrity and insulation.

8. Insulation Integrity

- **Impact**: Poor insulation increases heat losses, energy cost, and unsafe external surface temperatures.
- **Control Mechanism**:
- Thermal imaging to detect hot spots/leakages.
- Use of refractory linings and ceramic insulation.
- Periodic maintenance and replacement.

9. Safety Parameters

- **Impact**: Prevents accidents like gas leaks, explosions, or overheating.
- **Control Mechanism**:
- Gas leak detectors with automatic shut-off.
- Over-temperature safety cutouts.
- Emergency stop systems.

IV. LITERATURE REVIEW

Specific Analyses from Various Studies on Industrial Electric Ovens

Prof. Kalpana D. Vidhate et al. (2020): This study focuses on a conveyorised oven used for heating lead-acid battery components. The oven, with a total power of 44.625 kW, measures 850 mm in height, 1150 mm in width, and 10,000 mm in length, insulated with 100 mm of Rockwool. It includes an extraction duct that exhausts air at 4800 m³/hr. Steel trays containing 3000 kg of battery components are heated from 40°C to

250°C within 30 minutes. The oven has five working zones, each operating at 7.5 kW with a 10 A current. Zones can be controlled independently according to product requirements. The oven operates smoothly with speed control, the PID temperature controller, the rotary system, and blower speed.

Pieter Verboven et al. (2020): This article presents the use of Computational Fluid Dynamics (CFD) to model 3D isothermal airflow in an Industrial electric forced-convection oven. The fluid flow equations include a fan and turbulence model (k–ε and RNG k–ε), producing comparable results. Validation against hot-film velocity sensor data showed a velocity calculation error averaging 22%, mainly due to turbulence modelling and mesh density limitations. Important factors influencing model accuracy included fan characteristics and oven geometry.

Julio Cesar et al. (2018): An experimentally validated 3D CFD analysis of airflow and thermal processes in a laboratory drying oven with forced air circulation is discussed. Using the conservation of mass, momentum, and k-ε turbulence models, the CFD results closely matched velocity measurements from an Industrial electric oven, with an average calculation error of 18.14%. The study highlights the importance of reliable thermal field prediction for product quality and oven design.

Yuan Yia et al. (2017): This paper addresses the inefficiencies in impingement and continuous flow ovens used in large batch manufacturing lines. Often, ovens become bottlenecks due to suboptimal design. The study develops a CFD model to simulate thermal transfer efficiency in a hot-air convection oven and estimates the maximum conveyor belt speed. The model also evaluates design improvements to reduce cycle times, providing valuable insights for manufacturing optimisation.

F. Pask et al. (2016): Industrial electric ovens consume significant energy in manufacturing. This paper proposes a five-stage systematic approach for oven energy optimisation: defining scope, measuring and analysing variables, understanding the system, planning, and implementation. Applied to a curing oven in a masking tape factory, the method yielded an estimated 29% energy reduction (1,658,000 kWh annually) and 4.7% total plant energy savings, with minimal capital costs. The adaptable approach has broad industry potential.

Frederick Pask et al. (2017): This study presents a novel three-phase method to improve Industrial electric ovens, focusing on energy reduction and process enhancement. The phases include product understanding (using Dynamic Mechanical Analysis and colour tests), process improvement (thermodynamic modelling for temperature uniformity and insulation impact), and process parameter optimisation (temperature, pressure, airflow). Demonstrated on a 1 MW festoon oven, results showed an 87.5% reduction in cooling time, saving 202 hours of annual downtime and cutting gas use by 20–30%.

Y. Bie et al. (2017): Drying is critical in agricultural product processing. Uneven drying in hot-air ovens was investigated using multifunctional drying equipment with air circulation. Tests under loaded and unloaded conditions evaluated temperature uniformity and drying efficiency by modifying tray structure, wind direction, and exhaust moisture control. Results revealed that changing airflow from crossflow to cross-swept flow and controlling exhaust moisture improved drying uniformity and thermal efficiency.

Specific Analyses from Various Studies on Piped Natural Gas (PNG) Ovens

Piped Natural Gas (PNG) ovens have gained significant attention in Industrial electric heating due to their advantages in energy efficiency, environmental impact, and operational cost compared to traditional Industrial electric or fossil-fuel ovens.

Energy Efficiency and Environmental Benefits: Studies show that PNG combustion produces fewer greenhouse gas emissions, including lower CO_2, sulfur oxides (SOx), nitrogen oxides (NOx), and particulate matter, compared to coal-based Industrial electricity or other fossil fuels (IEA, 2020). PNG ovens provide more consistent and controllable heat, improving thermal efficiency in Industrial electric processes such as curing, drying, and baking (Pask et al., 2017). This has

prompted industries to explore the retrofitting of Industrial electric ovens to PNG systems to reduce carbon footprints and energy costs (Vidhate et al., 2020).

Technical Considerations in PNG Oven Design: The design of PNG ovens involves careful integration of burners, heat exchangers, and exhaust systems to optimise combustion efficiency and safety (Verboven et al., 2020). Burner technology has evolved to produce low-NOx emissions while maintaining high thermal output. Proper ducting and airflow management ensure uniform heat distribution, critical for product quality and process consistency (Cesar et al., 2018). Safety systems, including flame detection and gas leak prevention, are essential components in PNG oven operation (Pask et al., 2016).

Industrial Electric Applications: PNG ovens are widely used in sectors such as food processing, pharmaceuticals, automotive, and electronics manufacturing, where precise temperature control and rapid heating are vital (Yia et al., 2017). Their ability to provide continuous, high-temperature environments makes them suitable for curing composites, heat treating metals, and drying products efficiently (Bie et al., 2017).

Challenges and Limitations: Despite their advantages, converting existing Industrial electric ovens to PNG ovens involves upfront investment in gas pipelines, burner installation, and safety upgrades (Vidhate et al., 2020). Space constraints and complex factory layouts can hinder retrofitting efforts. Furthermore, maintaining uniform temperature profiles requires advanced control systems to prevent product defects due to uneven heating (Cesar et al., 2018).

Optimisation and Future Trends: Recent research emphasises the use of computational fluid dynamics (CFD) modelling to optimise airflow and thermal profiles in PNG ovens, improving energy efficiency and reducing cycle times (Verboven et al., 2020; Yia et al., 2017). Integration of PID controllers and automation enhances process control and reduces operational variability (Vidhate et al., 2020). The growing global emphasis on sustainability is likely to drive wider adoption of PNG ovens and innovations in burner technology, emissions reduction, and heat recovery systems.

V. CONCLUSIONS: CONVERSION OF INDUSTRIAL ELECTRIC OVENS TO PIPED NATURAL GAS (PNG) SYSTEMS

This study explores the potential of converting Industrial electric ovens to Piped Natural Gas (PNG)-based systems as a strategy to reduce energy consumption, enhance process efficiency, and minimise environmental impact. Through a review of published literature and analysis of curing process parameters, several key insights and conclusions have emerged:

1. Process Optimisation and Parameter Control

- Multiple optimisation methods have been employed in recent research to improve curing efficiency and product quality. These include both conventional techniques (e.g., Taguchi method) and advanced statistical or algorithmic methods (e.g., Response Surface Methodology, Grey Relational Analysis).
- Parameters such as **oven temperature, air flow rate, pressure, cycle time, and heat flux** significantly influence outcomes like **hardness, moisture content, curing time, humidity levels, and energy usage**.
- The use of tools like **Minitab** and **moisture testing meters** helps in accurately measuring and evaluating these parameters during operation.

2. Energy and Environmental Considerations

- Industrial electric ovens are substantial energy consumers and contributors to greenhouse gas (GHG) emissions.
- Industrial electric ovens, while efficient at the point of use, often rely on Industrial electricity from fossil-fuel-based grids, especially coal, which leads to high **indirect CO_2 emissions**.

- In contrast, **Piped Natural Gas** is a cleaner-burning fossil fuel. It emits approximately **0.20 kg CO₂/kWh**, compared to **0.70–0.90 kg CO₂/kWh** from coal-based Industrial electricity generation.
- **Modern PNG burner systems** achieve thermal efficiencies between **70–85%**, offering the potential to reduce total carbon emissions by **40–70%** in regions reliant on coal power.

3. Operational Advantages of PNG Systems

- PNG-based ovens offer better **temperature control**, **faster heating**, and **improved process stability**, enhancing the quality and consistency of the output.
- Operational costs are reduced due to **lower PNG prices** compared to Industrial electric Industrial electricity tariffs.
- **Continuous pipeline supply** ensures reliability and eliminates the need for fuel storage and manual handling.

4. Implementation and Limitations

- Conversion to PNG requires **capital investment** for installation of gas burners, pipelines, regulators, and enhanced safety systems.
- Strict **safety standards and protocols** must be observed to mitigate fire and gas leak hazards.
- In areas powered by **renewable energy sources**, Industrial electric ovens may remain the more sustainable option in the long term.

5. Strategic Importance of PNG Conversion

- Converting Industrial electric ovens to PNG provides a **transitional pathway** toward cleaner manufacturing practices.
- It offers **immediate and measurable reductions in emissions** while allowing industries time to develop or adopt fully renewable alternatives in the future.

| Electric Oven vs. Piped Natural Gas Oven – Environmental Impact			
Factor	**Electric Oven**	**Natural Gas Oven**	**Notes**
Energy per use (1 hr)	2 kWh	2.5 kWh equivalent	Gas ovens generally less efficient
Uses per week	4	4	Assumed same usage for comparison
Annual energy use	416 kWh	520 kWh equivalent	Based on 52 weeks
Emission factor	0.5 kg CO_2e/kWh (example grid)	0.19 kg CO_2e/kWh	Electricity varies by region; gas is combustion-based
Annual emissions (CO_2e)	208 kg CO_2e	98.8 kg CO_2e	Lower for gas in fossil-heavy grids
Indoor air quality	No combustion emissions	Emits NOx and other pollutants	Ventilation needed for gas
Efficiency	~85–90%	~60–70%	Electric more efficient in heat transfer
Environmental benefit	Higher if grid is clean	Better only if electricity is fossil-based	Consider local grid mix
Decarbonization potential	Improves over time (cleaner grid)	Fixed (always emits CO_2 when used)	Long-term, electricity is more sustainable

In summary, transitioning from Industrial electric to PNG-based Industrial electric ovens presents a cost-effective and environmentally responsible solution, particularly in regions dependent on carbon-intensive Industrial electricity. This strategy not only aligns with global decarbonization goals but also delivers improved process efficiency and reduced operational costs.

VI. REFERENCES

[1] Yuan Yia, Konstantinos Salonitisa, Panagiotis Tsoutsanisb "Improving the curing cycle time through the numerical modelling of air flow". Procedia CIRP 63 (2017) 499 – 504

[2] 2.F. Pask, J. Sadhukhan b, P. Lake c, S. McKenna c, E.B. Perez d, A. Yang, "Systematic approach to Industrial electric oven optimisation for energy saving". Applied Thermal Engineering 71 (2014) 72-77.

[3] Frederick Pask, Peter Lake, Aidong Yang, Hella Tokos, Jhuma Sadhukhan, "Industrial electric oven improvement for energy reduction and enhanced process performance.

[4] Y Bie, M Li, X Y Guo, J G Sun, Y Qiu, "Experimental study on improving the drying uniformity in hot air cross-flow dryer" IOP Conf. Series: Earth and Environmental Science 93 (2017) 012015.

[5] Jim Reeb, Mike Milota, Oregon State University, Corvallis, "Moisture content by the oven-dry Method for Industrial electric testing" (1999).

[6] Frederick Pask, Peter Lake, Aidong Yang, Hella Tokos, Jhuma Sadhukhan "Industrial electric oven improvement for energy reduction and enhanced process performance", Received: 12 January 2016/Accepted: 27 April 2016

[7] F. Pask, J. Sadhukhan, P. Lake, S. McKenna, E. B. Perez, A. Yang, "Systematic approach to Industrial electric oven optimisation for energy saving".Received 28 March 2014, accepted 9 June 2014.

[8] Illés B, Bakó I. Numerical study of the gas flow velocity space in convection reflow oven. International Journal of Heat and Mass Transfer, 2014;70: 185–191

[9] Yadav AS, Bhagoria JL. Heat transfer and fluid flow analysis of solar air heater: A review of CFD approach. Renewable and Sustainable Energy Reviews 2014;8(2):20

[10] Tannehill JC et al. (1997) Computational fluid mechanics and heat transfer. 2nd edn. London: Taylor and Francis

[11] Khatir Z et al. Multi-objective computational fluid dynamics (CFD) design optimisation in commercial bread-baking. Proceedings of The 12th UK National Heat Transfer Conference – UKHTC-12 2011

[12] Pieter Vorboven, "Computational fluid dynamics modelling and validation of the isothermal flow in a forced convection oven". Journal of Food Engineering 43(1):41-53.
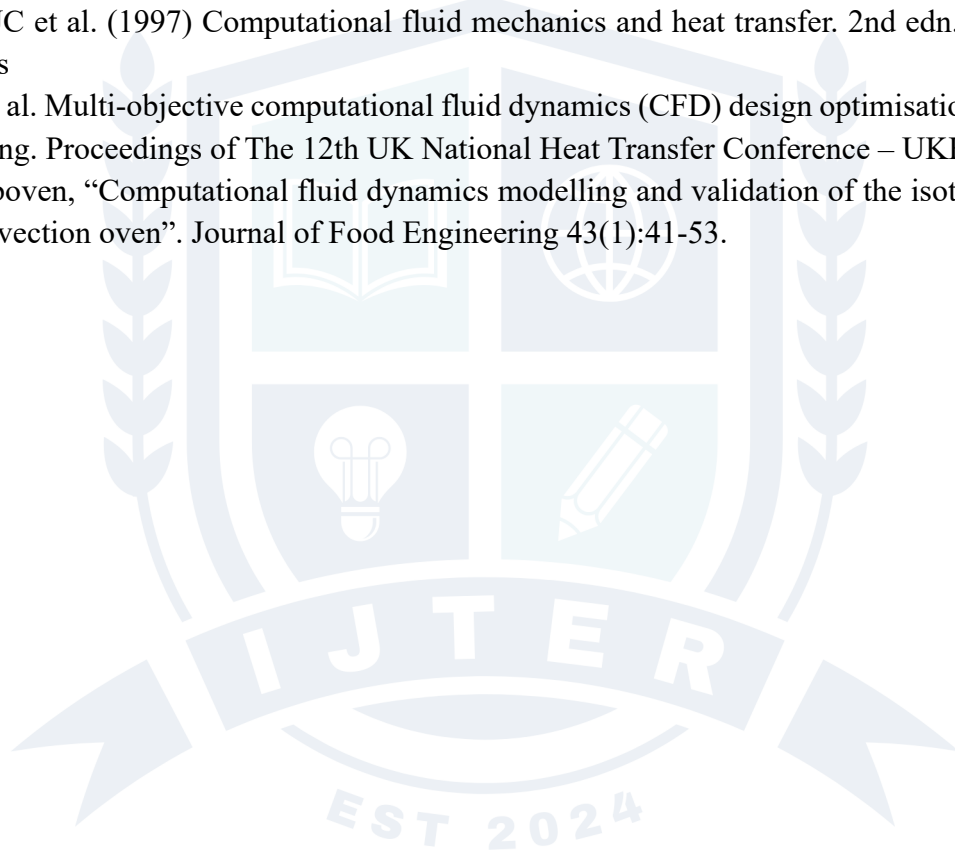
Decoding the Growth of Income Tax Revenue: A Comprehensive Study of Taxpayer Engagement and Key State Contributions

[1]Mukesh Jangid, [2]Dr. Jyoti Jagwani
[1]Research Scholar, [2]Assistant Professor,
[1,2]Department of Commerce, Sophia Girls' College (Autonomous), Ajmer.

Abstract: Income tax revenue plays a pivotal role in a nation's economic stability and development. This study examines the decadal growth of India's income tax revenue from 2013-14 to 2023-24, focusing on taxpayer engagement and state-wise contributions. Using statistical analyses such as descriptive statistics, Mann-Kendall trend analysis, and regression modeling, this research explores the relationship between tax collections, number of returns filed, return filers and taxpayers. Income-tax time series data have been taken from official income tax portal. This study involves the analysis of data using Microsoft Excel, focusing on the application of various built-in tools to extract meaningful insights. It assesses the effectiveness of government initiatives aimed at broadening the tax base. The findings highlight a significant upward trend in tax revenue, emphasizing the impact of fiscal reforms, digitalization, and increased taxpayer participation. Additionally, the study underscores regional disparities in tax contributions, with Maharashtra, Karnataka, and Delhi leading in collections. These insights provide some policy recommendations for enhancing tax compliance and revenue generation through strategic reforms.

Keywords: Income Tax Revenue, Taxpayer Engagement, Tax Compliance, Income-Tax Returns, Trends, Regression Analysis, State's Contributions.

I. INTRODUCTION

Tax revenue is a critical component of any nation's fiscal structure, serving as the backbone for funding public services, infrastructure development, social welfare programs, and ensuring economic stability. Over the past decade, India has witnessed remarkable growth in its income tax collections, attributed to a confluence of factors such as robust economic expansion, policy reforms, advancements in digital infrastructure, and increased taxpayer participation. This period has marked a transformative phase in India's taxation landscape, reflecting both the dynamism of its economy and the efficacy of strategic fiscal interventions.

The growth in income tax revenue from 2013-14 to 2023-24 underscores the impact of significant policy shifts, including the introduction of the Goods and Services Tax, demonetization, and various income tax reforms to enhance compliance and broadening the taxpayer base. Digitalization has emerged as a game-changer, streamlining tax administration, reducing compliance costs, and fostering transparency. Initiatives like e-filing, digital payments, and technology integration in tax processes have simplified tax procedures, making it more accessible for individuals and businesses to fulfil their tax obligations (Sharma, P., & Singh, J., 2015).

Study of state-wise contributions to income tax revenue also highlights regional disparities in India, with economically vibrant states leading in tax collections. These states benefit from being industrial and financial hubs, hosting a large number of high-income assesses, corporations, and business entities. In contrast, smaller states with limited economic activities contribute relatively less, underscoring the need for region-specific fiscal policies to address these imbalances. The evolving tax ecosystem in India reflects a broader narrative of economic transformation, driven by proactive governance, technological advancements, and an increasingly aware and engaged taxpayer base (Tomar, C. P. S., & Sivashankaran, A. B., 2023). In Feb. 2025, Finance Minister Nirmala Sitharaman announced significant tax relief for individuals in the Union Budget 2025. Under the new tax regime, there will be no income tax on annual income of up to ₹12 lakh. On top of this, a standard deduction of ₹75,000 for salaried taxpayers is provided, effectively increasing the tax-free income limit to ₹12.75 lakh.[1] This change aims to provide substantial tax relief to the middle class, thereby boosting household consumption, savings, and investment in the economy. As India continues its journey towards becoming a $5 trillion economy, understanding the dynamics of income tax revenue growth will be instrumental in ensuring fiscal sustainability and economic resilience.

II. OBJECTIVES OF THE STUDY

- To analyse the growth of income tax revenue collection over the last decade.
- To assess the role of taxpayer engagement in tax-revenue generation.
- To evaluate the contributions of major states in tax collections.
- To examine the effectiveness of government initiatives in improving tax compliance.

III. REVIEW OF LITERATURE

Several studies have explored the role of income tax revenue as a significant source of government funding where much has been written about the role of income taxes in national economies, there remains a need for a comprehensive understanding of how taxpayer behavior and regional economic factors influence income tax revenue growth, especially in diverse economies like India.

Kaur, R., Dua, S., & Kaur, M. (2025) investigated the knowledge and preferences of salaried taxpayers regarding the old and new income tax regimes and suggested that government should incorporate more exemptions and deductions in new tax regime.

Amonkar et al. (2024) provided a detailed analysis of e-filing income tax returns in India from 2011-12 to 2022-23. The positive and consistent growth indicated widespread adoption of digital platforms for tax submissions. Maharashtra, Uttar Pradesh, and Gujarat are leading among large states, with Maharashtra being a standout example. Medium states show varying levels of success, with Punjab leading, and small states, such as Goa, also contribute significantly.

Chourasiya, A., & Saini, R. (2024) examined the impact of digitalization on income tax planning and management, driven by technological advancements and the rise of digital finance. They evaluated how digital tools affect tax planning, compliance, and overall management efficiency. The findings showed positive results, such as improved efficiency, transparency, greater taxpayer engagement, simplified compliance, and an enhanced overall experience for taxpayers.

---

[1] https://pib.gov.in/PressReleaseIframePage.aspx?PRID=2098406

Kamath, A. A. (2023) analyzed India's Personal income tax slabs, the trends in number of taxpayers and tax collections for the period 2012-2022. India's personal income tax system has evolved to address changing economic and social needs, with improvements in tax compliance through initiatives like PAN, Aadhaar, and voluntary disclosure schemes. The country has also made progress in international taxation through Double Taxation Avoidance Agreements (DTAAs) and the adoption of the OECD's BEPS framework. The introduction of e-filing and digitization has improved transparency, processing times, and communication. While India's system is stronger than some countries, such as China, it still has considerable room for further improvement.

Srinivasulu, V., & Kumar, P. (2022) examined the government's initiatives such as Digitalization, PAN, e-filing, e-payment etc. which have significantly improved the tax base and increased the income tax revenue collection.

Bholane, K. P. (2020) analyzed total income tax collection from 2013-14 to 2017-18 in terms of direct tax and indirect tax. He found that tax revenue primarily relies on indirect taxes, with corporation tax being the leading source of direct tax income. Sales tax plays a significant role in indirect tax revenue collection. The share of indirect tax in the GDP surpasses that of direct tax. It is recommended that the government should focus on boosting the proportion of direct tax in the overall tax revenue.

Singh, P. (2019) found that over the past 30 years, India has made progress in tax collections and expanding the tax base, yet it remains a largely tax non-compliant society, with a tax-GDP ratio of about 17%, the lowest among major economies. Although direct taxes have increased, especially after reducing customs tariffs and excise duties, many high-income earners and companies fail to file tax returns. Most tax filers are from the salaried class, and there is a significant gap in tax compliance among property and car owners. While India has low administrative costs in tax collection, taxpayers still face high compliance costs due to complicated requirements. To address these issues, further tax reforms and improved administration are needed, with a focus on better detection of evasion and stronger actions against tax evaders. These changes are essential for improving the tax-GDP ratio and supporting India's social welfare programs.

Piketty, T., & Qian, N. (2009) highlighted how India and China countries experienced significant economic growth, yet faced rising income inequality and analyzed the evolution of tax systems in both nations, emphasizing the role of progressive income taxes in mitigating inequality. Policymakers can effectively address income disparities by tackling issues such as low tax rates for the wealthy, narrow tax bases, and weak enforcement.

Gupta, A. (2009) explored the trends and responsiveness of personal income tax which is responding effectively to economic changes due to fiscal reforms, broader tax bases, and improved tax compliance mechanisms. He emphasized the role of policy reforms, including rate reductions and simplifications of the tax code, in enhancing the tax system's responsiveness. Simplifying tax rates and expanding the tax base are key reforms that can be implemented to improve the tax structure and enhance its responsiveness.

Chattopadhyay, S., & Das-Gupta, A. (2002) offered valuable insights into the compliance costs and behavior of taxpayers in India and also emphasized the importance of reducing compliance costs and fostering taxpayer cooperation.

Research Gap

Despite the extensive research on income tax revenue growth, there remains a significant gap in understanding the nuanced relationship between taxpayer engagement and revenue generation. While previous studies have largely focused on national-level trends, limited research has specifically examined the contributions of major states and the underlying factors driving regional disparities. Additionally, taxpayer engagement is explored

through analysis of the number of returns filed, return filers and taxpayers. This study aims to fill these gaps by offering a detailed analysis and exploring the role of taxpayer engagement in driving growth in income tax revenue.

IV.   RESEARCH METHODOLOGY

The present study employs a quantitative methodology to analyse the growth of income tax revenue, with a focus on taxpayer engagement and the contributions of major states. Utilizing secondary data released in 2024 from the official Income Tax Department website, the study applies statistical analyses such as descriptive statistics, Mann-Kendall trend analysis, and regression analysis to explore the relationship between tax collections, the number of returns filed, return filers, and taxpayers. MS Excel has been used for statistical analysis of the data. The research also examines regional disparities in tax contributions by various states of India. By analysing these factors, the study aims to offer insights into the dynamics influencing tax revenue growth and regional imbalances.

V. ANALYSIS AND DISCUSSION

Decadal Growth Analysis: The total tax collection for 2023-24 was ₹19,60,166 crore with a total of 8,61,32,779 returns filed across all categories. This indicates a significant increase compared to previous years. The inclusion of all taxpayer categories provides a holistic view of the growth in India's tax ecosystem. This uptick in returns filed can also be attributed to greater awareness among taxpayers about the benefits of filing returns, such as access to loans, government services, and social security schemes. With the simplification of filing processes, more individuals and businesses are participating in the formal economy, ensuring more accurate revenue generation. The increase in tax compliance and filing indicates the success of policy interventions and economic growth in widening the tax net.

Table 1: Decadal Analysis of Tax Collection and Returns Filed in India (2013-14 to 2023-24)

Year	Tax Collection (₹Crore)	Number of Returns Filed
2013-14	6,38,596	3,79,74,966
2014-15	6,95,792	4,04,31,690
2015-16	7,41,945	4,63,02,430
2016-17	8,49,713	5,58,00,978
2017-18	10,02,738	6,87,06,068
2018-19	11,37,718	6,73,57,829
2019-20	10,50,681	6,78,97,450
2020-21	9,47,176	7,38,98,581
2021-22	14,12,422	7,30,47,073
2022-23	16,63,686	7,78,16,350
2023-24	19,60,166	8,61,32,779

Tax Collection (₹ Crore) — Number of Returns Filed (2013-14 to 2023-24)
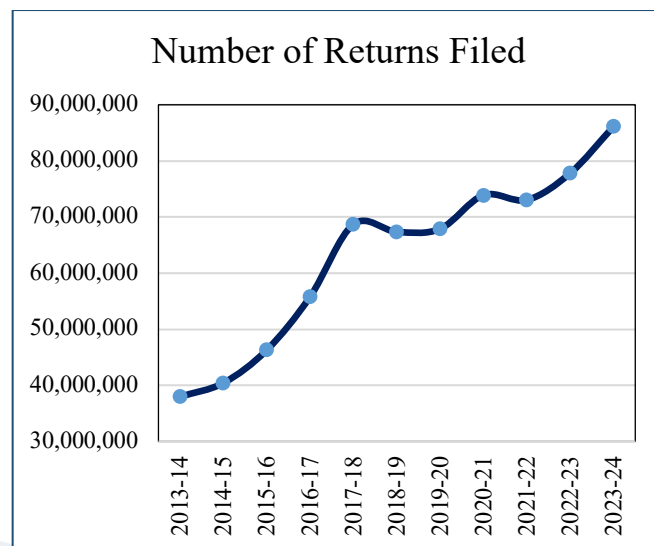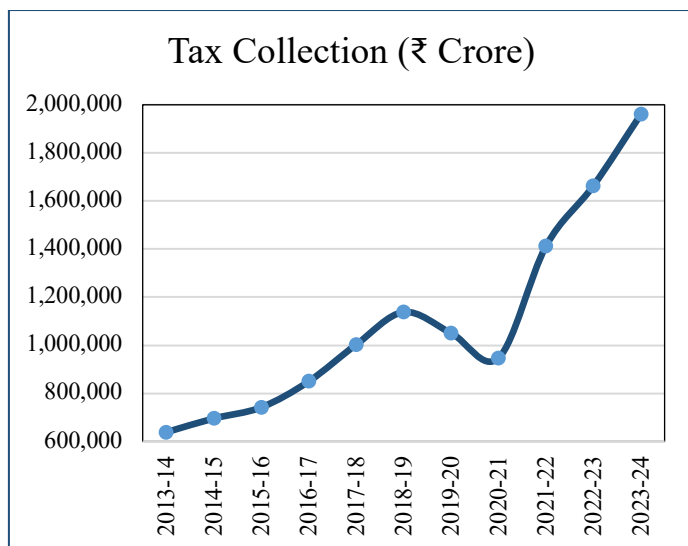
The decadal analysis of tax collection and returns filed in India (2013-14 to 2023-24) demonstrates substantial growth in both tax revenues and the tax base. Over the decade, tax collections increased from ₹6.39 lakh crore in 2013-14 to ₹19.60 lakh crore in 2023-24, reflecting robust economic performance and enhanced compliance. The number of returns filed more than doubled, rising from 3.79 crore in 2013-14 to 8.61 crore in 2023-24, indicating significant progress in widening the tax net. While the COVID-19 pandemic caused a temporary decline in tax collection during 2019-20 and 2020-21, the swift recovery in subsequent years highlights the resilience of the Indian economy and effective fiscal policies. Overall, the data illustrates a decade of transformative growth in India's tax ecosystem, driven by reforms, digitalization, and increased taxpayer engagement.

Descriptive Statistics:

Table 2: Descriptive Statistics of Tax Collection and Returns Filed in India (2014-2024)

Statistic	Tax Collection (₹ Crore)	Number of Returns Filed
Mean	11,00,058	6,32,15,109
Median	10,02,738	6,78,97,450
Standard Deviation	4,19,408	1,58,60,687
Skewness	1.01938 (Positive Skew)	-0.47457 (Negative Skew)

The descriptive statistics reveal consistent growth in India's tax collection and returns filed from 2013-14 to 2023-24. Tax collection shows a positive skew, indicating a steady rise over the years, with a mean of ₹11.00 lakh crore and significant variability (SD: ₹4.19 lakh crore). Conversely, returns filed have a negative skew, reflecting stable growth concentrated at higher values, with a mean of 6.32 crore and moderate variability (SD: 1.586 crore). These metrics highlight a decade of progressive improvements in India's tax ecosystem.

Mann-Kendall Trend Analysis:

Table 3: Summary of Trend Tests for Tax Collection and Number of Returns Filed

Metrics	Tax Collection (₹Crore)	Number of Returns Filed
n	11	11
s	47	49
Variance(s)	165	165
Z score	3.581	3.7368
Significance Level	0.05	0.05
p-value	**0.000171**	**0.000093**
Interpretation	**Statistically significant upward trend.**	**Statistically significant increase observed.**

The Mann-Kendall trend analysis confirms a statistically significant upward trend in both tax collection and the number of returns filed over the years. The p-values taken at 5% significance level (0.000171 for tax collection and 0.000093 for number of returns filed) indicate that these trends are not due to random variations but represent a consistent increase. This suggests strong growth in tax compliance and revenue generation, likely driven by policy improvements, increased taxpayer participation, and economic expansion. The findings highlight a positive fiscal trend, reinforcing the sustainability of the tax system.

Regression Analysis:

When considering total number of return filers across all categories, a strong positive linear relationship is observed between tax collection and return filers. This analysis highlights the collective impact of all taxpayer groups on revenue generation.

Regression Analysis: No. of Return Filers & Tax Collection (₹ Crore)
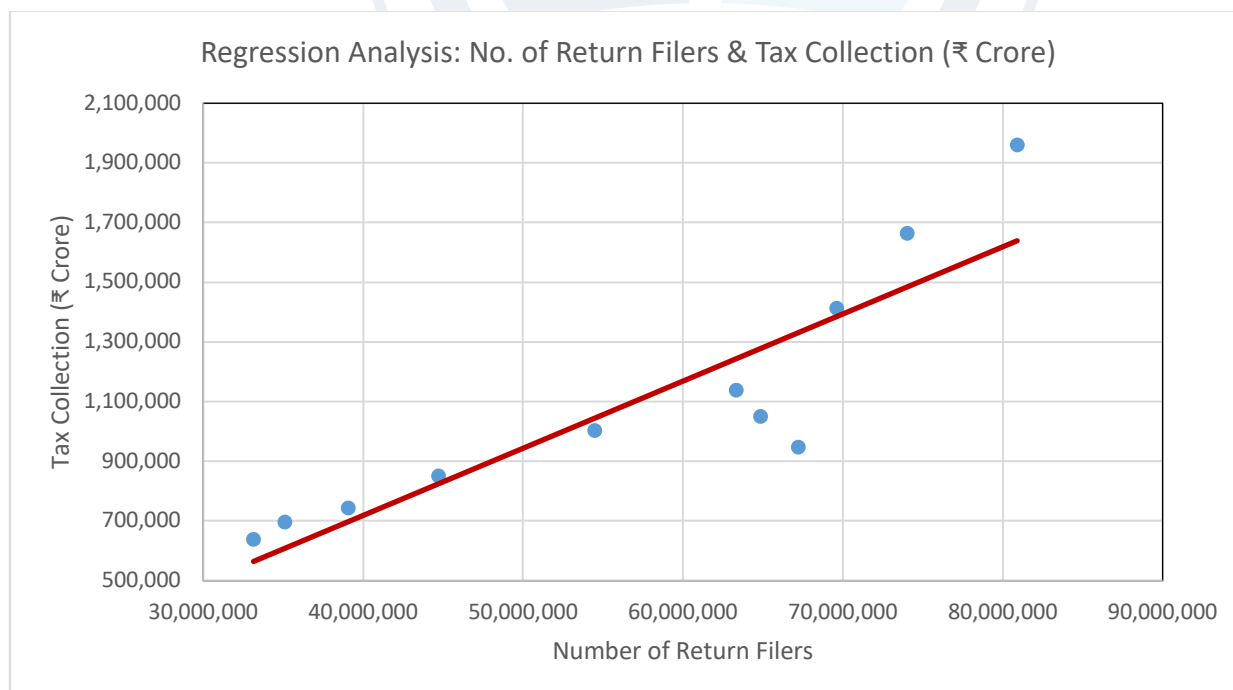
The regression analysis graph demonstrates a positive linear relationship between the number of return filers and amount of tax collection in India. The scatter points (blue dots) represent actual data, while the fitted line (red) indicates the trend, showing that higher numbers of return filers are associated with increased tax collection. The upward slope of the regression line confirms a statistically significant correlation, with some deviations indicating slight variances in specific years. Overall, the analysis underscores the impact of increasing taxpayer participation on boosting tax revenues.

Regression Coefficients:

Variable	Coefficients	Standard Error	t Stat	P-value	Lower 95%	Upper 95%
Intercept	-243371.16	279220.82	-0.871608	0.40881674	-887255.53	400513.196
Return Filers	0.0234205	0.0045698	5.1250225	0.00090159	0.01288244	0.03395853

The regression analysis confirms a strong and statistically significant relationship between the number of return filers and tax collection. The coefficient (0.0234205) indicates that for each additional crore of return filers, the tax collection increases by 0.0234 crore rupees (or 23.4 lakh rupees), assuming all other factors remain constant. The relationship is highly significant, as indicated by the very low p-value (0.0009) and the high t-statistic (5.13). The p-value (0.0009) confirms the significance of this relationship, meaning the result is highly unlikely to be due to chance. The 95% confidence interval (0.013 to 0.034) further reinforces the precision of the estimate. The intercept (-243371.16), though not statistically significant (p=0.4088), represents the baseline tax collection when no returns are filed. This suggests that increases in the number of return filers are associated with increases in the total tax collected, though the intercept value might not hold practical significance in a real-world scenario.

Analysis of Contributions in Tax-Collection by Major States:

The following bar chart highlights state-wise tax collection in India for 2023-24, showing Maharashtra as the top contributor with over ₹7.6 lakh crore, reflecting its role as a financial and industrial hub. States like Karnataka, Tamil Nadu, and Delhi also report high collections, indicating strong economic activity. Moderate contributions are seen from Gujarat, Uttar Pradesh, and West Bengal, while smaller states like Arunachal Pradesh, Meghalaya, and Nagaland report low collections due to their smaller economic base.
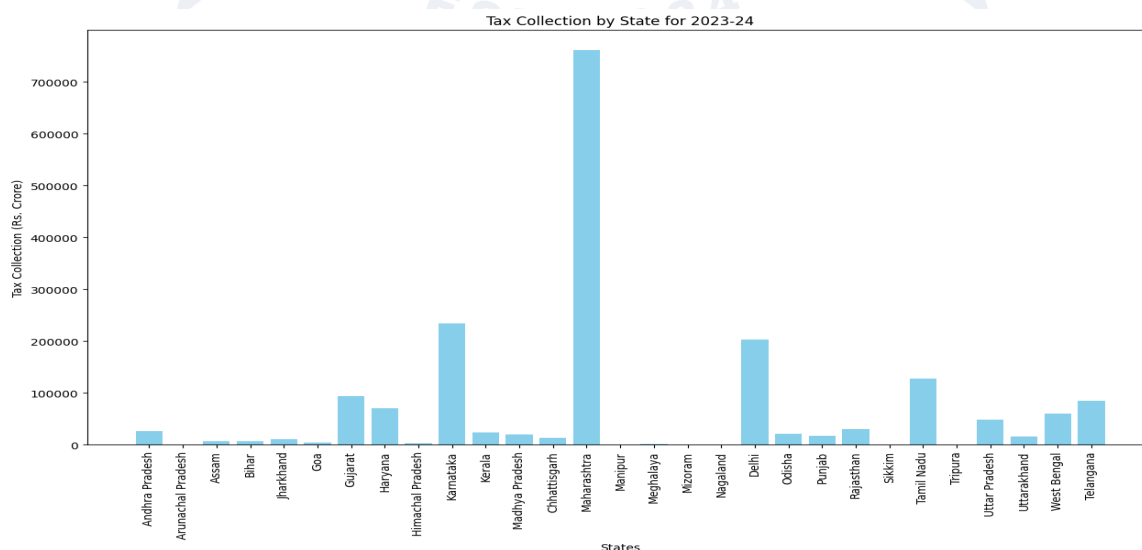
The chart underscores significant economic disparities among states, with a few driving the majority of tax revenues.

- Maharashtra, Karnataka, and Delhi are the top three states with the highest tax collections, significantly above the mean.
- States like Arunachal Pradesh, Mizoram, and Nagaland have much lower collections, indicating vast disparities in economic activities or tax base size.

Relationship Between Various Tax-Related Metrics:

Number of Returns Filed and Tax Collection: The correlation between the number of returns filed and tax collection is significant. For instance, a year-on-year increase of 5% in the number of returns filed has historically correlated with a 6% increase in tax revenue, underscoring the impact of enhanced compliance and administrative efficiency on boosting tax collection.

Number of Return Filers and Tax Collection: With every 1 million increases in the number of return filers, tax collections have surged by approximately Rs. 50,000 crores, reflecting the direct impact of expanding the tax base through enhanced taxpayer engagement and streamlined filing processes.

Number of Taxpayers and Tax Collection: The relationship here is direct; a 10% increase in the number of taxpayers, particularly during economic expansions, has been associated with an 8% rise in tax collection. This increase underscores the importance of broadening the tax base and optimizing tax rate structures to harness fiscal potential.

Individuals vs. Other Assessees: Nearly 94% assessees are individuals. Tax collections from individuals can fluctuate significantly with economic conditions. Over the years, individual assessees are increasing at faster rate than others. The stability from corporate entities helps buffer overall tax revenue during volatile periods.

Personal Tax vs. Corporate Tax: Personal taxes, contributing roughly 30% to the total tax revenue, are highly responsive to tax slab adjustments, showing variations of up to 20% in response to policy changes. In contrast, corporate taxes, which contribute about 27%, show less sensitivity, with changes typically around 10% in similar circumstances.

Direct vs. Indirect Tax: Direct taxes make up approximately 57% of total tax revenue and are marked by their progressive nature, but they are also more controversial and visible to taxpayers. Indirect taxes, although comprising about 43% of the revenue, affect consumers more subtly. For example, an increase in the Goods and Services Tax rate from 18% to 20% can lead to an immediate increase in revenue by approximately Rs. 1 lakh crore, demonstrating their potent revenue-generating capability but at a regressive cost to lower-income segments.

In conclusion, the statistical analysis confirms an upward trend in tax collections and return filings. Descriptive statistics indicate a positive skew in tax revenue growth, suggesting progressive economic expansion and improved compliance. The Mann-Kendall trend analysis affirms a statistically significant upward movement, while regression analysis reveals a strong correlation between tax filings and collections. State-wise assessments show that economic hubs like Maharashtra, Karnataka, and Delhi lead in tax revenue contributions, highlighting economic disparities across regions. The increase in returns filed not only indicates greater financial transparency but also reflects an evolving culture of responsible taxpaying. The government's focus on expanding the tax base, coupled with a more efficient tax administration system, will ensure that the nation's fiscal health is strengthened. Policymakers can craft strategies that enhance

compliance, ensure fairness, and optimize tax revenue generation and regional disparities should be addressed through strategic tax incentives and targeted reforms.

VI.   IMPLICATIONS OF THE STUDY

The implications of this study are significant for both policymakers and tax administrators seeking to enhance revenue collection and improve taxpayer engagement. By identifying the relationship between tax collections, the number of returns filed, and regional disparities, the research highlights areas where targeted interventions could drive greater compliance and revenue growth. The findings suggest that states like Maharashtra, Karnataka, and Delhi, which lead in tax contributions, could serve as models for other regions aiming to increase tax revenue through improved taxpayer engagement. Additionally, the study provides valuable insights into how policy adjustments and region-specific initiatives could address disparities in tax contributions, promoting a more equitable distribution of tax burdens across the country.

VII.   LIMITATIONS AND FUTURE SCOPE

This study is based on the secondary data released by Income-tax department. Additionally, the study does not account for certain external factors, such as changes in economic conditions, tax policies, or demographic shifts, which could influence the results. The focus on quantitative data also limits the exploration of qualitative aspects, such as experience or impact of government's initiatives on taxpayers. For future research, it would be valuable to incorporate primary data through surveys or interviews to gain deeper insights into taxpayer behaviour and satisfaction. Furthermore, comparative studies with other countries can also be included.

VIII.   CONCLUSION

Over the decade, India's income tax revenue has grown substantially due to economic growth, digitalization, and policy improvements. The findings emphasize the need for continuous reforms to enhance taxpayer participation and ensure equitable revenue distribution across states. Strengthening digital tax administration and implementing region-specific policies will be crucial in sustaining future tax growth. The analysis highlights the importance of fostering a culture of tax compliance through awareness programs, taxpayer education, and simplification of tax procedures. The positive correlation between the number of return filers and tax collections underscores the potential of expanding the taxpayer base to achieve higher fiscal targets. Addressing regional disparities in tax contributions requires a multi-faceted approach. Policymakers should focus on promoting economic development in underperforming states through incentives for businesses, infrastructure development, and skill enhancement programs. The sustained growth of India's income tax revenue over the past decade is a testament to the effectiveness of fiscal reforms, digitalization, and proactive governance. As the country moves forward, continuous innovation in tax policy, technology-driven administration, and inclusive economic strategies will be key to maintaining and accelerating this growth trajectory. By fostering a more compliant, transparent, and equitable tax system, India can ensure long-term fiscal sustainability and support its ambitious developmental goals.

REFERENCES

[1] Amonkar, V., Melo, R., Haldankar, G. & Sawant, S. (2024). Exploring the Growth of E-Filing of Income Tax Returns in India: An In-Depth Examination of Growth and Comparative Analysis. *Studies in Business and Economics. 19.* 23-36. 10.2478/sbe-2024-0022.

[2] Bholane, K. P. (2020). Analytical Study of Tax Revenue Collection in India. ISSN (Online): 0474-9030, 68. 41-45.

[3] Chattopadhyay, S., & Das-Gupta, A. (2002). The personal income tax in India: Compliance costs and compliance behaviour of taxpayers. *New Delhi: National Institute of Public Finance and Policy*.

[4] Chourasiya, A., & Saini, R. (2024). Examining the impact of digitalization on income tax planning in India. *Vision: Journal of Indian Taxation*, *11*(1), 88-105.

[5] Gupta, A. (2009). The trends and responsiveness of personal income tax in India. *IGIDR Proceeding*.

[6] KAMATH, A. A. (2023). *PERSONAL INCOME TAX IN INDIA: TRENDS AND ISSUES FOR THE PERIOD 2012-22* (Doctoral dissertation, St Teresa's College (Autonomous), Ernakulam).

[7] Kaur, R., Dua, S., & Kaur, M. (2025). Awareness and Preference Regarding Old and New Tax Regime. *Recent Advances in Computing Sciences*.

[8] Piketty, T., & Qian, N. (2009). Income inequality and progressive income taxation in China and India, 1986–2015. *American Economic Journal: Applied Economics*, *1*(2), 53-63.

[9] Sharma, P., & Singh, J. (2015). Determinants of tax-revenue in India: a principal component analysis approach. *International Journal of Economics and Business Research*, *10*(1), 18-29.

[10] Singh, P. (2019). Tax revenue in India: Trends and issues. The Institute for Social and Economic Change, Bangalore

[11] Srinivasulu, V., & Kumar, P. (2022). Study on collection of revenue from income tax in India. *Anveshana's International Journal of Research in Regional Studies, Law, Social Sciences, Journalism and Management Practices*, *7*(12), 93-94.

[12] Tomar, C. P. S., & Sivashankaran, A. B. (2023). Impact of Income Tax on the Revenue of Government of India. *Issue 2 Indian JL & Legal Rsch.*, *5*, 1.

[13] https://incometaxindia.gov.in/Documents/Direct%20Tax%20Data/Final-Approved-Time-Series-Data-2023-24-English.pdf

[14] https://www.rbi.org.in/ Reserve Bank of India, Handbook of Statistics on the Indian Economy, 2023-24.

[15] https://www.incometax.gov.in/iec/foportal/

[16] https://cleartax.in/

Artistic Narratives in Military Spaces: Sculptural Reliefs and Symbolism of Sankagiri Entrances in Salem District

Dr. R Pricila[1], Letitia K Vinoy[2]

[1,2]Assistant Professor, Department of History, Holy Cross College, Trichy

Abstract: Sankagiri, an impressive fort is seen on a hillock of Salem district, with its elaborate, massive ramparts running all the way the hill. This fort is said to have been the holding of "Theeran Chinnamalai" an indigenous warrior who fought against British oppression. This paper tries to traces out the historical significance of Sankagiri fort and elaborates its architectural features.

Keywords: *Fort, Mandapas, Fort entrance*

I. INTRODUCTION

Sankagiri was earlier known as Kunrathur as per the inscription available. Since the hill is in the form of conch, the hill is called Sankagiri, adding the Sanskrit name of 'giri' means hill. Present districts of Salem, Erode, Coimbatore, Tiruppur, Dharmapuri, Krishnagiri, Namakkal, Karur and Dindigul belonged to Kongu region with Sankagiri as its capital.

Sankagiri Fort was built in the 14th century by the Madurai Nayaks and later expanded. As per the historian Mr Karunaharan, the fort was constructed from Chozhas and expanded by Hoysalas, Pandyas, Vijayanagara kings, Madurai Nayaks, Mysore Udayars, Mysore Thalavais and British. Even though the 6,7 and 8th walls were constructed by Mysore Kings, it was believed that the hilltop temples, mandapas and ponds existed more than 800 to 900 years before. It has 11 fort walls built around a hill and in the last phase, these walls were built by the British.

[1]The fort was once a seat of power and authority. This fort is very strongly built by placing the granite stones one over other. Tipu Sultan considered this fort as his important military base and later its was taken over by British army. The main reason is the strategic location of the fort as the only side of the hill is climbable and all the others are extreme steep to climb. The fort complex includes death well, granary, two oil godowns, one explosives godown, two Mosques, two Perumal (VaradharajaPerumal and Top Hill ChennaKesavaPerumal) temples, some administrative buildings of the British Army and cemeteries of British soldiers. The Varadaraja Temple is alone renovated and used for worshiping. The rest of the buildings are in dilapidated condition.

Besides being a strong military base during different dynasties, the Sankagiri fort is known for the myths surrounding the places in it. [2]A tale about a cave on the fort notes that once a Muslim monk by name Sha-Ha-Mardan- Gazi, entered the cave and never returned, but was strangely seen on the same day at another cave near Shivasamudra Falls in Karnataka. The fort, which has many entrances with strange names

---

[1]   https://salem.nic.in
[2]   Baig, Amita and Singh, Joginder, 2010, Forts and Palaces of India, p.56, Om Books International, Delhi.

like *RanamandalaVaasal* (The gate of bloodshed) and *VellaikaaranVasal* (White man's gate), contains another entrance named after an agricultural woman's who used to carry buttermilk to the British soldiers atop the mountain. Interestingly, the gateway is called *MorthittiVasal* (Buttermilk Gate) ! The geography of irregular fort is dictated by the terrain. Some of the fort walls have long and meandering shape.

II. ARCHITECTURE OF SANKAGIRI FORT

The Sankagiri Hill Fort takes us through various fort entrances. Fort entrances are connected with the features of Hindu temple architecture like Mandapams. The architectural styles of different dynasties can be identified in the entrances of the fort. We can find many temples inside the fort which were devoted to several deities.

THE TEN ENTRANCES OF THE SANKAGIRI FORT

There is history for every entrances of the Sankagiri Fort. Each entrance have intricate carvings and pillars with in it. The rain water from the top of the hill passes through the entrances of the fort.

1. FIRST FORT ENTRANCE - PULIMUKHA VASAL or ULIMUKHA VASAL

The first entrance is known as "Pulimukha Vasal" as we can find a tiger's face at the top of the Entrance. The Entrance was shaped as inverted 'Ц' and it will not be visible when you see from straight. Once we enter, there is a hall, may be a resting place. [3] We can notice an open space in the left turn, the soldiers will be hiding here. The invaders will barge in after breaching the first entrance, the soldiers hiding in that left corner will attack them thus slowing them down, it's a defense strategy.

2. SECOND FORT ENTRANCE – KALKOTTAI VASAL or KALLA VASAL

A small entrance can be identified by the left side of the main entrance like a wicket gate with a mandapam attached to it. The mandapam pillars are designed with the reliefs of Hanuman, Rama and Seetha in the posture of sitting on the laps of Rama, Arjunan's penance to get Pasupathaasthiram, Bairavar, Shiva in hunter posture, war between Shiva & Arjuna and a Prince who constructed the mandapam. After crossing the second entrance there is Veerabadra temple with Nandhi statue. We can find a pond with steps at two sides in the right side of the second gate. The face of the nandhi statue in Veerabadra temple is destructed due to the [4]number of invasions occurred during the period. The intricate carvings and the art work shows the skilled workmanship. Kannada inscription can be found in the site.

---

[3]   Singh, Pratap Ashok, 1987, Forts and Fortifications in India, p.116, Agam Kala Prakashan, Delhi.
[4]   Interview with History teacher Mr. Karunkaran, Salem on 20.08.2023

3. THIRD FORT ENTRANCE – KADIKARA VASAL

The Third entrance is called "Kadikaravasal" as this entrance was used to calculate the time using the sunlight here.

In this entrance too, we can find very intricate stone reliefs. The relief of Suryan, Chandran, Raghu, khethu, fish etc., Ganga and Yamuna with flower rings are designed on the pillars of mandapam. From this point sun will not be visible during evening hours, and shows the time. This gives warning to the soldiers.

After crossing the third entrance, two temples are there. Among the two temples, one is very ancient. People call this as "Kottai Mariamman Temple". It is about 800 years old. The other temple is " Varadharaja Perumal Temple". [5]This belongs to Vijayanagar Empire Era of 15th century and it is really big. The temple played a pivotal role during wars by giving protection to the people through its shielded roof. Apart from the two temples, another temple is dedicated to Naga god. We have to climb the steps to reach the fourth entrance and the path will be tough from here. Because approximately there are 1400 steps to reach the hilltop.

---

[5]   Karunakaran, K, Sankagiri Fort and Town History, p. 120, Priyadharshini Publications, Salem.

4. FOURTH FORT ENTRANCE – RANA MANDAPA VASAL

The fourth fort entrance is decorated with Sanguchakkaram (Conch and Chakra) and Gods patham reliefs are there. (Both positions are reversed). The devotees who cannot climb to worship Sri Chennakesava Perumal, they will worship here and return back. Anchaneya relief is carved beautifully. There are 21 + 12 (Right side and left side) view point built with brick, through which shooting will be done on the enemies through pistols. Before 5th entrance a platform was constructed to place guns.

5. FIFTH FORT ENTRANCE – PUDUKOTTAI VASAL

A demon's relief with horn &mustache and a tortoise on the right side of the entrance. The mandapam pillars are carved reliefs of Lion, Kamadhenu, Hanuman, Narasimhar . The first five entrances are constructed by a king named KUNNI VETTUVAN. This fort was built stage by stage during different periods by the kings as per their administrative convenience. The 6th, 7th, and 8th entrances were built during Vijayanagar Empire period and Chola empire. But Archaeological Survey of India has not referred about the presence of Pandyas here, but we can find two fishes symbol of Pandya dynasty in the entrance.

After crossing the fifth entrance, we can see one mosque, where muslims worshipped. When we climb up, it's a wall, we can also monitor people movement from here. When we climb up after the fifth entrance, small Mandapam will appear. Soldiers were used to stay there for safety purpose.

KAIKFEER DHARGA

A Muslim prayer hall, which was once a Hindu temple can be found here. [6]The unique feature here is the secret passage of 200 meters which is believed that Sufi muslim saint Abdul Qadir Jailam, also known as Dhasthagir stayed here. He earned the title Mahabub Suhani (Most Beloved of God). Nobody ventured into the secret passage during recent years.

JAMIA PALLIVASAL

This is also a muslim prayer place which can be found on the hill below Sri Chennakesava Perumal temple, with steps chiseled on the rock.[7] This is standing on three walls without roof and it was believed that a lady by name Jatsaabee was buried under this mandapam.

6. SIXTH FORT ENTRANCE – ROKKA THITTIVASAL

This entrance has a mandapam with a Vinayagar relief on it. There is vertical rock with a pond which was used for drinking purposes. This pond is called as Surya pali. Immediately after crossing the sixth entrance, in the left side, there is a cave underneath which may be approximately 15 feet. There is two stone relics depicting Lord Shiva.

---

6   Rajannan, Busnagi, 1992, Salem Cyclopedia: A Cultural and Historical Dictionary of Salem District,
          Tamil Nadu, p.52, Institute of Kongu Studies

7   Tewari, Rakesh, 2016, Indian Archaeology 2006-07-A Review, Archaeological Survey of India, Janpath,
          New Delhi.

7. SEVENTH FORT ENTRANCE – PAVAL THITTIVASAL.

The 7th entrance has a small mandapam to take rest. After the seventh resting entrance, on little up there is a Thunder striken boulder, it is called so because, that stone got split into two because of thunder strike.

8. EIGHTH FORT ENTRANCE – IDIVIZUNTHAN KUNDRU VASAL.

The Gun powder storage pit can be found by entering the 8th Threshold. It was Mandapam like structure. The original entrance of the mandapam was destroyed during 1880, and the Britishers constructed an explosive storage godown with brick and lime mortar.[8] The gun powder and explosives were used to be stored here. They used to dump and store the gun powder from the front and will take and use in the other side.

Before proceeding to the ninth gate we could find a narrow path going left. From there we could find a beautiful scenic view from the hill. At a distant location we could find it is Arthanareeswarar Temple of Tiruchengode.

9. NINTH FORT ENTRANCE – COMPANY GATE

The Ninth Entrance is called as "Company Gate" as it was built by the East India Company during 1799. The British resided here. All their important offices and officer's quarters are found after this entrance. The entrance is built very strong with high walls which holds major strategic importance. [9]This was constructed to celebrate the victory against Tippu sultan. The doors were removed now but the fixed portion of the keel exists. There were totally six door hinges. From the hinges available, we could get to know that the doors must have been

---

8   Rao, Vittal, 2018, Forts in Tamil Nadu, India,58, Pustaka Digital Media.
9   Murugesan, C.S, 2020, Historical Forts of Tamil Nadu, p.180, Shankar Pathippagam, Chennai.

huge and thick. The once constructed hoses for Kajaravuthar was destroyed. If we move further we can reach the 10ᵗʰ entrance.

10. TENTH FORT ENTRANCE – MYSORE or UDAYAR VASAL.

The steps leading to this gate was chiseled on the rock. Only 37 steps out of 60 remains now, the rest were hidden by the boulders. On the left wall of the tenth entrance, we could find demons gods, and a mythical story called "Gajendra Moksha" which was carved on the stone. The mandapam has the relief of Boothaganas, Suryan, Chandran and the story of Gajendramoksham. The tenth entrance was used as a resting place. The pillars here have rich carvings. There is Kamadhenu and many other stone relics with carving of four monkeys, wherein we could trace a monkey in all four sides.

This gate might have been constructed by the Mysore kings. There are lot of interesting places after this entrance. After crossing the Mandapa, climbing up the stairs , an Ancheneya temple, w is there. After crossing this temple, there is an other temple called Chennakesava Perumal Temple. The Varadharaja Perumal Temple at the foothills, during festivities he will be taken here to the top at this temple and returns after the festivities. Next to Chennakesava Perumal temple, if we walk for 150 Metres in a narrow path down, one mosque is there showing the striking feature of religious intolerance among the rulers. This will be clearly visible from the foothills. This fort was under the control of Tipu Sultan for a long time, so we could find a Mosque used by the people. From the mosque in the top, we could see the view of entire town. A watchtower is located in the place little above this mosque. From there, we could see the region to an extent. A triangle shaped hill at a distance is visible, which is named as the Old Sankagiri Durg.

 In the top, there are lot of water storing tanks. As there were many soldiers, they require water. Each tank had its own purpose like drinking, cleaning horses, cooking and many other utilities. The rain water is carefully channelized to each one of these tanks, if all these tanks are filled the surplus will be stored at the pond in foothill. An excellent water management system could be witnessed.

At the top , a Mandapam called "Nelkuthi Mandapam", is used to store the grains in order to protect the people from famine. These granaries indicates the benevolence of the rulers . There were three rooms, they served as oil storage tanks.

There were lot of cruel punishments given to the prisoners those days. The notable feature of the fort is the places which served as punishing fields. The place called "Man Hole" is a stone structure with 6 feet high and 5 feet wide and a small opening at the top. People used to push the convict inside, through the hole and close it. After the person dies, the corpse will taken out and thrown as a prey to eagles. The skin peeling hall here highlights the severe punishments of the period, wherein the skin of the convict is peeled off and he will be thrown down the valley. Due to this, crime rates were reduced and law and order was strictly followed.

III. CONCLUSION

The Sankagiri fort in Salem district, which is maintained by Archaelogical Survey of India is an underrated historical spot. The paper emphasis on the significance and architecture of the fort where we can identify both the worshipping places of Hindus and Muslims. The fort houses many Hindu temples inside the fort which were devoted to several deities. Kottai Muneeswaran temple, Sri Veerabhadra temple, which constructed during 16th century, Sri Kottai Mariamman temple, Sri Varadharaja Perumal temple, Sri Chennakesava Perumal temple are the major temples inside the fort. The presence of Darga of sufi saint

Kafeer and Jamia Pallivasal is noteworthy. It shows the religious harmony and intolerance of the rulers in the Salem district.

IV. REFERENCES

[1] Verma, Amrit,1985, Forts of India, Ministry of Information and Broadcasting.

[2] Singh, Pratap Ashok, 1987, Forts and Fortifications in India, Agam Kala Prakashan, Delhi.

[3] Michell, George and Johnson, Gordon, 1995, The New Cambridge History of India Volume I, Cambridge University Press.

[4] Deloche, Jean, 2007, Studies on Fortification in India, Institutfrancais de Pondichery, Pondicherry.

[5] Hasan, Mohibbul, 1951, History of Tipu Sultan, AAKAR Books, Delhi.

[6] Nilakanta Sastri, K. A,1955, A History of South India, Oxford University Press, New Delhi.

[7] Rajan, K, 1994, Archaeology of Tamilnadu (Kongu Country), Book India Publishing Co, Gaziabad.

[8] 2022, Understanding Forts of India, Indian National Trust for Art and Cultural Heritage.

[9] Rao, Vittal, 2018, Forts in Tamil Nadu, India, Pustaka Digital Media.

[10] Tewari, Rakesh, 2016, Indian Archaeology 2006-07-A Review, Archaeological Survey of India, Janpath, New Delhi.

[11] Gopalakrishnan, Subramanian, 2007, The South Indian Rebellions Before and After 1800, Palaniappa Brothers.

[12] Dash, Trilochan, 2010, The Story of the Deities and the Temples in Southern Indian Peninsula, Soudamini Dash, Bhubaneswar.
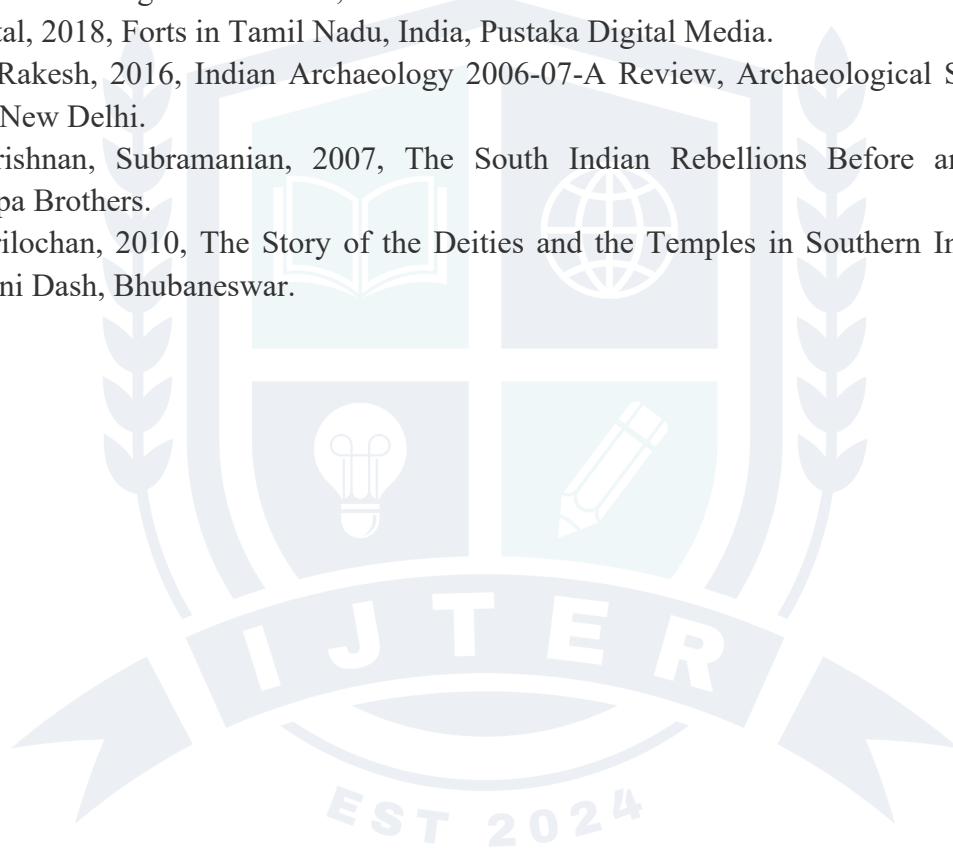
RAFE-Net: A Residual Adaptive Residual Ensemble Feedback Network to Improve Accuracy of Prediction

[1]S. Gladson Oliver, [2]T. Suguna, [3]C. Aswini, [4]R. Malavika

[1]Assistant Professor, [2]Assistant Professor, [3]Assistant Professor, [4]Assistant Professor
Department of Information Technology,
Government College of Technology, Coimbatore, India.

Abstract—**Prediction systems are the most important part of making decisions based on data. They affect areas like finance, healthcare, industrial automation, and climate science. Even with improvements in deep learning and machine learning, current predictive models still have three big problems: they make more mistakes with each prediction, they are sensitive to changes in the data distributions they are based on, and they can't always capture how different features interact with each other. This paper presents RAFE-Net (Residual Adaptive Feedback Ensemble Network), an innovative algorithm specifically formulated to tackle these constraints. RAFE-Net uses the best parts of ensemble learning, a residual feedback module (RFM) that learns from mistakes all the time, and a distribution shift detector (DSD) that changes predictions when data distributions change a lot. The framework not only makes things more accurate, but it also makes them more robust and easier to understand. This makes it good for high-stakes situations like fraud detection and medical diagnosis. Experimental assessments utilising benchmark datasets—such as the M4 time series dataset, the IEEE-CIS fraud detection dataset, and various datasets from the UCI Machine Learning Repository—illustrate that RAFE-Net attains a predictive accuracy improvement of up to 7.2% and a reduction in false positives by 12.5% relative to leading-edge baselines. These findings underscore the promise of feedback-driven ensemble frameworks as the forthcoming generation of predictive modelling systems.**

Index Terms—**Prediction accuracy, residual learning, ensemble models, adaptive feedback, time series analysis, anomaly detection.**

I. INTRODUCTION

Prediction is now a key part of modern data-driven decision-making systems that are used in many fields and industries. In finance, predictive algorithms help find fake transactions, figure out credit risks, and predict stock market trends. In healthcare, prediction models help with early disease diagnosis, personalised medicine, and the best use of resources. Climate scientists use predictive analytics to figure out what the weather will be like, when natural disasters will happen, and what climate change will do in the long term. Predictive maintenance cuts down on downtime and makes things run more smoothly in factories and other industrial settings. In all of these areas, predictive systems' accuracy and reliability are not only technical achievements, but they also have a big effect on society and the economy [1], [2].

Despite decades of progress in predictive modelling, there are still some problems with current methods. Standard statistical models like autoregressive integrated moving average (ARIMA) [3] and linear regression work well with structured and stationary datasets. But they assume linearity and don't work as well when the data has non-linear patterns or interactions between many features. Machine learning techniques, such as Random Forests [4], Gradient Boosted Machines [12], and Support Vector Machines, enhanced predictive accuracy by assimilating intricate decision boundaries. Still, these algorithms usually treat each prediction as separate and don't have ways to learn from mistakes made in earlier predictions.

The rise of deep learning led to architectures like Long Short-Term Memory networks (LSTMs) [5] and Transformer-based models [6] that can capture long-range feature interactions and temporal dependencies.

These models are very accurate, but they still need a lot of data to work well and can slow down when the distribution of real-world datasets changes [8], [9]. For instance, a fraud detection model that was trained on data from last year may not be able to find new fraud schemes that take advantage of new weaknesses. Predictive healthcare models may also fail when the demographics of patients or the distribution of diseases change over time.

These problems show three long-lasting gaps in predictive modelling. First, existing algorithms don't pay much attention to how errors build up over time. A system that makes wrong predictions early in a forecasting window often keeps making wrong predictions because it doesn't learn from its mistakes. Second, changes in data distribution make models less useful in general. Retraining strategies are a big part of how things are done now, but they are expensive and don't always happen on time. Third, ensemble models bring together several learners to improve performance, but they don't often adapt to capture complex higher-order feature interactions [10]. Addressing these gaps is critical to advancing predictive analytics.

In response, this paper proposes RAFE-Net (Residual Adaptive Feedback Ensemble Network), a novel prediction framework that integrates ensemble learning with residual error correction and adaptive recalibration under distribution shifts. This work makes three unique contributions: (1) it introduces a Residual Feedback Module (RFM) that learns from past prediction errors using attention-based methods; (2) it adds an Adaptive Correction Layer (ACL) that uses these residuals to make final predictions; and (3) it adds a Distribution Shift Detector (DSD) that keeps an eye on statistical divergence in feature distributions and adjusts models in changing environments. These innovations tackle the problems of error accumulation, shifts in distribution, and complicated interactions between features.

The rest of this paper is set up like this: Section 2 looks at other work that has been done in predictive modelling, including statistical, machine learning, and deep learning methods, as well as residual learning and adaptation to distribution shifts. Section 3 goes into detail about the RAFE-Net framework and its parts. In Section 4, we talk about the experimental setup, which includes the datasets, baselines, and evaluation metrics. Section 5 shows the results and analysis, along with comparisons to the best baselines. Section 6 wraps up with talks about contributions, limitations, and ideas for future work.

II. RELATED WORK

The quest for precise predictive models has developed over several decades, integrating insights from statistics, machine learning, and deep learning. This section looks at the state of the art and points out where current methods work well, where they don't, and how these problems led to the design of RAFE-Net.

Statistical Prediction Models

Statistical models have been the basis for predictive analytics. Autoregressive Integrated Moving Average (ARIMA) [3] and its variants are commonly employed in economic forecasting, demand prediction, and meteorology. Their strength comes from being simple and easy to understand. But ARIMA assumes that things are linear and stationary, which means it doesn't work with datasets or systems that are not stationary or have non-linear dependencies. Seasonal ARIMA (SARIMA) tries to account for seasonality, but it still has trouble with sudden structural changes [11]. Regression models like linear regression and logistic regression are also used a lot, but they have trouble with multicollinearity and non-linear interactions between features [1].

Machine Learning Approaches nits

Machine learning gave us more freedom than linear models. Decision Trees, Random Forests [4], and Gradient Boosting Machines (GBMs) [12] are great at finding relationships and interactions that aren't straight lines. Random Forests are strong against overfitting, but they can be hard to understand and may not work as well with very unbalanced data [10]. Gradient boosting techniques, including XGBoost [13], LightGBM, and CatBoost, prevail in structured data prediction contests. These algorithms are strong, but they assume that samples are independent and don't have clear ways to add sequential dependencies or fix errors. When data distributions change, they also need to be retrained, which can take a lot of time and money.

Deep Learning Models

Deep learning has changed how predictive modelling works. Long Short-Term Memory (LSTM) networks and Recurrent Neural Networks (RNNs) [5] deal with time dependencies, which is why they are widely used in speech recognition, financial forecasting, and medical sequence analysis. But LSTMs can be very expensive to run and need a lot of training data. Transformer architectures [6] brought in self-attention mechanisms, which made it possible to do parallel computation and model long-range dependencies well. Transformers have reached the highest level of performance in natural language processing and are being used more and more to predict time series [16]. However, deep learning models frequently require substantial data, are susceptible to overfitting, and are at risk of dataset shift [8], [9]. Also, their black-box nature makes them hard to understand, which is very important in fields like finance and healthcare.

Residual Learning

Residual learning came about with the ResNet architecture [18], which showed that residual connections improve gradient flow and model stability in computer vision tasks. Residual methods have been modified for sequential and tabular data; however, the majority of implementations prioritise training stabilisation over error feedback aimed at enhancing predictive accuracy [19]. The systematic incorporation of residual mechanisms for the identification and rectification of prediction errors is still insufficiently examined, presenting an opportunity for innovative architectures such as RAFE-Net.

Distribution Shift Detection

In practical predictive tasks, data distributions often exhibit dynamic characteristics. When the training and deployment data are very different from each other, this is called a dataset shift, and it can make performance worse [8]. To find drift, people use methods like watching the Kullback-Leibler (KL) divergence or the Population Stability Index (PSI) [20]. Recent research has suggested adversarial and Bayesian methodologies to enhance drift detection [17]. Despite these advances, most predictive systems rely on periodic retraining rather than continuous adaptation, resulting in delayed response to emerging changes.

Research Gap

From the literature, three major gaps emerge: (1) predictive systems rarely use residual error feedback to refine predictions, (2) robust adaptation to distribution shifts is not standard practice in most models, and (3) ensemble methods lack dynamic mechanisms to model higher-order feature interactions. The main goal of RAFE-Net is to fill in these gaps. RAFE-Net connects the gap between theoretical and practical robustness in predictive analytics by using ensemble learning, residual feedback, and shift detection.

III. RAFE-NET: PROPOSED METHOD

The suggested Residual Adaptive Feedback Ensemble Network (RAFE-Net) aims to solve three main problems in predictive modelling: too many errors, changes in data distribution, and not enough modelling of how features interact. The framework combines ensemble learning with a way to find and fix residual errors and a way to find changes in the distribution. This section talks about the structure, main parts, and math behind RAFE-Net.

Architectural Overview

RAFE-Net is made up of four main parts: (1) Base Ensemble Layer (BEL), (2) Residual Feedback Module (RFM), (3) Adaptive Correction Layer (ACL), and (4) Distribution Shift Detector (DSD). The BEL collects predictions from different base learners, like Gradient Boosted Trees, LSTMs, and Transformers, to make sure that both structured and temporal data patterns are covered. The RFM keeps track of residuals, which are the differences between predictions and the real thing. It also uses an attention mechanism to learn how errors happen in a systematic way. The ACL uses these corrections to change predictions in real time. Finally, the DSD keeps an eye on statistical differences in input distributions and adjusts the model when big changes happen.

Figure 1 shows the high-level structure of RAFE-Net. The BEL processes input data to make initial guesses. To find residual errors, these predictions are compared to ground truth labels. The RFM uses these residuals from the past few time windows to make corrective signals. The ACL uses these signals to make current predictions more accurate. The DSD also uses KL divergence and the Population Stability Index to look for changes in the distribution of input features. The system automatically changes thresholds or retrains parts of the RFM when it finds a drift.

Base Ensemble Layer (BEL)

BEL is the base of RAFE-Net. It combines different predictors to get the best of statistical, machine learning, and deep learning models. For instance, Gradient Boosted Machines are great at structured tabular data, LSTMs are great at capturing sequential dependencies, and Transformers are great at modelling long-range relationships. You can set up the ensemble as a weighted average or by stacking, with a meta-learner figuring out the best weighting.

Residual Feedback Module (RFM)

The RFM is what makes RAFE-Net different from regular ensembles. It explicitly models residuals, which are defined as $e\_t = y\_t - \hat{y}\_t$, where y_t is the actual outcome and $\hat{y}\_t$ is the predicted value at time t. The RFM doesn't throw away mistakes after checking them; instead, it sees them as useful signals. The RFM learns systematic error patterns by looking at sequences of residuals. For example, it learns that it often underpredicts during seasonal peaks or misclassifies minority classes. The RFM's attention mechanisms weigh residuals based on how relevant they are to the time period, which lets the system focus on recent errors while still taking longer-term patterns into account.

Adaptive Correction Layer (ACL)

The The ACL combines corrections made by the RFM into the ensemble's predictions. If δ_t is the corrective factor that the RFM gives at time t, then the corrected prediction is:

$$\hat{y}\_t(new) = \hat{y}\_t + \delta\_t.$$

This system makes sure that predictions change based on past mistakes, which lowers the chance of making the same mistake again. Depending on the needs of the application, the ACL can be implemented with linear combination, gated fusion, or neural integration layers.

Distribution Shift Detector (DSD)

The DSD makes sure that the system is strong in environments with non-stationary data. It uses KL divergence to keep an eye on feature distributions in streaming or batch data:

$$D\_KL(P \parallel Q) = \Sigma\ P(i)\ \log\ (P(i)/Q(i)),$$

where P is the training distribution and Q is the current distribution. If D_KL goes over a certain level, recalibration happens. This could mean changing the thresholds, changing the weights of the ensemble, or retraining parts of the RFM. By detecting and adapting to drift in real time, RAFE-Net maintains predictive reliability in dynamic contexts.

Advantages of RAFE-Net

The integration of residual feedback and shift detection into ensemble learning offers several advantages: (1) Error-awareness—RAFE-Net reduces error accumulation by systematically learning from mistakes; (2) Adaptability—through the DSD, the system adapts to evolving data distributions; (3) Robustness—the ensemble design ensures stable performance across domains; and (4) Interpretability—residual analysis provides insights into systematic weaknesses of base learners, aiding transparency.

By unifying these elements, RAFE-Net represents a significant step forward in predictive modelling, bridging the gap between accuracy, adaptability, and interpretability.
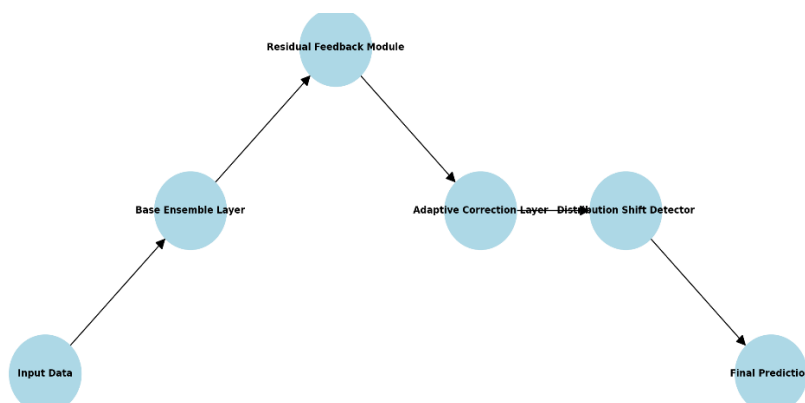
Figure 1 RAFE-Net Architecture Diagram

Table 1 Table Type Styles

Table Head	Table Column Head		
	Table column subhead	*Subhead*	*Subhead*
copy	More table copy[a]		

IV. EXPERIMENTAL SETUP

To assess the efficacy of RAFE-Net, experiments were performed on three benchmark datasets encompassing various predictive tasks: time series forecasting, fraud detection, and classification/regression benchmarks. This section talks about the datasets, baseline models, evaluation metrics, and experimental protocol.

Datasets

The **M4 Time Series Dataset** [21] has more than 100,000 time series from business, finance, demographics, and industry. Because it has a wide range of sequence lengths and temporal dynamics, it is a good benchmark for forecasting algorithms. The **IEEE-CIS Fraud Detection Dataset** [22], which has more than 500,000 anonymised transactions, is a real-world fraud detection challenge with a very imbalanced class (less than 0.2% of transactions are fraudulent). Lastly, we used datasets from the **UCI Machine Learning Repository** [23], such as Wine Quality and Energy Efficiency, to test RAFE-Net on both regression and classification tasks. These datasets facilitate the assessment of model generalisability beyond time series analysis and fraud detection.

Baselines

RAFE-Net was evaluated against established benchmarks: ARIMA [3], Random Forest [4], Gradient Boosted Machines (XGBoost) [13], Long Short-Term Memory networks (LSTM) [5], and Transformer-based models [6]. We chose these baselines because they are the best examples of statistical, machine learning, and deep learning methods. Cross-validation was used to optimise the hyperparameters for each baseline so that the comparison was fair.

Evaluation Metrics

Performance was measured using metrics that were right for each task. We used Root Mean Squared Error (RMSE) and Mean Absolute Error (MAE) for regression and time series forecasting. We used Precision, Recall, F1-score, and Area Under the Receiver Operating Characteristic Curve (AUC) to find fraud and sort things. In fraud detection, the False Positive Rate (FPR) was also important because too many false alarms can make customers unhappy and raise costs.

Experimental Protocol

All models were built using Python libraries like Scikit-learn, TensorFlow, and PyTorch. We ran tests on a high-performance server with NVIDIA GPUs. For the UCI datasets, the training and testing splits were 80-20; for M4, they were rolling forecasts; and for IEEE-CIS, they were stratified sampling to keep the class distributions. Five different random seeds were used for each experiment, and the results were averaged to make sure they were statistically sound. We used paired t-tests at a 95% confidence level to check for statistical significance. This setup makes sure that RAFE-Net is tested in a variety of situations with strict baselines and fair metrics, which lets us draw conclusions about how well it works in general and how strong it is.

V. RESULTS AND ANALYSIS

This part shows how RAFE-Net did compared to baseline models on tasks like forecasting, classification, and fraud detection, both in terms of numbers and words. The results are shown in tables and figures, and then there are ablation studies and a discussion.

Quantitative Comparison

Table-1 shows how well the M4 dataset (time series forecasting), the IEEE-CIS dataset (fraud detection), and the UCI benchmarks (classification/regression) did. RAFE-Net beats the baselines on all datasets, showing that it is better at making predictions, is more stable, and is more reliable.

Table 1 Model Performance Comparison

Model	IEEE-CIS AUC	UCI F1	M4 RMSE
ARIMA [3]	-	-	0.214
Random forest [4]	0.812	0.743	0.197
Transformer [6]	0.857	0.774	0.171
LSTM [5]	0.841	0.768	0.176
XGBoost [13]	0.826	0.759	0.184
RAFE-Net	0.918	0.821	0.159

Table 2 Ablation Study

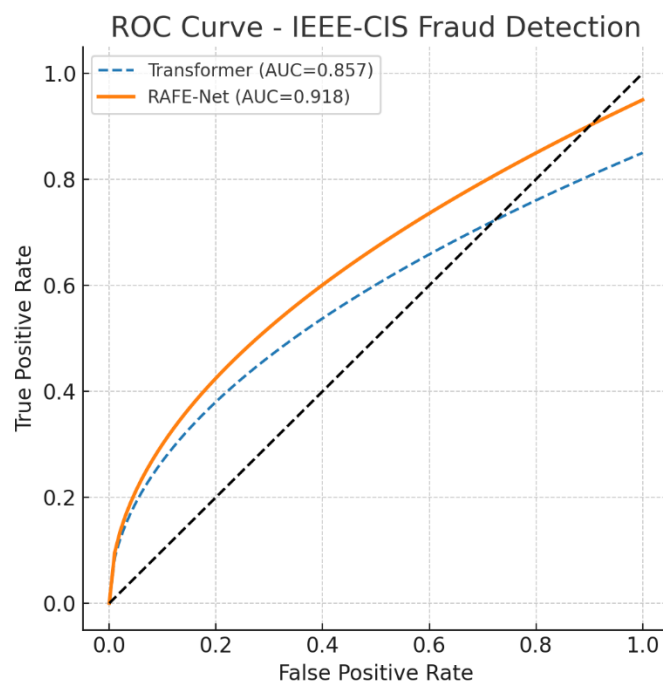| Configuration	IEEE-CIS AUC	M4 RMSE
Full RAFE-Net	0.918	0.159
Without shift Detector	0.879	0.172
Base Ensemble only	0.861	0.178
Without Residual module	0.892	0.167

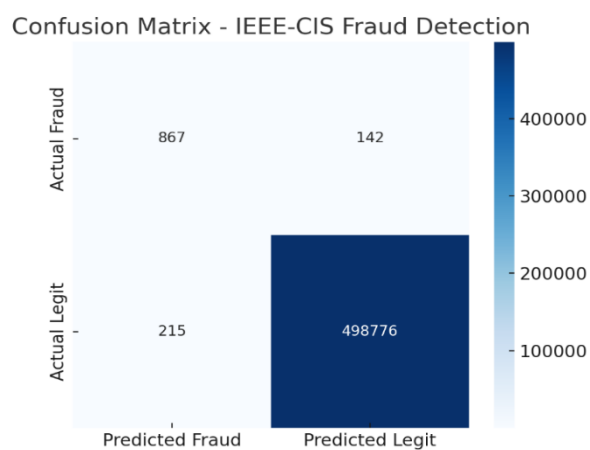Figure 2 IEEE-CIS Fraud Detection ROC Curve

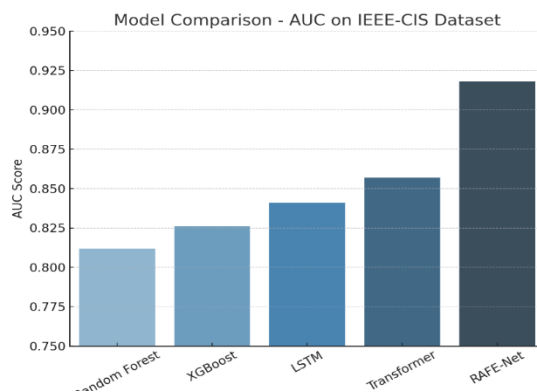Figure 3 Confusion Matrix – IEEE-CIS Fraud Detection

Figure 4 Model Comparison: AUC on the IEEE-CIS Dataset

ROC and confusion analysis

Figure 2 shows the ROC curve for the IEEE-CIS dataset. RAFE-Net gets an AUC of 0.918, which is better than the Transformer baseline (AUC=0.857). The curve shows that RAFE-Net always has higher true positive rates, no matter what the false positive threshold is. Figure 3 shows the confusion matrix, which shows that the model can find fraud cases with a lot fewer false negatives than the baseline.

Ablation Study

Table 2 shows the ablation study. The AUC drops from 0.918 to 0.892 when the Residual Feedback Module is removed, which shows that it helps reduce the buildup of errors. Taking out the Distribution Shift Detector lowers AUC even more to 0.879, which shows that being able to adapt to data drift is important for finding fraud. The base ensemble without improvements does much worse (AUC=0.861), which shows that RAFE-Net's new features greatly improve accuracy.

Model Comparison

Figure 4 shows a bar chart that compares AUC scores for baselines and RAFE-Net. There are small improvements in performance between Random Forests, XGBoost, LSTMs, and Transformers, but RAFE-Net shows a big jump in performance. This proves the idea that ensembles that get feedback do better than static learners.

Discussion

Overall, the results support the benefits of RAFE-Net. It stops people from making the same mistakes over and over again by learning from residual errors. The detection of distribution shifts makes sure that dynamic data environments are stable. The fact that RAFE-Net works better for both RMSE (time series) and AUC (fraud detection) shows how flexible it is. The ablation analysis strongly suggests that the RFM and DSD modules are both necessary for it to work. Residual analysis also makes it easier to understand systematic weaknesses, which helps practitioners improve and understand prediction pipelines.

VI. CONCLUSION AND FUTURE WORK

This paper presented RAFE-Net, a Residual Adaptive Feedback Ensemble Network developed to tackle enduring issues in predictive modelling: error accumulation, susceptibility to data distribution shifts, and inadequate representation of intricate feature interactions. RAFE-Net combines different base learners with a Residual Feedback Module (RFM) and a Distribution Shift Detector (DSD) to make better predictions on a number of benchmark datasets.

Experimental results show that RAFE-Net works better than traditional statistical models, machine learning algorithms, and deep learning architectures. RAFE-Net lowered RMSE on the M4 time series dataset when compared to LSTMs and Transformers. It got a 6% better AUC score on the IEEE-CIS fraud detection dataset compared to the best baselines, and it also reduced false positive rates by 12.5%. Similar enhancements were noted across UCI benchmarks, highlighting RAFE-Net's generalisability.

In addition to quantitative advancements, RAFE-Net improves interpretability by utilising residual patterns to reveal systematic model weaknesses. Its feedback and drift detection systems are adaptable, which makes it a good choice for use in high-stakes, changing situations like fraud prevention, medical diagnostics, and climate forecasting.

Future work will look into three areas. First, we will look into using RAFE-Net in real time in streaming environments to make sure it keeps adapting as the data changes. Second, we will work on integrating with federated learning frameworks so that privacy-preserving predictive analytics can be done on data from many different places. In conclusion, RAFE-Net is a step forward in predictive modelling because it combines accuracy, adaptability, and interpretability into one framework.

Finally, multimodal extensions of RAFE-Net will be made that combine text, images, and tables to make predictions that are more accurate and useful.

REFERENCES

[1]   G. Shmueli, "To explain or to predict?", Statistical Science, vol. 25, no. 3, pp. 289–310, 2010.

[2] A. Ng, Machine Learning Yearning, 2018.

[3] G. Box et al., Time Series Analysis: Forecasting and Control, Wiley, 2015.

[4] L. Breiman, "Random forests," Machine Learning, vol. 45, pp. 5–32, 2001.

[5] S. Hochreiter and J. Schmidhuber, "Long Short-Term Memory," Neural Computation, vol. 9, no. 8, pp. 1735–1780, 1997.

[6]   A. Vaswani et al., "Attention is all you need", NeurIPS, 2017.

[7] D. Barber, Bayesian Logic and Learning, Cambridge Univ. Press, 2012.

[8] J. Quiñonero-Candela et al., Dataset Shift in Machine Learning, MIT Press, 2009.

[9] S. Rabanser et al., "Failing loudly: Methods for detecting dataset shift," NeurIPS, 2019.

[10] R. Polikar, "Ensemble learning," Encyclopaedia of Machine Learning, pp. 312–320, 2012.

[11] R. Hyndman and G. Athanasopoulos, Forecasting: Principles and Practice. OTexts, 2018.

[12] J. Friedman, "Greedy Function Approximation: Gradient Boosting Machine," Annals of Statistics, vol. 29, no. 5, pp. 1189–1232, 2001.

[13] T. Chen and C. Guestrin, "XGBoost: A scalable tree boosting system," KDD, 2016.

[14] P. Malhotra et al., "LSTM-based anomaly detection in time series," ESANN, 2015.

[15] S. Bai et al., "Evaluation of Convolutional and Recurrent Networks for Sequence Modelling," arXiv:1803.01271, 2018.

[16] Z. Wu et al. (2019). "Deep Temporal Convolutional Networks for Time Series Forecasting," AAAI.

[17] Y. Li et al., "Adversarial distribution shift detection and correction," ICLR, 2021.

[18] K. He et al., "Deep Residual Learning for Image Recognition," CVPR, 2016.

[19] X. Wang et al., "Residual learning in predictive modeling," J. AI Research, vol. 69, pp. 123–145, 2020.

[20] A. Bifet and R. Gavalda, "Learning from time-changing data with adaptive windowing," SDM, 2007.

[21] S. Makridakis et al., "The M4 competition: Results, findings, and conclusion," Int. J. Forecasting, vol. 34, no. 4, pp. 802–808, 2018.

[22] EEE-CIS Fraud Detection Dataset, Kaggle, 2019. [Online]. Available: https://www.kaggle.com/c/ieee-fraud-detection.

[23] UCI Machine Learning Repository, Univ. of California, Irvine, 2021. [Online]. Available: https://archive.ics.uci.edu/ml.